Characterizing performance of the radar system for breathing and heart rate estimation in real-life conditions

by

Xinyang Zhang

Thesis submitted to the
Faculty of Graduate and Postdoctoral Studies
In partial fulfillment of the requirements
For the M.A.Sc. degree in
Electrical and Computer Engineering

School of Electrical Engineering and Computer Science
Faculty of Engineering
University of Ottawa

© Xinyang Zhang, Ottawa, Canada, 2017

Abstract

Contact-less human detection and monitoring using radar technology has been recently applied in many areas including search-and-rescue for earthquake victims, fall detection, gait analysis and detection of other human activities. Radars can also provide important information about a persons state of health by monitoring the level of activities, heart and breathing rate. Also it can be used to generate warnings if some of the monitored parameters are outside of predefined limits. The major application of this work is for monitoring in-mates and their activities.

This thesis deals with characterizing the performance of the radar system used for monitoring a single person in a contained environment. This thesis is experimentally based and during the thesis a large number of experiments were performed in order to monitor subjects in realistic conditions. The thesis explores feasibility of using the radar with a single radio-frequency channel input and two algorithms for breathing and heart rate estimation when the subject is at different relative orientation towards the radar as well as in different postures. Algorithm one is using Fast Fourier Transformation (FFT) and algorithm two is using Empirical Mode Decomposition (EMD) with Minkowski distance. We also detect the zones where the subject is when the subject is moving. Since this exploratory analysis provides initial features for classifications and algorithms for breathing and heart beat estimation, it can represent a foundation for future works on designing systems that track subjects and their breathing in real-time.

Acknowledgements

I would like to express my gratitude to all those who helped me during the writing of this thesis. My deepest gratitude goes first and foremost to Professor Miodrag Bolic and Professor Sreeraman Rajan, for their constant encouragement and guidance. They have walked me through all the stages of the writing of this thesis. Without their consistent and illuminating instruction, this thesis could not have reached its present form.

Secondly, I would like to express my heartfelt gratitude to Dr. Isar Nejadgholi, who led me into the world of EMD. I am also greatly indebted to all of the students in our team. I am deeply grateful for the guidance and support they have provided me during my research.

Last my thanks would go to my beloved family for their loving considerations and great confidence in me all through these years. I also own my sincere gratitude to my friends and my fellow classmates who give me their help and time in listening to me and helping me work out my problems during the difficult courses of graduate study.

Table of Contents

List of Tables and Figures

Chapter 1

Background and Significance

Breathing rate estimation and heart beat rate estimation provide measures of s subject's state of life, posture and health. Stop breathing is a dangerous condition that if it takes a long time, can lead to death, or other health problems.

This project is based on the realistic detection of different kinds of human signals. The goal of this project is to use adaptive filters to estimate the heart beat signal and breathing signal in a minimal mean square error sense.

As we know, such an observation has a significant meaning in detecting human signals. Through detecting human body signals, we can reliably gauge the status of all body parts and determine whether they are operating normally or otherwise. For example, by detecting the heart beat, we can calculate the heart rate. When the heart rate is not within the scope of the standard range, the subject is required to go to the hospital and carry out a detailed examination in order to be treated for cause of illness. This highlights the importance of detecting these human signals, as they can be used to understand complex conditions. For example, when a motivated subject is tense or nervous, their body signals may differ from the normal. In such a situation, a machine capable of reading their vitals could detect these anomalies, which can help shorten the medical response time. Our bodies may sometimes send us some indicators to tell us there may be something (ie headaches, dizziness, fatigue), but we often overlook these signals. However, if we examine them using the proper equipment, we can then analyze the readings from an unbiased, rational point of view.

In recent years, several studies have explored new approaches to estimate breathing rate using minimal contact (non-disturbing) sensors. [1] explored the ability of a tri-axial accelerometer worn on the torso to record breathing activity and to calculate Breathing rate (wireless). They compared their breathing rate (BR) estimation with nasal cannula sensor and showed a correlation of 0.870-0.928. Johnston and Mendelson [2] used a photoplethysmographic signal that was recorded by a reflectance pulse oximeter sensor mounted on the subject's forehead. Their Breathing rate analysis was subsequently processed by a time domain filtering and frequency analysis; they showed, qualitatively, a good agreement between their approach and respiratory belts. [3] estimated respiratory rate using a sensitive thermal infra-red (IR) camera (thermal sensitivity of 0.025C); They measured

airflow due to temperature difference resulting from respiratory activity. Accuracy of Breathing rate estimation between 83% and 98% depending on the tested subjects (10 participants) was reported.

Previous work with radar tended to detect life signs, respiration rates, and heartbeat rates, using a transmitted signal with fixed values of its frequency and power [4] [5]. Operating at 1.6 GHz and 2.4 GHz, direct-conversion Doppler radars have been integrated in 0.25 lm CMOS and BiCMOS technologies [6]. Heart and respiration activities were detected using a modified Wireless Local Area Network PCMCIA card and a module combining the transmitted and reflected signals [7]. Other systems operating in the Ka-Band were described in [8] [9] using a low-power double sideband transmission signal.

The demand for contact-less heart monitoring has increased lately, especially for long duration monitoring and for patients with particular conditions. This research is to detect life signs so that we can extract the breathing signal and the heartbeat signal from signals using continue wave Radar (CW Radar) in different situations, such as normal breathing, breathing with movement, holding breathing, breathing with fan, breathing with water and so on. In this section, we will first introduce different systems and techniques for monitoring breathing and heart rate. Then we will present the motivation of the thesis, followed by the contributions and the thesis overview

1.1 Background

1.1.1 Vital Signs

Breathing rate

Breathing (which in organisms with lungs is called ventilation and includes inhalation and exhalation) is a part of respiration. The rate at which breaths occur, usually measured in breaths per minute, is called the ventilation rate, or, by long-standing convention, the respiratory rate (despite that in precise usage ventilation is a hyponym, not a synonym, of respiration).

Human respiration rate is measured when a person is at rest and involves counting the number of breaths for one minute by counting how many times the chest rises. An optical breath rate sensor can be used for monitoring patients during a magnetic resonance imaging scan. [10] Respiration rates may increase with fever, illness, or other medical conditions.

The typical respiratory rate for a healthy adult at rest is 12-20 breaths per minute. [11] Average resting respiratory rates by age are: [12] [13] [14]

- birth to 6 weeks: 30-40 breaths per minute
- 6 months: 25-40 breaths per minute
- 3 years: 20-30 breaths per minute

- 6 years: 18-25 breaths per minute
- 10 years: 17-23 breaths per minute
- Adults: 12-18 breaths per minute
- Elderly >= 65 years old: 12-28 breaths per minute
- Elderly >= 80 years old: 10-30 breaths per minute

Heartbeat rate

Heart rate is the speed of the heartbeat measured by the number of contractions of the heart per minute (bpm). The heart rate can vary according to the body's physical needs, including the need to absorb oxygen and excrete carbon dioxide. It is usually equal or close to the pulse measured at any peripheral point. Activities that can provoke change include physical exercise, sleep, anxiety, stress, illness, and ingestion of drugs.

Many texts cite the normal resting adult human heart rate range from 60-100 bpm [15]. Tachycardia is a fast heart rate, defined as above 100 bpm at rest. [16] Bradycardia is a slow heart rate, defined as below 60 bpm at rest. Several studies, as well as expert consensus indicates that the normal resting adult heart rate is probably closer to a range between 50-90 bpm. [17]

1.1.2 Radar types

Radars have been widely used for detection of vital signs such respiration and heart activity [18] [19] [20] and human activity [21] [22] [23] [24]. The two main radar technologies used for this purpose are the pulsed radar (UWB) and continuous-wave (CW) radar. The pulsed radar transmits short duration modulated pulses and then receives the echo from reflecting objects, while the CW radar transmits and receives a continuous electromagnetic wave.

Microwave doppler radar has gained popularity in wireless sensing applications, such as volume change sensing [25], life detection [26], and cardiopulmonary monitoring [27]. Recently, much interest has been paid to the topic of non-contact vital sign detection using a Doppler radar. The Doppler radar first captures and down converts the wireless signal that is phase modulated by the physiological movements, and then identifies the human heartbeat and respiration rates by processing the baseband signal. This wireless radar detection can help us to collect the bio-signals when subjects are walking, moving their hand, holding their breath and so on.

Using CW Radar to detect and process signal, its working frequency is generally: 450MHz, 1.8GHz, 2.4GHz, 5GHz, 24GHz, 27GHz. There is a trade-off while choosing different frequency bands: the higher transmission frequency, the higher detection sensitivity, but the detection distance and the penetration will decline; the lower emission frequency, so the lower detection sensitivity, but the detection range and penetration will improve.

1.1.3 Applications

Radars for detecting vital signs

The first attempt of using continuous wave (CW) radars in medical applications for human body monitoring was in 1970s by Lin [28]. CW radars measured the modulation of phase of the reflected signal from the human chest displacement. In 1991, Chuang used CW radars to detect human breathing in a high clutter environment [29]. A lot of work has since been done in remote sensing of human breathing and stop breathing detection.

Stress level detection

Several patents discussed measuring the stress level of a human by examining and detecting the heartbeat rate and its variability [30]. However, heartbeat detection is a challenging problem if the subject is not settled in a specific scenario, and the signal reflected from the heart displacement is highly attenuated. [31] In a breathing pattern classification has been performed using the nasal pressure signal. Apneas, hypopneas, flow-limitation, and snoring were detected. We can detect a stress level marker of a human breathing if we are able to detect different breathing patterns using our radar system.

Suicide warning system

A suicide warning system has been developed between 2009 and 2013 [32]. It relies on a low-cost radar from GE. The system is capable of detecting breathing and heart signals and performing classification in order to detect stop breathing event. Relatively high specificity and sensitivity of the system is reported after Phase II of the project. However, all the experiments were performed without additional noise sources. This work is an excellent starting point for our project.

Detection of falls

Detection of falls using the radar was performed in [33] where it was observed that different parts of the human body move at different velocities during fall which can be recognized using radars. Another method was invented to detect falls by inspecting the distance of the torso from the floor [34].

Posture and gait estimation

Regarding posture detection, a biometric radar system was invented for identifying positional states of people using neural networks. The system requires training. Biometric research using radars is relatively new. Gait recognition is one possible method to distinguish between ways people walk.

1.1.4 Review of algorithms for estimating breathing and heart rate using radars

The challenges of using the 24 GHz Doppler radar in human stop breathing detection are: Narrow Band Interference (NBI), Null Detection (ND) points, target position, noise due to the movements of human body parts, movements while sleeping, any non-stationary targets such as water drops falling from taps, changing water level in washrooms, swinging decorations, and small fans. All of these challenges increase the false alarm rate. The effect of the unwanted movements becomes worse when the carrier frequency is higher. In 2007, Park used the arctangent demodulation to solve the null detection point problem [35]. In 2008, Li used the complex signal demodulation technique to solve the ND points problem, suppress the stationary clutter reflected from the non-moving parts in the human body and the room, and remove the random body movements [36]. In 2009, Chioukh compared between three radar systems operating at 5.8 GHz, 24 GHz and 35 GHz. The results show that the highest sensitivity detection can be achieved with the system at the highest frequency [37]. G. Sun proposed a screening method based on Amplitude Probability (AP) distribution analysis for detecting the disordered breathing [38]. Sun studied the amplitude distribution of the breathing signal that fall below a certain threshold level. In 2013, Kagawa proposed a noncontact screening system with two microwave radars for the diagnosis of sleep apnea-hypopnea syndrome. Kagawa used two inexpensive 24 GHz microwave Doppler devices [39].

Spectral analysis using Fourier transform was applied to detect the respiration and heart fundamental frequencies in [18] and [19]. In [40], an infant monitoring system was designed using CW radar which was able to monitor the infant breathing rate. As in [19], spectral analysis was performed for breathing rate estimation. In [20] [41], CW radar was used for assessment of heart rate variability (HRV) and respiratory sinus arrhythmia (RSA). The heart rate was estimated by searching for the local peaks of radar returns using the autocorrelation method.

Narayanan discriminated between the movements behind the wall of the human chest and the arm or the wrist using a Doppler radar system with Empirical Mode Decomposition (EMD) followed by the Hilbert spectrum. Other classification methods based on EMD are [42]. EMD has also been used to remove the noise and sensor motion artifacts before doing breathing and heartbeat estimation [43]. However, other methods have been used to process the signal after removing the artifacts. It was stated by the authors:"the EMD algorithm contains a number of heuristic and ad-hoc elements which makes it hard to guarantee its accuracy and limit its applicability".

1.2 Motivation and Problem Statement

This thesis is a part of a large project with the goal of detecting suicide events of inmates in prisons. The suicide events will be detected by estimating breathing rate and classifying the activities of the inmates. If it is detected that the person is stationary and that he or

she is not breathing then the alarm should be generated. A number of design choices and requirements were made prior to the start of the project and they were carried throughout the project. One of the choices were to select continuous wave radar operating at 24 GHz since the signal at this frequency will not be able to penetrate through concrete walls and therefore the radar will be able to monitor only a single person in a cell. In addition, this high frequency should provide enough resolution for estimating heart rate. Other choices that have been made are that the size of the room where experiments were performed is limited to the size of the prison cell and that only one person is monitored over time without any obstacles between the radar and the person.

The experiments and development of the algorithm as a part of this thesis were done in parallel with developing the CW radar by our industrial partner K&G Spectrum Inc., Gatineau, Quebec, Canada. A number of experiments were performed on intermediate versions of the radar and results from these experiments helped improving the radar and the overall system. However, this caused problem in evaluating some of the methods since different experiments were done with different versions of the radar.

As mentioned above, this thesis is a part of a larger project. The objective of this thesis was to characterize performance of the radar and breathing and heartbeat rate estimation algorithms in challenging real-life conditions. Majority of the research publications that deal with breathing and heart rate estimation consider situations when the person sits in front of the radar or deal with classifying the activities when the person is moving. The objective was to perform the experiments and provide initial breathing and heart rate estimation to show that current radar and these algorithms are capable of estimating breathing and heart rate. We evaluated the following scenarios:

- Characterizing breathing in case of interferences such as water movement in the same zone as the subject. To the best of our knowledge, the only published method of monitoring inmates for suicide detection involves the use of pulsed radars done by General Electric [24] [23]. Limitation of this study is that the effect of common interferences in correctional facilities were ignored.
- Characterizing breathing and heartbeat at different posture and orientations towards the radar. This is usually ignored in papers or only classification is performed without extracting breathing and heart rate.
- Detection of the zone where the subject is when the subject moves.

Classical approach in estimating breathing and heart rate is to perform discrete Fourier transform and to detect maximum peak in the frequency range of interest. The maximum peak in the range of breathing frequency should correspond to the breathing frequency. This naive approach has several problems especially in realistic situations such as when estimating breathing rate at different postured including:

- The multiple breathing frequency harmonics may have a magnitude higher than the magnitude of the first breathing frequency harmonic.

- Any human body part displacements while breathing will generate multiple frequency components. These frequencies overlap with the human breathing frequency range.

Therefore, we developed initial algorithm for estimating breathing and heart beat that relies on modifying the original DFT based approach, as well as we developed algorithms based on Empirical Mode Decomposition (EMD). EMD has been mainly used for classification of activities [44] [42] and removing noise [43]. Many Intrinsic Mode Functions (IMFs) will have a frequency spectrum in the range of the human breathing frequency range and it is difficult to decide which of these IMFs is related to the human breathing activity. In this thesis, an automated detection of IMF was adapted from other research areas and applied to specifying the IMF that corresponds to breathing.

1.3 Contributions

The major research contributions of this work are listed below:

- Modifying FFT and EMD based algorithms to detect more reliably heart and breathing rate. To the best of our knowledge, this is the first reported attempt to reliably determine breathing rate from radar signals in many different conditions including interference in the environment (with water flow, with fan on), different postures (sitting, standing, or lying down) and breathing conditions (normal breathing, holding breath, breathing with movement).

Other contributions include:

- Performing a large number of experiments in different real-life conditions.

The results of this thesis provided features and initial algorithms used by other team members for breathing and heartbeat rate estimation.

1.4 Thesis overview

This thesis is structured as follows.

Chapter 1 provides background information on the basic principles of radar model, motivation and problem statement, contribution, as well as applications. Also, contains the review of algorithms for estimating breathing rate and heartbeat rate using radar.

Chapter 2 introduce the experimental set up. In addition, it describes all the sensors used in the experiments including the radar system and the reference sensors: ECG and breathing belt.

Chapter 3 outlines two basic algorithms which are used for the analysis of the radar signals: Modified FFT, EMD with Minkowski distance. At the end of the chapter, the algorithm for estimating the distance (zone) between the subject and the radar while the subject is moving is presented.

Chapter 4 discusses the breathing and heart rate estimates of the two algorithms which are applied on data obtained while the subject is sitting in front of radar with normal breathing.

Chapter 5 compares the breathing and heart rate estimates of the two algorithms applied on the experimental data obtained while the subject is standing, sitting and lying down with normal breathing using two algorithms.

Chapter 6 compares the breathing and heart rate estimates of the two algorithms applied on the experimental data obtained while subject is facing the radar and when the subject is oriented sideways or backwards relative to the radar.

Chapter 7 discusses the results of estimating the distance while the subject is walking.

Chapter 8 provides the conclusions and future work.

Chapter 2

Experiments set-up, reference system and radar system

In this chapter, we will describe the Radar system, belt system, ECG sensors system and explain experiments in different environments.

2.1 CW Radar System

We use phase-modulated continous wave (CW) radar. Microwave doppler radar has gained popularity in wireless sensing applications, such as volume change sensing [25], life detection [26], and cardiopulmonary monitoring [27]. Recently, much interest has been paid to the topic of non-contact vital sign detection using a Doppler radar. The Doppler radar first captures and down converts the wireless signal that is phase modulated by the physiological movements, and then identifies the human heartbeat and respiration rates by processing the baseband signal. This wireless radar detection can help us to collect the bio-signals when subjects are walkIing, moving their hand, holding their breath and so on.

Using CW Radar to detect and process signal, its working frequency is generally: 450MHz, 1.8GHz, 2.4GHz, 5GHz, 24GHz, 27GHz. There is a trade-off while choosing different frequency bands: the higher transmission frequency, the higher detection sensitivity, but the detection distance and the penetration will decline. On the other side, lower emission frequency results in lower detection sensitivity, but the detection range and penetration improve.

This project studies the human respiratory signal detection and estimation at short distances up to 5 m. In the experiment there are no obstacles, which means the requirements for the penetration are relatively low. Also, bio-signals are weak signals, therefore the detection sensitivity needs to be high.

In our experiments, we used the SR4505 continuous wave (CW) radar produced by K&G Spectrum Inc., Gatineau, Quebec, Canada shown in Figure 2.1. The Radar is a mono-static millimetric wave radar in which the transmitter and the receiver antennas are at the same

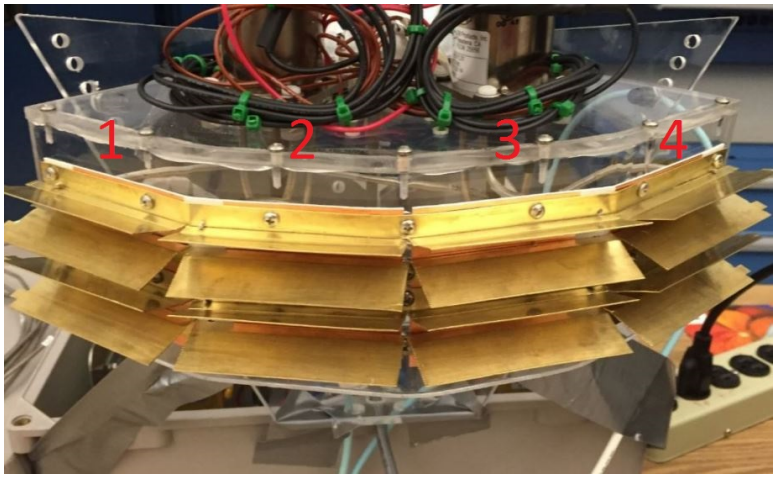

Figure 2.1: Radar System

location from the perspective of the target. The transmitter sends out a direct sequence spread-spectrum (DSSS) waveform which is a bi-phase shift keying (BPSK) modulated signal with a 24.125 GHz centre frequency. In order to measure the range, pseudo-random noise codes (PN codes) are used. PN codes generated from a code generator are used to trigger the pulse generator to shift each pulse actual transmission time. This is called a pulse position modulation (PPM) scheme. The parameters of the radar include: centre frequency: 24.125 GHz; frequency band: 500 MHz; transmitted power: 17 mW; and dynamic range: 120 dB.

During the course of the project the radar has been improved and changed. Several versions of the radar that we used include:

October 2014: Radar with noise level of +/- 20mV, single antenna, 20 x 3 degree antenna beamwidth or 90 x 5 degree antenna beamwidth was used. The zone size was 3 m. With this radar we were only able to focus on the person chest due to very narrow beamwidth of the antenna. In addition, narrow beamwidth provided the highest SNR which allowed for estimating accurate heart and breathing rate. A 10x7 area was cordoned off in room STE 3013 laboratory at the University of Ottawa. The Radar was placed at on a tripod of approximately 3 feet in height.

Dec 2015: Radar with Quad antenna (4 pair of antennas with 70 x 20 degree antenna beamwidth with coaxial switch) was used. Noise level was +/- 20mV. The zone size was reduced to 0.75 m. The goal of this version of the radar was to evaluate the antennas and the overall system for estimating breathing rate. The antennas was built and installed in a way to cover the whole room. Manual antenna switching was possible through K&G Spectrum software. The SNR decreased significantly in comparison to the radar from October 2014 by 27dB. The experiments were also done at the University of Ottawa.

May 2016: Radar with Quad antenna (4 antenna with 70 x 20 degree antenna beam width) with 1 electronic switch and one 4way power splitter was used. Noise level was improved to +/- 4mV. The SNR improved in comparison to the version from Dec 2015

by 10dB. The fact that there was an electronic switch allowed for possibility to automatically switch between the four antennas. However this was not attempted in this thesis. Significant improvements in processing speed and A/D conversion were achieved. The experiments were done at the Carleton University in a room that has size of about 3 m x 4 m.

Oct 2016: The switch was replaced with higher quality electronic switch. In comparison with the previous versions of the radar where only one pair of receiving and transmitting antennas were active, in this version of the radar all four antennas are always transmitting while there can be only one receiving antenna turning on. This made radar more sensitive to detecting person but also to picking up noise and the clutter. The experiments with that version of the radar were also performed at the Carleton University.

The radar shown in Figure 2.1 has four antennas (version from December 2015). Each antenna has 50 zones with 0.75 meter in one zone. The scan area is about 70 degrees in the vertical plane and about 20 degrees in the horizontal plane to make sure it can scan the whole room. Even though the versions of the radar from May and October 2016 supported high speed switching between the antennas, the software for providing the automated switching was not provided. Therefore, in all the experiments only one antenna pair was active except in the experiments done in October 2016 where four transmitting and one receiving antenna were active. Again in that case, the receiving antenna was not switched during the experiment.

There are two mode of collecting data from radar: dwell mode and scan mode. For dwell mode, there is only one zone which is selected to detect the bio-medical signals from human beings. For scan mode, we will turn on up to 50 zones to send and receive the bio-medical signals which means we can also detect in which zone the subject is.

The radar was usually set in the scanning mode where it collects one sample per zone starting from the predefined minimum zone and finishing at the predefined maximum zone. After that, the radar starts scanning again from the minimum zone. The sampling rate per zone is the sampling rate of the radar divided by the number of zones. For example, in the experiments done in May and October 2016, the zones are set between 4 and 12 (the size of the zone is 0.75 m) and the sampling rate was about 905 Hz per those nine zones.

2.2 Belt and ECG sensors System

In this project, we use the signals collected from belt as breathing reference signals and use the signals collected from ECG sensors as the heartbeat reference signals. What we used is the machine named BioRadio shown in Figure 2.2. The size of this device is about 10 by 15 centimeters and the device was attached to the waist of the subject. Data between the device and the computer was transferred by Bluetooth communication. The sampling rate of all the sensors is 256 H

In this project, we use the signals collected from belt as breathing reference signals and use the signals collected from ECG sensors as the heartbeat reference signals. The

device used was BioRadioTM from Great Lakes NeuroTechnologies, US, shown in Figure 2.2. The size of this device is about 10 by 15 centimeters and the device was attached to the waist of the subject. Data between the device and the computer was transferred by Bluetooth communication. The sampling rate of all the sensors is 256 Hz.

Figure 2.2: setup equipment of belt and ECG sensors

The number of the channels is eight. In this project, we use only two channels. Channel one is used to detect the heart beat signal; channel two is used to detect breathing signal.

For the heart beat signal detection, we can use three ECG electrode based on lead one configuration where one electrode is attached to the left arm, another to the right arm, and the ground electrode is connected to the leg.

The breathing belt was attached around the chest of the subject to detect the chest movement when the subject is breathing.

The Belt and ECG system is shown in Figure 2.2

2.3 Experiment setup

This research is on how to extract the breathing signal and the heartbeat signal from human beings signals while using continue wave Radar (CW Radar) in different situations, such as normal breathing, breathing with movement, holding breathing, breathing with fan, breathing with water and so on. The experiments were done in different places during winter 2014 to summer 2016. Ethics approvals are shown in the Appendix for the experiments done at the University of Ottawa and at Carleton University.

In all the experiments, the radar described above was used to acquire the signal. There was always only one subject in the environment where the experiments were done. The subject always wore referecence sensors: the breathing belt and ECG electrodes. The CW radar was always stationary and the subject was in front of the radar. The breathing belt was placed around the chest and is used to get the breathing signal from the subject's chest. ECG electrodes are placed in lead 1 configuration on the right and the left arm and the right leg and are used to extract the heart rate.

All the data is collected, tored and processed off-line. Processing was done in MATLAB. Results obtained after processing radar signal are compared against the breathing rate extracted from the breathing belt and heart rate extracted from the ECG signal. Mean absolute error is commonly reported as the performance metric.

The experiments were performed in the Labs at the University of Ottawa and Carleton University. The experiment set-up, the picture of the experiment and the overall goal of the experiment are described next:

1. The experiment performed in the research laboratory at the University of Ottawa. The purpose of this experiment was to extract the breathing and heart rate of a stationary subject when the radar points directly to the subject's chest. The radar from October 2014 (described in Section 2.1) was used. It had only one receiving and one transmitting antenna with 90 x 5 degree antenna beamwidth which means it can cover 5 degrees in the horizontal plane and 90 degrees in the vertical plane. The experimental set-up is shown in Figure 2.3. We can see the radar was placed on the desk facing to the door in the research laboratory. Since the radar had very narrow beam, the subject was placed at positions A, B or C always in front of the radar.

2. The experiment performed in the anechoic chamber at the University of Ottawa.

   Figure 2.4 shows the setup where the radar was placed on the paper pillar in the anechoic chamber at the University of Ottawa. The reason of placing the radar on the paper pillar is to make sure that the radar is as the same hight as the subject's chest. The radar is also implemented using only one receiving and one transmitting antenna. The beamwidth of the antenna is 70 x 20 degrees. The goal of this experiment is to determine the quality of the extracted breathing signal when more realistic antenna is used than in the previous experiment because the use of the antenna with the beamwidth of 70 x 20 degrees resulted in having the signal with much lower SNR as described in Section 2.1.

3. The experiment performed in the research laboratory at the University of Ottawa with the radar placed in the upper corner of the laboratory.

   The goal of this experiment was to evaluate the quality of the received signal when the radar is placed high to emulate placement an upper corner of the room. This placement of the radar would correspond to the realistic placement for the application of monitoring in-mates in prisons. Figure 2.5 shows the radar that is the same as the one in Figure 2.4. Because the hight of radar is no longer as the same hight as subject's chest, we have to calculate the distance and the angle. Because the radar

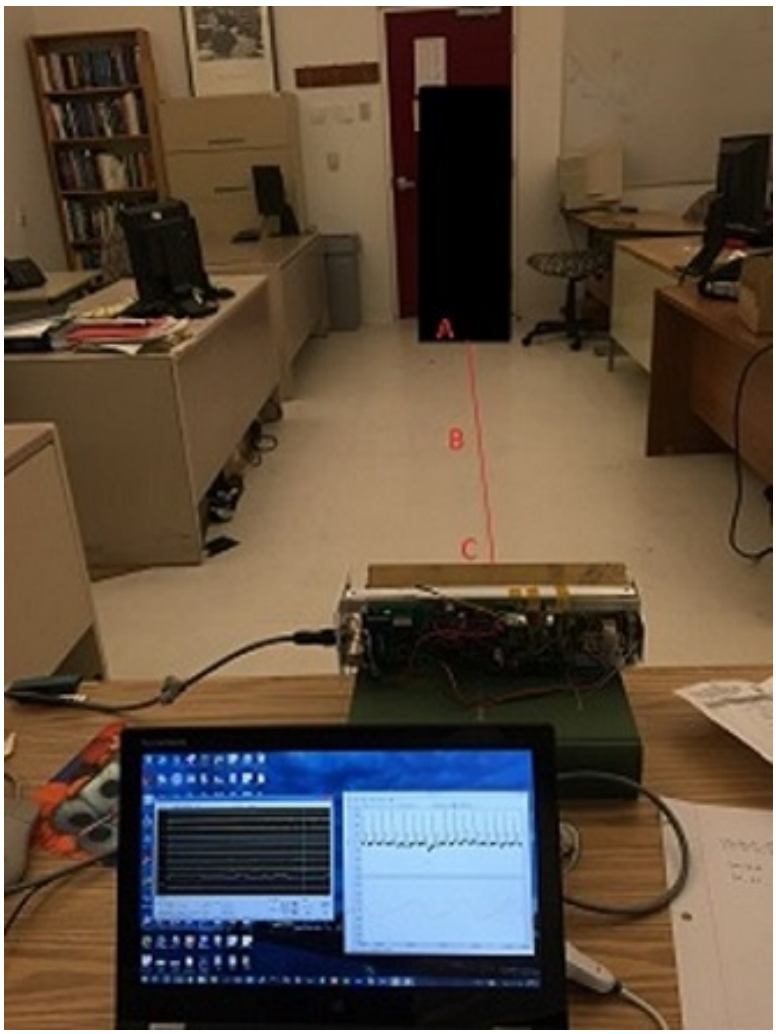

Figure 2.3: Experiment setup in the lab at the University of Ottawa

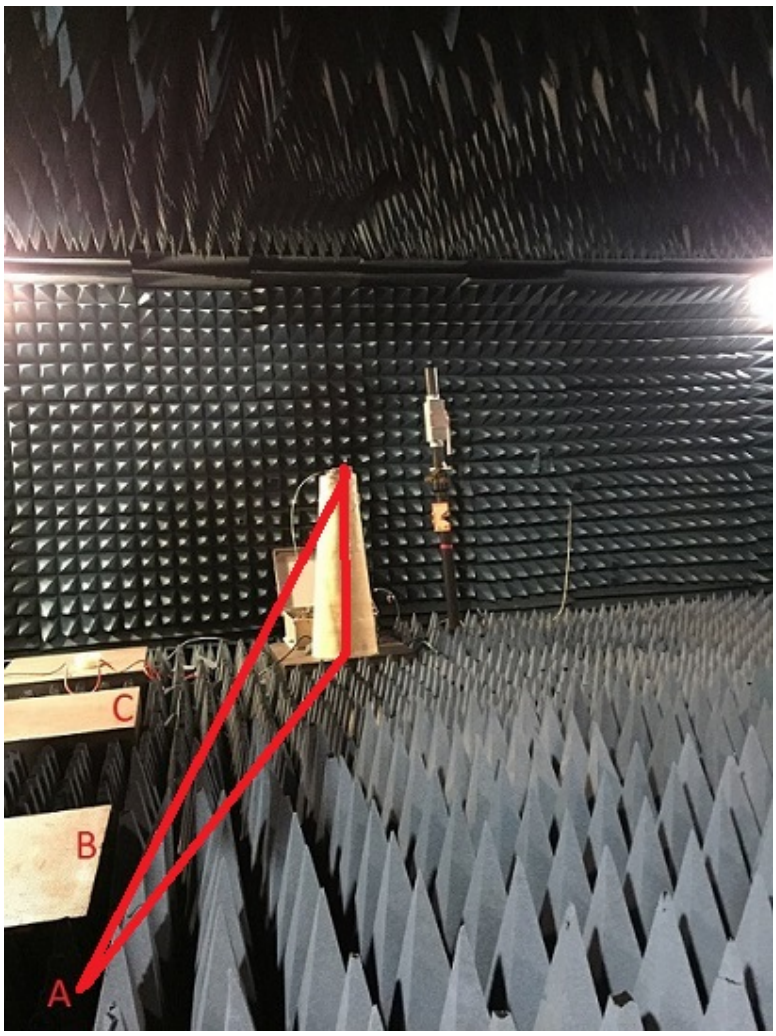

Figure 2.4: Experiment setup in the anechoic chamber at the University of Ottawa

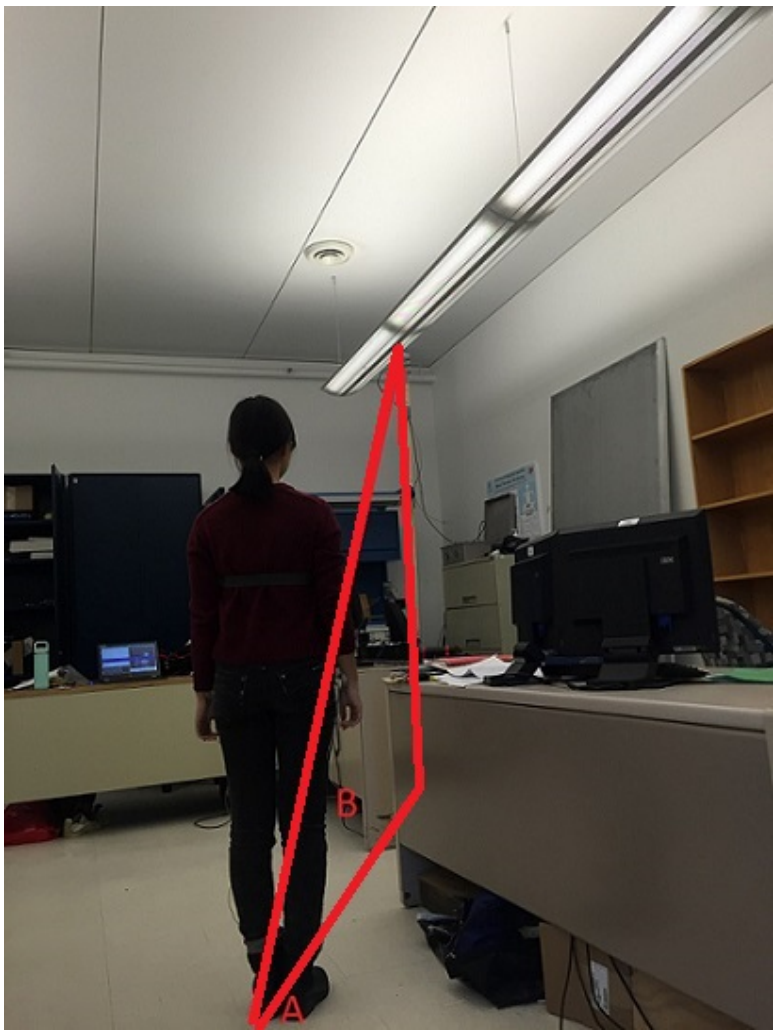

Figure 2.5: Experiment setup in the research lab at the University of Ottawa

is same as in Figure 2.4, there is still only one antenna with the beamwidth of 70 x 20 degrees.

4. The experiment performed in the research laboratory at Carleton University with the radar placed in the upper corner of the laboratory.

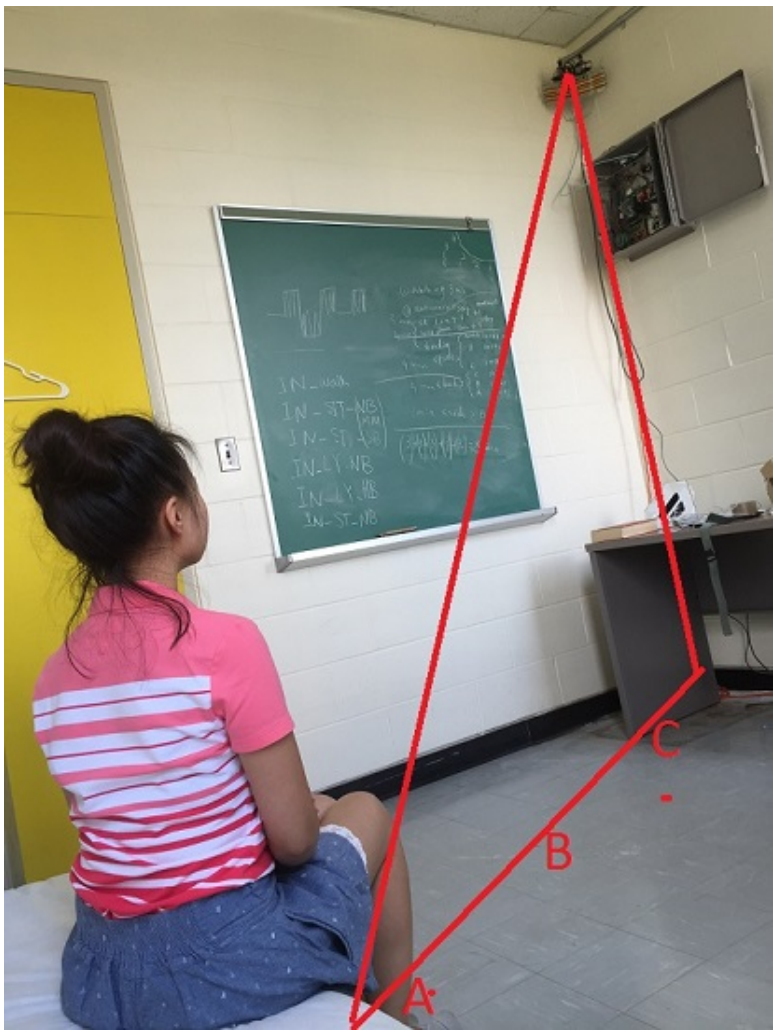

Figure 2.6: Mock-up prison cell at Carleton University

The goal of this experimental setup is to make a mock-up prison cell. The radar is placed in the upper corner in the room in the same way as it would be placed in the prison cell. The room is of similar dimensions as the prison cell and it has concrete walls, similar type of bed and the metal toilet that is obtained from Correctional Services Canada. Figure 2.6 shows the setup with the CW radar placed on the top right corner facing the room. This setup is used for the experiments performed with the versions of the radar from May and October 2016. The radar has four pairs of antennas. For majority of the experiments we use the antenna two, which is the second from the left. The beamwidth of each antenna is 70 x 20 degrees.

Chapter 3

Algorithms for processing the radar signal

In this chapter, we will discuss the algorithms that are applied to estimate breathing heartbeat rate.

3.1 The model of the radar signal

In this section, we will introduce a mathematical model of the received radar signal.

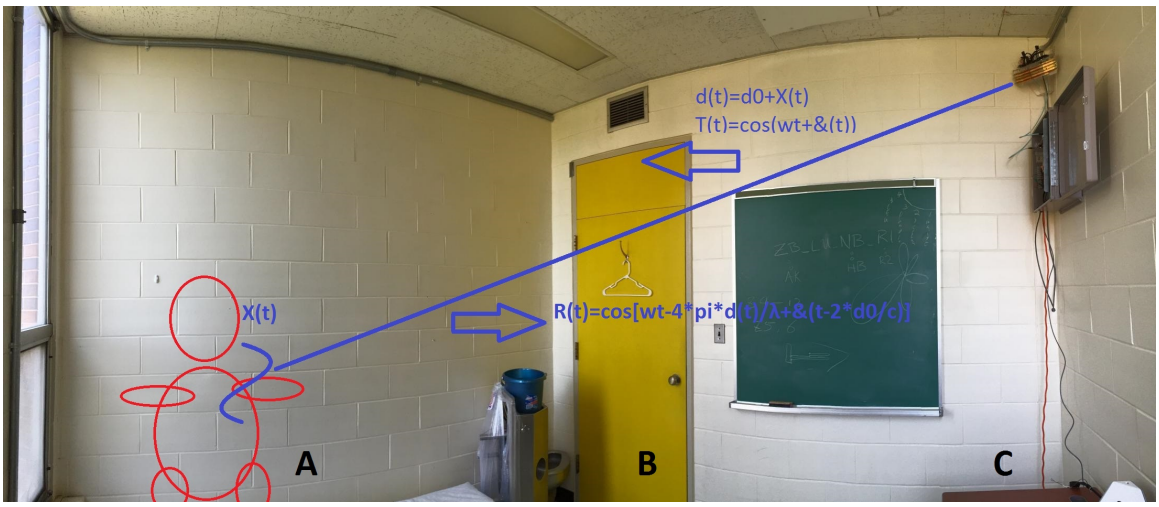

Figure 3.1: Radar System in empty room

Based on Doppler theory, any target that moves periodically reflects the transmitted signal with its phase modulated by the time varying position of the target [45].

One of our environmental setups of the non-contact Doppler radar used for the detection of vital signs is illustrated in Figure 3.1. A CW Radar is placed at the corner of the room. A radio-frequency continuous-wave quadrature signal T(t) is transmitted and reflected by the human body: [46].

$$T(t) = cos(\omega t + \phi t) \tag{3.1}$$

where ω=2πf denotes the angular frequency of the carrier, and ϕ(t) represents the time-varying phase noise of the transmitted signal.

The reflected signal from the subject's chest contains information about the chest displacement including movements due to heartbeat and respiration. From the theory of Fourier series, any time-varying periodic displacement x(t) can be viewed as the combination of a series of single-tone signals. Therefore, for the ease of analysis and without loss of generality, x(t) is assumed to be single tone,

$$x(t) = x_h(t) + x_r(t) = m_h sin(w_h t) + m_r sin(w_r t) \tag{3.2}$$

where x_r(t) and x_h(t) represent, respectively, the body movements caused by respiration and heartbeat, which in turn can be approximated as sinusoids with amplitudes m_h and m_r and frequencies w_h and w_r, respectively. The chest displacement variation caused by respiration is between 1mm and 12mm [47]. The chest displacement due to heartbeat alone ranges between 0.1mm and 0.5mm [48]. This displacement is the concern of this work. Moreover, at rest, the frequency that corresponds to the respiration rate varies between 0.1 Hz and 0.3 Hz, whereas the frequency that corresponds to the heartbeat rate changes between 1 Hz and 3 Hz.

Assuming that the subject is located at a nominal distance d_0. The total distance that the signal travels between the transmitter and receiver is 2d(t), where d(t)=d_0+x(t).

If the signal T(t) is reflected by the subject, then the received signal R(t) is approximated as:

$$R(t) = cos[\omega t - \frac{4\pi d_0}{\lambda} - \frac{4\pi x(t)}{\lambda} + \phi(t - \frac{2d_0}{c})] \tag{3.3}$$

where R(t) is the received signal at the radar, ω is the frequency of the radar system, c represents the signal propagation speed (i.e., the speed of light) and $\lambda = c/f$ is the wavelength.

The baseband signal B(t) after the down-conversion is approximated as: [46]

$$B(t) = cos[\frac{4\pi x_h(t)}{\lambda} + \frac{4\pi x_r(t)}{\lambda} + \Phi] \tag{3.4}$$

where Φ includes the phase noise as well as the component $\frac{4\pi d_0}{\lambda}$. By combining 3.4 and 3.2 we get:

$$B(t) = cos[\frac{4\pi m_h sin(w_h t)}{\lambda} + \frac{4\pi m_r sin(w_r t)}{\lambda} + \Phi] \tag{3.5}$$

This signal is non-linear. Having quadrature receiver would help us extracting just the phase of the signal which is then linearly related to the sinusoidal components of breathing and heartbeat. However, our radar has only one receiver input and therefore the receiver signal is similar to the signal $B(t)$ shown in 3.5. However, the signal appears to be sinusoidal if the components $\frac{4\pi m_h sin(w_h t)}{\lambda}$ and $\frac{4\pi m_r sin(w_r t)}{\lambda}$ are small and in these cases Fourier analysis is a reasonable approach. In case the displacement is relatively large, there will be a large number of spectral peaks in the frequency domain due to non-linearity of the signal. Even though we apply Fourier analysis in these cases as well, some other methods such as EMD might perform better.

3.2 Algorithm One: Modified FFT

In this section we explain our processing steps that rely of finding the maximum peak of the spectrum after applying discrete Fourier transform in the range of breathing and heartbeat frequencies. The discrete Fourier transform is implemented using Fast Fourier Transform (FFT). Windowing is applied before the Fourier transform resulting in much clearer peaks in the frequency spectrum. Different window functions are used to crop the signal in time domain and we found that the effects of different windows on the signal spectrum are not the same. The rectangular window has a narrow main lobe and large side lobes and has the highest accuracy of frequency identification and the lowest accuracy of amplitude identification; the Blackman window has wide main lobe, small side lobes and has the lowest accuracy of frequency identification and the highest accuracy of amplitude recognition. After trying the rectangle window, triangular window, Hamming window and Blackman window, we decided to use Hamming window and Blackman window. We show below examples of frequency spectrum after applying rectangular and Hamming windows.

- Rectangular Window

  "Each window is described by its functional form in the continuous time-domain, f(t), and its Continuous-time Fourier transform (CTFT), F(jω). In the following discussion, τ represents the one-sided duration of the window in the time-domain." [49] Figures 3.2 through Figure 3.5 present the plots of window functions in the time-domain and their CTFTs.

  The rectangular window, which is also called a uniform window or a box car window due to its shape, is defined as follows: [49]

$$f(t) = \begin{cases} 1 & \mid t \mid \leq \tau \\ 0 & \text{elsewhere} \end{cases} \tag{3.6}$$

and its CTFT is:

$$F(j\omega) = \frac{2\tau sin(\Omega\tau)}{\Omega\tau}, -\propto < \Omega < \propto \tag{3.7}$$

Therefore, the CTFT of a rectangular window function represents a sinc function. Plots of a rectangular window are given in Figure 3.2 [49]

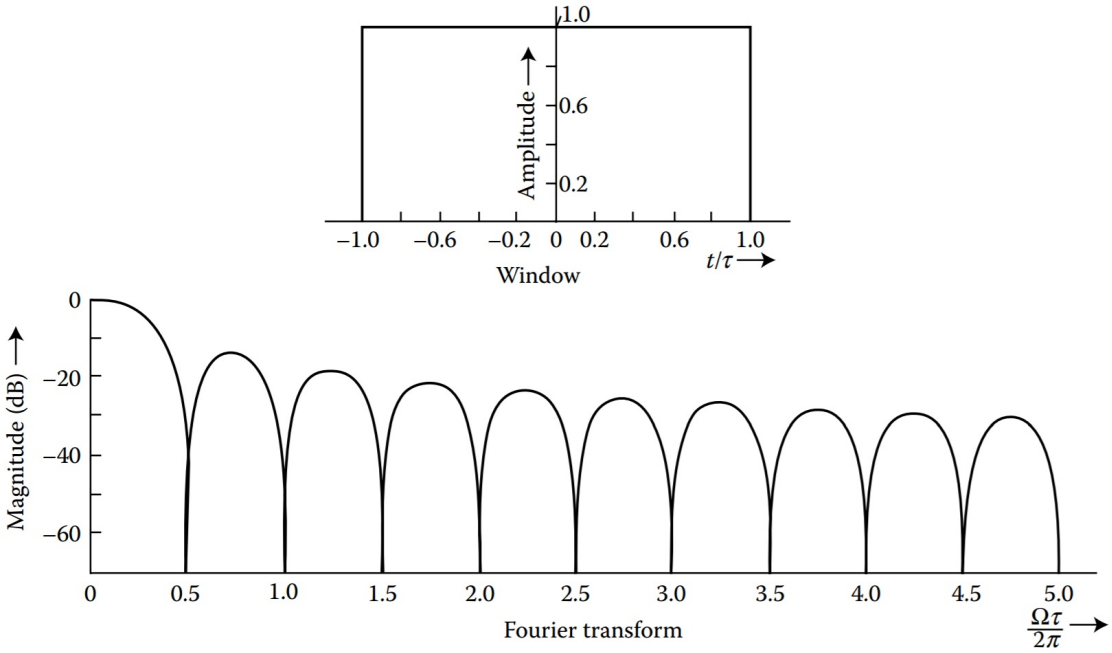

Figure 3.2: Rectangular Window

The normalized half main-lobe width (NHMLW) of the rectangular window is 0.5. The maximum side lobe level (MSLL) of this window, which is also the same as the first side-lobe level (FSLL), is about 13 dB [49]. Application of the window on radar signal shown in Figure 3.4. In this case, the subject is sitting in front of radar with normal breathing for 3 minutes. Figure 3.3 shows the radar signal in frequency domain and Figure 3.4 shows that the radar signal after applying rectangular window in frequency domain. We can find that the rectangular window helps in reducing noise.

- Hamming window

  This window can be thought of as an optimized form of the Hann window and was proposed by Hamming. The coefficients of this window are optimized so as to obtain the minimum FSLL. Its functional form is represented by [49]:

$$f(t) = \begin{cases} 0.54 + 0.46cos(\frac{\pi t}{\tau}) & \mid t \mid \leq \tau \\ 0 & \text{elsewhere} \end{cases} \tag{3.8}$$

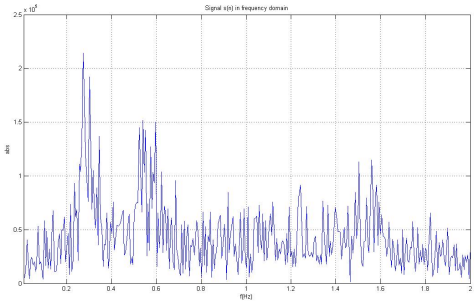

Figure 3.3: Radar signal in frequency domain

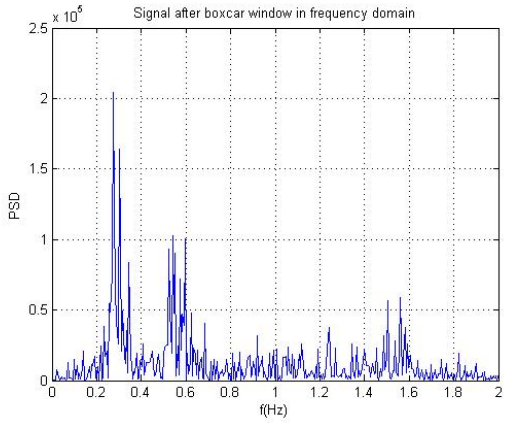

Figure 3.4: Radar signal after rectangular window in frequency domain

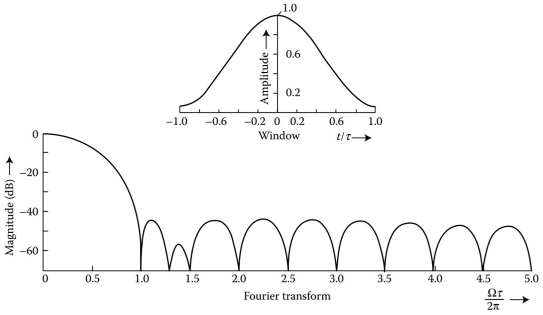

Figure 3.5: Hamming Window

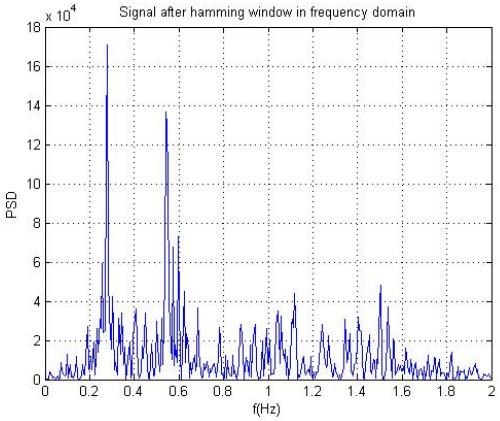

Figure 3.6: Radar signal after hamming window in frequency domain

whose Fourier transform can be written as follows: [49]

$$F(j\omega) = 1.08[\frac{sin(\Omega\tau)}{\Omega}] + 0.46[\frac{sin((\Omega + \frac{\pi}{\tau})\tau)}{\Omega + \frac{\pi}{\tau}} + \frac{sin((\Omega - \frac{\pi}{\tau})\tau)}{\Omega - \frac{\pi}{\tau}}], -\propto < \Omega < \propto \quad (3.9)$$

The time domain and Fourier domain plots are shown in Figure 3.5. From these plots, we can see that the maximum side lobe level (MSLL) is about 42 dB and the side lobes fall at the rate of $\frac{1}{\Omega}$. This slow fall-off rate is due to the small discontinuity (0.08) at the edges of the window. However, the first side lobe level (FSLL) of this window is about 44 dB [49].

After applying hamming window on radar signal with normal breathing, radar signal in frequency is shown in Figure 3.6.

Figure 3.3 shows the radar signal in frequency domain and Figure 3.6 shows that the radar signal after applying Hamming window in frequency domain. We can see

that the Hamming window helps in reducing noise. Comparing with Figure 3.4 and Figure 3.6, we can find that in this case for radar signal analysis, hamming window works better than rectangular window.

3.2.1 Steps of the modified FFT algorithm

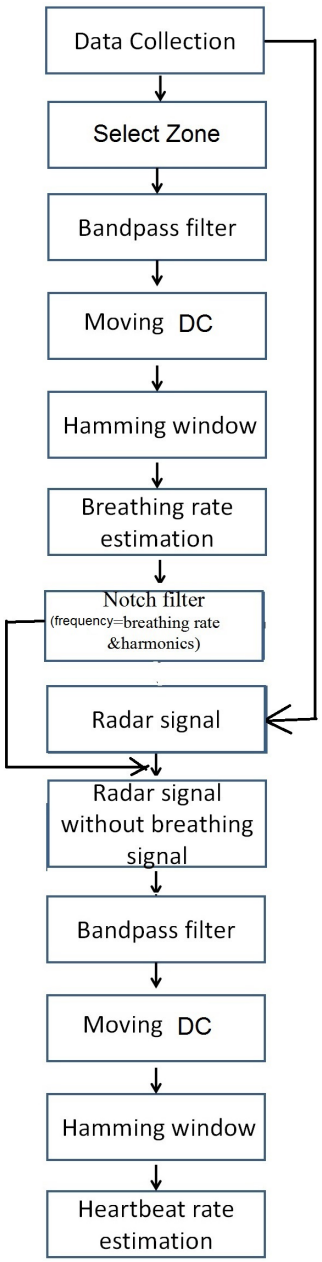

Figure 3.7: Algorithm one: Modified FFT

Figure 3.7 shows the basic steps of the algorithm including:

- Data collection: In this program data is processed off-line and it is entered from the file. The zone where the subject is is entered if known or it is estimated if it is not known in advance.
- Processing breathing signal
  - Bandpass filter: Applying IIR butterworth bandpass filter with the cut-off frequencies of 0.1 Hz and 2 Hz.
  - Removing DC component of the signal because sometimes signals have shift in time domain.
  - Hamming window: the window is applied on the whole input signal.
  - Breathing rate estimation: Applying FFT to present the filtered and windowed signal.

    After applying FFT, the frequency at which the magnitude of the spectrum is the largest is selected as the breathing frequency.
- Processing heartbeat signal
  - Notch filter is used to remove estimated breathing signal and its harmonics from original signal before the heart rate is estimated in the next steps.

    The reason why we have to remove breathing signal first to be able to extract heartbeat signal is because the ratio of the magnitude of breathing signal to the magnitude of heartbeat signal is very high. Therefore, we have to first remove breathing signal from the original signal, and then use the steps shown below to estimate heartbeat rate.
  - Bandpass filter IIR butterworth filter in the range of 0.8 to 2 Hz.
  - Hamming window is applied on the signal without breathing components.
  - Maximum of the spectrum (FFT) in the range of interest is used to estimate the heartbeat rate.

3.3 Algorithm Two: EMD with Minkowski distance

Empirical Mode Decomposition (EMD) is a method of signal decomposition that allows for separating the observed signal into a set of intrinsic mode functions (IMFs) and a residual function. Each IMF represents an oscillatory mode with one instantaneous frequency.

An IMF is a function that must satisfy two basic conditions [50]:

- The number of extrema and the number of zero crossings must be either equal or different by no more than one in the entire data set.
- The mean value of the envelope defined by the local maximums and the envelope defined by local minima is zero. Thus, an IMF represents a simple oscillatory mode embedded in the signal.

EMD algorithm is composed of the following step in order to obtain a set of IMFs: [50]

- Identify the extrema (local maximum and minimum).
- Interpolate the local extrema using cubic spline to obtain the upper and the lower envelopes.
- Calculate the local mean value of upper and lower envelopes
- Subtract $m_1(t)$ from original signal obtaining the first component

$$h_1(t) = x(t) - m_1(t) \tag{3.10}$$

- Examine if $h_1(t)$ satisfies the two basic requirements as described above to be an IMF.
- If not, the sifting process is repeated treating $h_1(t)$ as a new original signal.

The process continue until $h_1(t)$ is an IMF designated as $C_1(t)$. So we obtain the residue by the formula:

$$r_1(t) = x(t) - C_1(t) \tag{3.11}$$

The sifting process continues using $r_1(t)$ as our new signal and applies the steps described above. At the end of the algorithm, we obtain a set of IMFs and a residue. The first IMF contains the highest frequency oscillation that exists in the signal. Then, each IMF contains lower frequency of oscillations than the one extracted just before. Finally, the original signal may be written as:

$$x(t) = \sum_{i=1}^{n} C_{\mathrm{i}}(t) + r_{\mathrm{n}}(t) \tag{3.12}$$

3.3.1 Minkowski distance

The Minkowski distance is a metric in a normed vector space which can be considered as a generalization of both the Euclidean distance and the Manhattan distance. In this thesis, the Minkowski Distance (d_{mink}) computes the Euclidian distance between two vectors X and Y and is defined as: (from chapter 2.3.6 in [51])

$$d_{\mathrm{mink}} = (\sum_{i=1}^{n} \mid x_{\mathrm{i}} - y_{\mathrm{i}} \mid^2)^{1/2} \tag{3.13}$$

Where x_i and y_i are the i^{th} respective samples of the observed Radar signal and the extracted IMF.

The redundant IMFs have shape and frequency content different than those of the original signal. So the value of d_{mink} will be minimal when the distance between the original signal and the IMF is minimum. When IMFs is not appropriate, the value of d_{mink} present a maximum value.

3.3.2 Steps of the EMD with Minkowski distance algorithm

Figure 3.8 shows main steps of the algorithm. These steps are further explained below:

- Data collection: In this program data is processed off-line and it is entered from the file. The zone where the subject is is entered if known or it is estimated if it is not known in advance.
- Processing breathing signal
  - EMD: The algorithm that was discussed in Section 3.3.
  - Hamming window: We apply Hamming window on each IMF before applying FFT.
  - Apply FFT and find maximum peak of each IMF. This maximum peak corresponds to the estimated rate of each IMF.
  - Minkowski distance: Using Minkowski distance we find the right IMF of breathing signal. Then, the rate of that IMF is the estimated breathing rate of the radar signal.
- Processing heartbeat signal
  - Notch filter is applied to remove estimated breathing rate and its harmonics from original signal.
  - EMD: applying EMD on the signal with removed breathing components to get new IMFs.
  - Hamming window
  - Apply FFT and find the frequency of the maximum peak of the spectrum which represents estimated rate of IMFs.
  - Minkowski distance: using Minkowski distance select the right IMF. The rate of that IMF is the estimate of the heart rate.

3.4 Algorithm for walking position detection

In this section, our goal is to detect the position of a subject that moves relative to the radar. The idea is that the zone where the subject is will have the largest energy. As explained before, the radar scans pre-defined number of zones where each zone is 0.75 m.

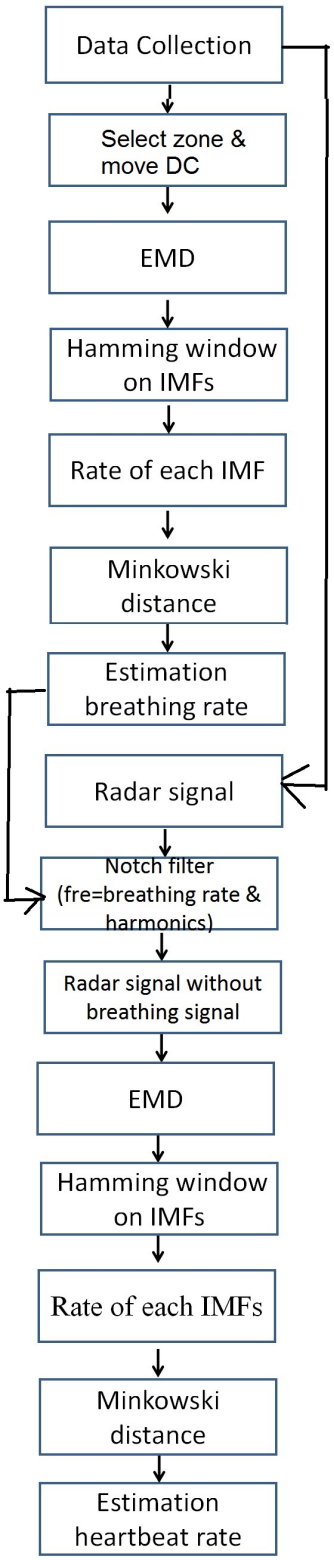

Figure 3.8: Algorithm Two: EMD with Minkowski distance

The subject is first walking towards the radar and then away from the radar, as shown in Figure 2.3. From the algorithm shown in Figure 3.9, we can see that after collecting the data, we will select one zone (assume that zone number i is from 1 to n) and divide data into 5 second segments (assume total segment number is j); apply filters and window on each segment; calculate energy of each segment E(i,j). Finally, finding the maximal energy E(:,j) of each segment j gives us the zone where the subject is. Results are shown in Chapter 7.

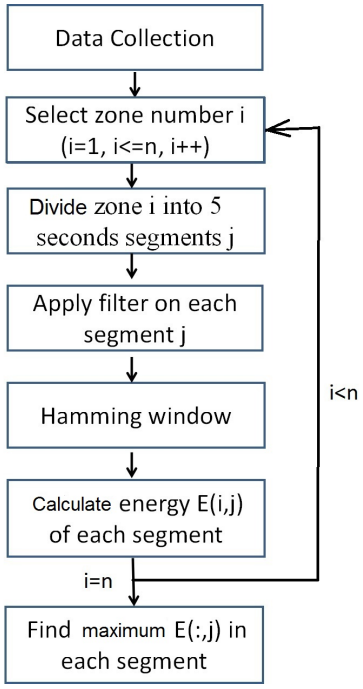

Figure 3.9: Algorithm Three: Algorithm for walking detection

Figure 3.9 shows the steps for algorithm that are also explained below:

- Data collection: Using radar system for data collection.
- Select zone: n is the total number of the zones. Here in a loop we calculate energy of the signal in each zone.
- The signal is divided in 5 second segments.
- Applying filter to remove DC component in each segment.
- Hamming window: Applying Hamming window on each segment.
- Calculate energy: Energy E(i,j) represents the energy of the signal during five seconds for zone i and segment number j.
- Repeat the loop to fine all energy components E(i,j).

- Find max energy in each time segment: maximum energy represents the right zone where the subject is.

Chapter 4

Breathing and heart rate estimation of stationary subjects using modified FFT and EMD

The goal of this chapter is to estimate the heart and breathing rate when the subject is not moving and is oriented towards the radar. Two algorithms were compared: modified FFT algorithm and EMD with Minkowski distance.

The experiments set up in lab at Carleton University are shown in Figure 2.6. These experiments allow us to detect bio-signals when the subject is breathing normally in a room that corresponds to a "prison cell". The radar was placed on the wall in the corner of the room, facing the center of the room at an angle. There are three marks on the floor: mark A, B and C. The distance to the radar from points A, B and C are 4.7 meters, 3.2 meters and 2.5 meters, respectively.

The experiments were conducted on October 21st, Nov 3rd, and Nov 17th, 2016. In these experiments, subjects sit down at mark A shown in Figure 2.6 for normal breathing experiments. The radar has a beamwidth of 20 degrees in the horizontal plane and 70 degrees in the vertical plane.

The reference signals are described in Section 4.1. The results from the radar signals are shown in Section 4.2. The comparison of all the estimate breathing rates and heartbeat rates, as well as their respective reference breathing rates and heartbeat rates are shown in Section 4.3.

We will first show the signals from the radar and reference sensors in both time and frequency domain before and after processing for one subject and for a window of 30 seconds. The purpose of this section is to show what the signals look like and what estimates can be obtained from 30 second samples of these relatively clean signals. At the end of this chapter, we compared estimates from the radar signal against the values estimated from the reference signals for 3 subjects and for 3 minute signals.

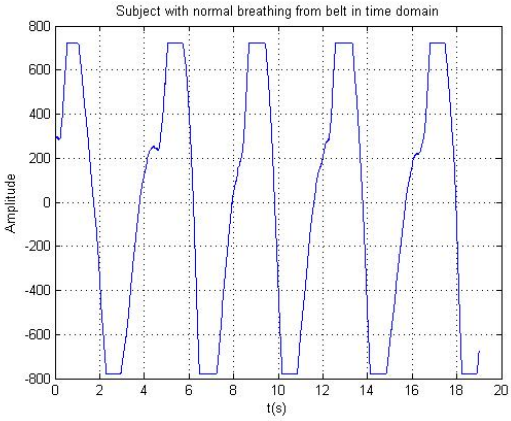

Figure 4.1: Breathing signal from the belt sensor from the subject with normal breathing

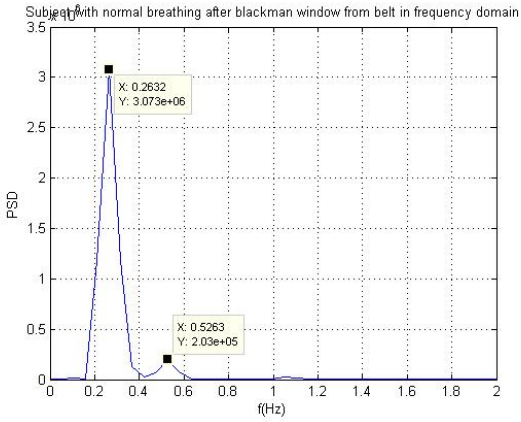

Figure 4.2: Breathing signal from the belt sensor in frequency domain after applying Blackman window from the subject with normal breathing

4.1 Reference signals from belt and ECG

The data in time-domain collected from the belt and ECG sensors is shown in figures 4.1 and 4.3 for the duration of 18 seconds.

After applying FFT on the reference breathing signal, we can find the maximum of the spectrum that corresponds to the fundamental breathing rate. The reference breathing rate is approximately 0.2632 Hz, as shown in Figure 4.2.

After applying FFT on the reference heartbeat signal, we can calculate the reference heartbeat rate to be approximately 1.421 per second, as shown in Figure 4.4.

After finding the reference breathing rate and reference heartbeat rate, we will estimate the breathing rate and heartbeat rate from the radar system. Then, we compare them to find the error between the estimated and the reference values.

The results are shown in Section 4.2, while the findings are explained in Section4.3.

4.2 Breathing and heart rate estimated from the radar signal

4.2.1 Breathing Rate estimation using modified FFT

This section is about breathing rate estimation using modified FFT for the subject with normal breathing when the subject is sitting.

The 30 seconds data in Figure 4.5 is from zone 8 and is collected from the radar system when the subject is sitting and breathing normally. After using modified FFT, we can find

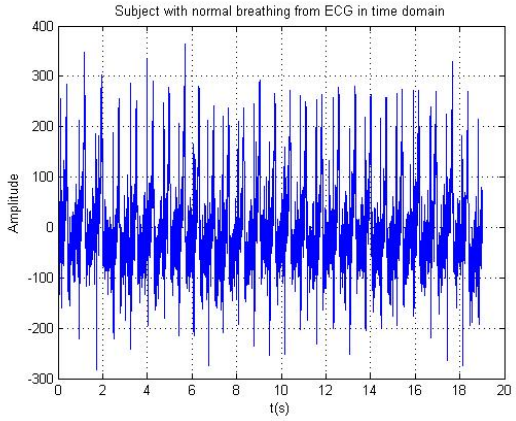

Figure 4.3: ECG signal from the subject with normal breathing

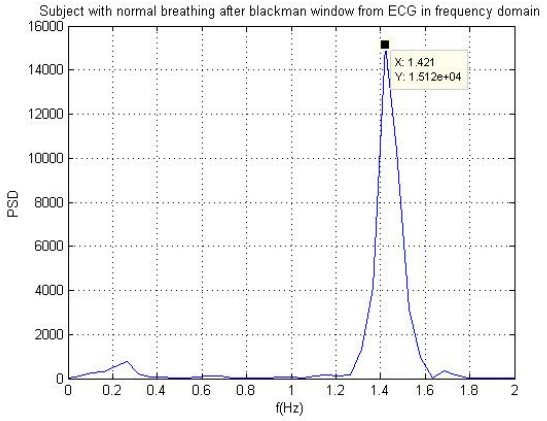

Figure 4.4: ECG signal from the subject with normal breathing in frequency domain after applying Blackman window

that the estimated breathing rate is about 0.2414 Hz, as shown in Figure 4.6. Comparing it with the reference breathing rate from the belt which is 0.2632, we can calculate that the error is 0.0218 per second, which is 8.28% off from the reference breathing rate.

4.2.2 Breathing Rate estimation using EMD

The same 30 seconds of data as in Section 4.2.1 is shown in Figure 4.5 and is processed using the EMD method. We extract thirteen (13) IMFs shown in Figure 4.7.

The next step of the algorithm includes applying FFT and finding the frequency that corresponds to the highest peak of the spectrum of each IMF. The obtained estimates in Hz for all 13 IMFs are:

breathing_rate_of_imf 1 = [393.4705];

breathing_rate_of_imf 2 = [121.0997];

breathing_rate_of_imf 3 = [121.0997];

breathing_rate_of_imf 4 = [30.2749] ;

breathing_rate_of_imf 5 = [30.2749];

breathing_rate_of_imf 6 = [6.8619] ;

breathing_rate_of_imf 7 = [1.5862] ;

breathing_rate_of_imf 8 = [1.1034];

breathing_rate_of_imf 9 = [0.2759];

breathing_rate_of_imf 10 = [0.1724] ;

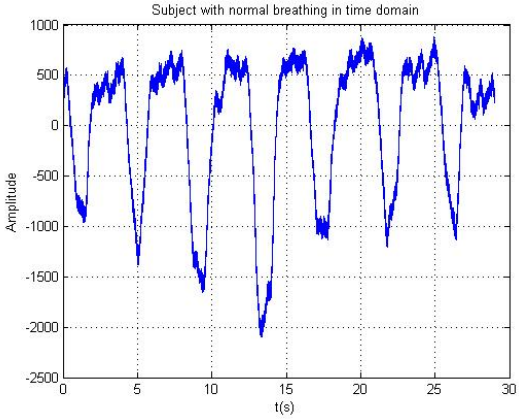

Figure 4.5: Breathing signal from the radar sensor from the subject with normal breathing

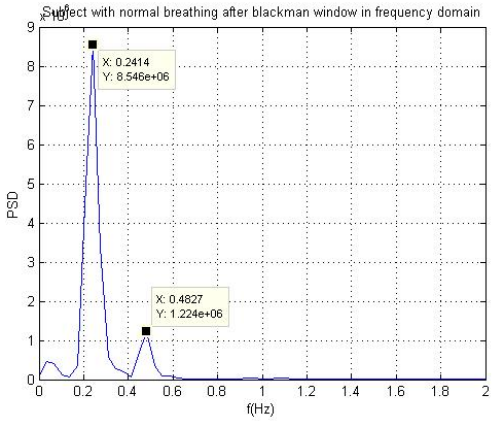

Figure 4.6: Breathing signal from the radar in frequency domain after applying Blackman window from the subject with normal breathing

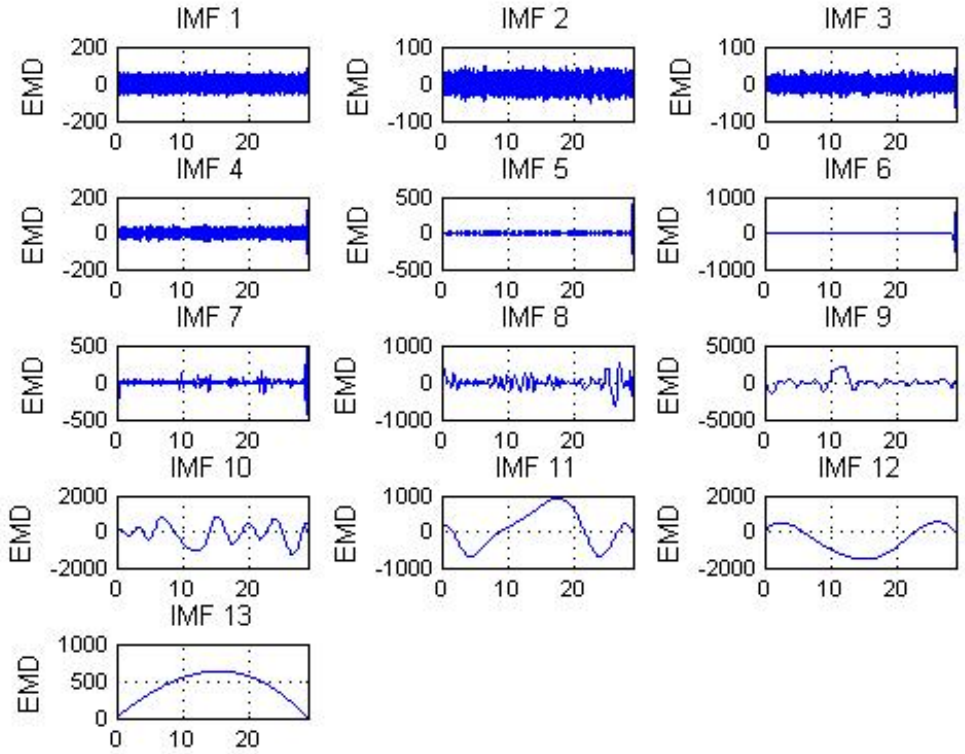

Figure 4.7: IMFs of the breathing signal from the radar with the subject breathing normally

breathing_rate_of_imf 11 = [0.0690];

breathing_rate_of_imf 12 = [0.0690] ;

breathing_rate_of_imf 13 = [0.0345];

To determine which IMF corresponds to our breathing signal, we use the Minkowski distance which was explained in Chapter 3.3.1. The results obtained after applying the Minkowski distance on each IMF are shown in Figure 4.8. The minimum corresponds to IMF 9 and therefore the estimated breathing rate is equal to the estimated rate of IMF 9 which is 0.2759 Hz. Comparing this value with the reference breathing rate 0.2632 Hz from the belt, we find the error to be 0.0127 Hz, which is 4.82% off from the reference breathing rate in this case.

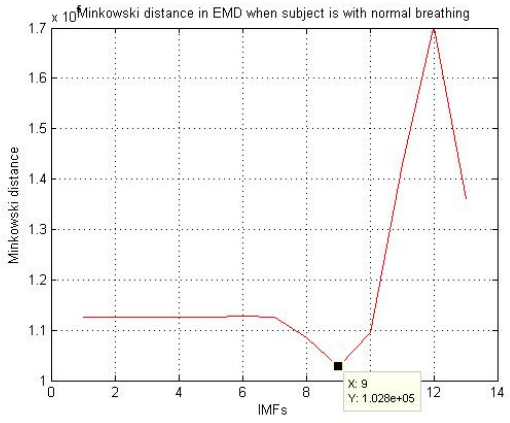

Figure 4.8: Minkowski distance for the IMFs shown in Figure 4.7

Obtained results in Section 4.2.1 and Section 4.2.2 show us that both modified FFT and EMD provide good results in this 30 second segment.

4.2.3 Heart rate estimation using Modified FFT

This subsection deals with the estimation of the heart rate from the radar system using modified FFT with the same 30 second data. After applying the breathing estimation algorithm, we estimated the breathing rate from the radar system to be 0.2414 Hz. Because the energy of the breathing signal is much higher than the energy of heartbeat signal, it is necessary to remove the breathing signal from the collected radar signal so that we can estimate the heart rate more accurately.

In this case, we used a notch filter to remove the estimated breathing signal at 0.2414 Hz in the frequency domain together with its second, third, fourth and fifth harmonics. The

reason for removing them from the breathing signal is that some of these harmonics might appear in the range of frequencies of the heart rate and it is possible that the energy of the breathing signal's harmonics are still larger than the energy of the heartbeat signal. The comparison of the radar signal before and after removing the breathing signal is shown in Figure 4.9. From Figure 4.9, we can clearly see that the power of the radar signal changes significantly. After removing the estimated breathing signal, the radar's signal power reduces.

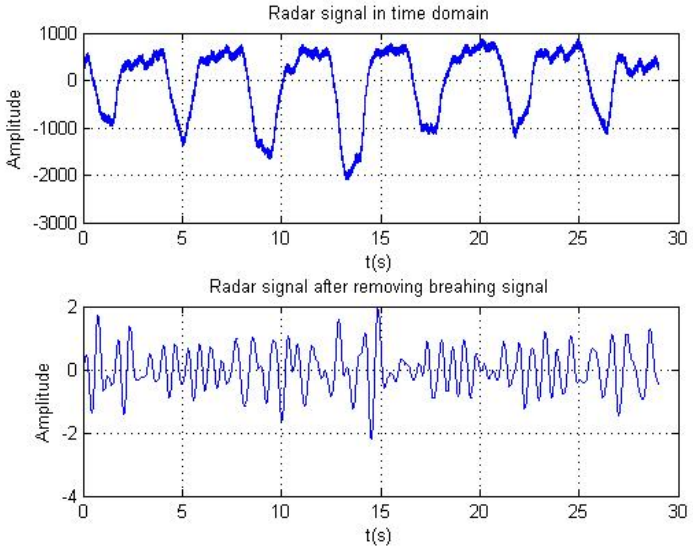

Figure 4.9: The comparison of the original radar signal before and after removing the breathing signal

The use of modified FFT to estimate the heart rate is shown in Figure 4.10.

From Figure 4.10, we can gather that the estimated heartbeat rate is about 1.552 Hz. Comparing it with the reference heart rate of 1.421 which we get from ECG sensors, the error is 0.131 Hz, which is 9.22% off from the reference heart rate.

Also from Figure 4.10, we note that there are two peaks at x= 0.931 Hz and x = 1.552 Hz. One possible reason for the peak at 0.931 Hz is the intermodulation product between the breathing and heartbeat signals. The peak 0.931 Hz is very close to the frequency that corresponds to (heart rate - 2 x breathing rate).

4.2.4 Heart rate estimation with using EMD

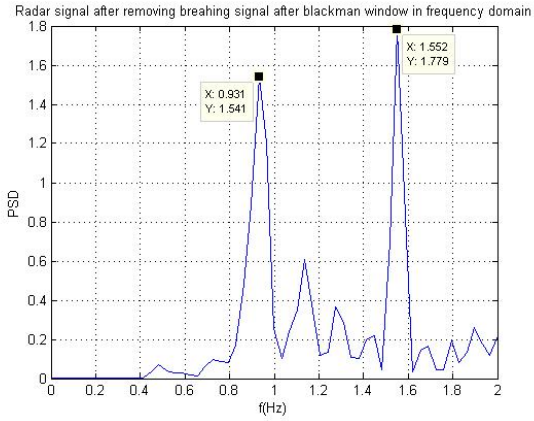

Figure 4.10: Heart rate of Subject D with normal breathing after applying Blackman window and notch filter in the frequency domain

This subsection deals with the estimation of the heart rate from the radar system using EMD with the same 30 sec data.

After applying the EMD method on the radar signal without the breathing signal, we can estimate the heart rate. In this case, we find that there are eight IMFs shown in Figure 4.11.

After applying FFT on each IMF and finding the frequency that corresponds to the maximum peak we obtain the following rates for each IMF:

Heartbeat_rate_of_imf 1 = [1.5862];

Heartbeat_rate_of_imf 2 = [0.8965];

Heartbeat_rate_of_imf 3 = [0.3448];

Heartbeat_rate_of_imf 4 = [0.2069];

Heartbeat_rate_of_imf 5 = [0.0690];

Heartbeat_rate_of_imf 6 = [0.1034];

Heartbeat_rate_of_imf 7 = [0.0690];

Heartbeat_rate_of_imf 7 = [0.0345];

To figure out which IMF is our estimate heartbeat signal, we use the Minkowski distance as it is explained in Chapter 3.3.1. After applying the Minkowski distance on each IMF, we get the results shown in Figure 4.12. We see that the minimum of Minkowski distance is IMF 1, which allow us to estimate the heart rate to be 1.5862 Hz. Comparing with the reference heartbeat rate 1.421 which we get from ECG, the error margin is 0.1652, which is 11.62% off from the reference heartbeat rate.

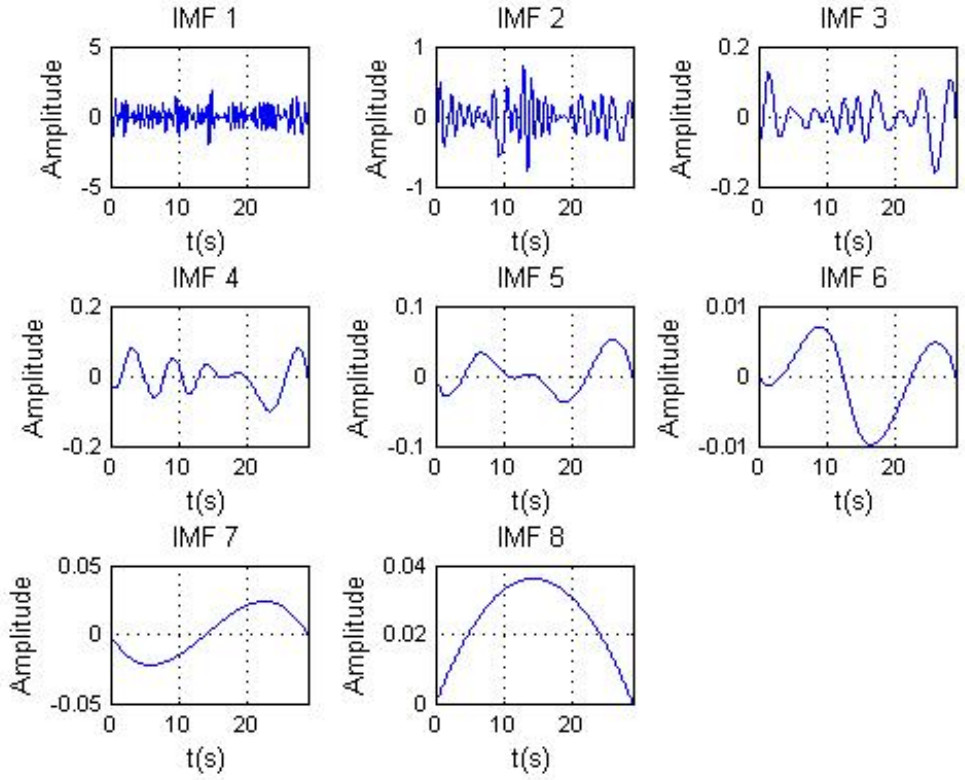

Figure 4.11: IMFs of radar signal after removing breathing signal when subject is sitting while breathing normally

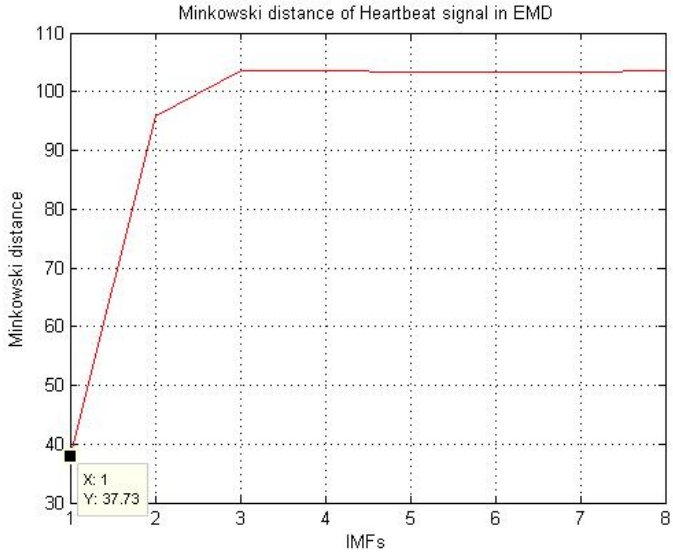

Figure 4.12: Minkowski distance for the IMFs shown in Figure 4.11

Section 4.2.1 to Section 4.2.4 covers one segment, which represents 30 seconds. In total, we have 18 segments of data, each spanning 30 seconds. The results and comparisons of these 18 segments are shown in Section 4.3.

4.3 Discussion

In Section 4.2.1 to Section 4.2.4 above, one segment of 30 seconds worth of data was analysed. In order to better show the result, in this subsection we present results of the same experiment for three subjects sitting with breathing normally. The data is collected from the radar and reference sensors for three minutes for each subject. This means we have six 30 second segments for one subject and a total of 18 segments for this experiment.

In this section, we will analyse the difference between breathing rate estimation and heartbeat rate estimation using modified FFT and EMD. The comparison of modified FFT and EMD with the reference belt signals are shown in Figure 4.13, Figure 4.14, and Figure 4.15. The detailed results and statistics of the estimates of all the 18 segments are compared in Figures 4.16, Figures 4.17, and Figures 4.18.

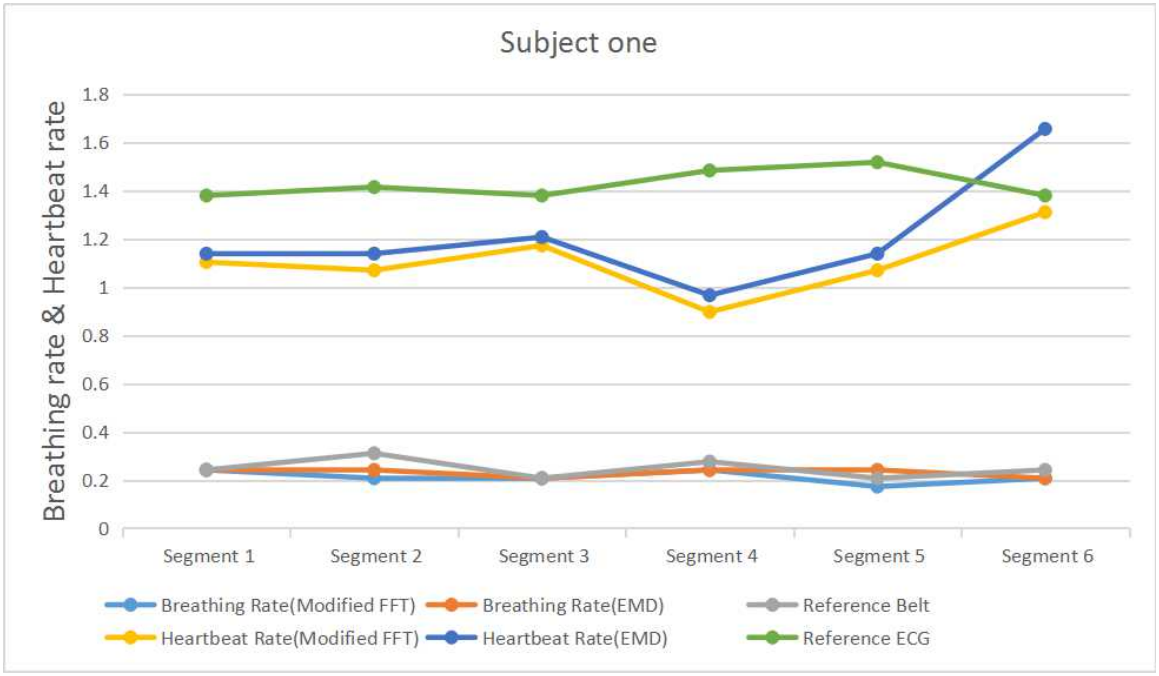

Figure 4.13: Comparison of breathing and heart rate estimation using modified FFT and EMD with reference belt and ECG signals of subject 1

Table 4.16 shows four results: one is the estimated breathing rate from the modified FFT, a second is the estimated breathing rate from the ECG, a third is the estimated heartbeat rate from the modified FFT, and a fourth is the estimated heartbeat rate from the ECG. The estimated breathing rate and heartbeat rate must be compared with the

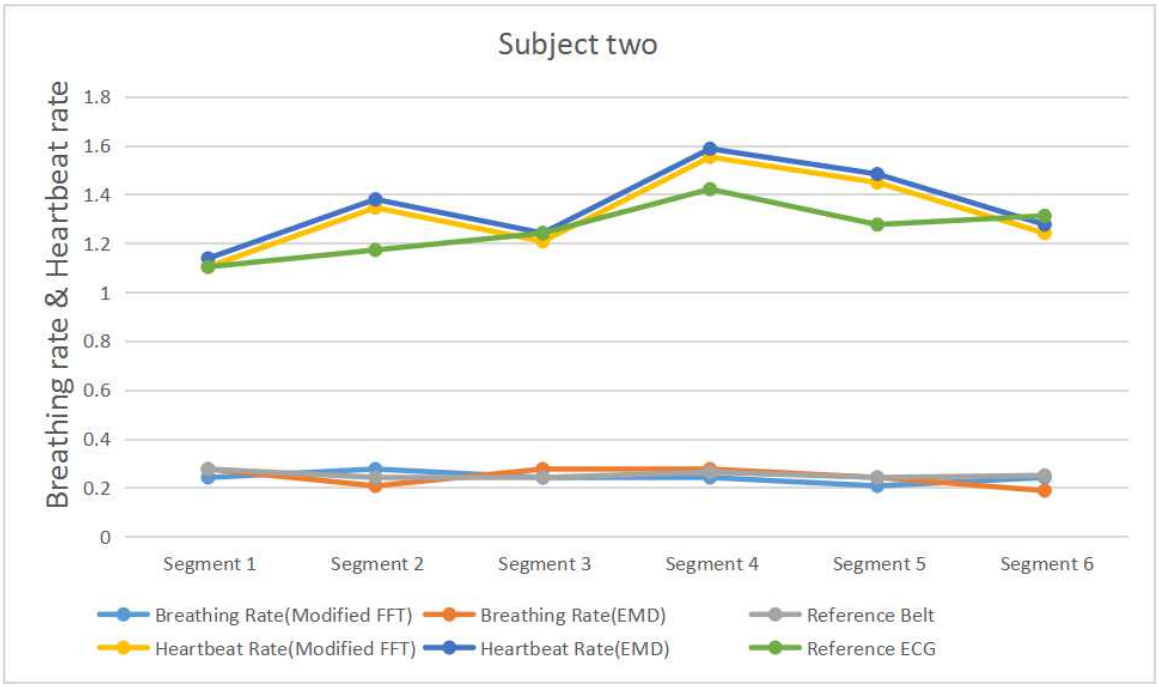

Figure 4.14: Comparison of breathing and heart rate estimation using modified FFT and EMD with reference belt and ECG signals of subject 2

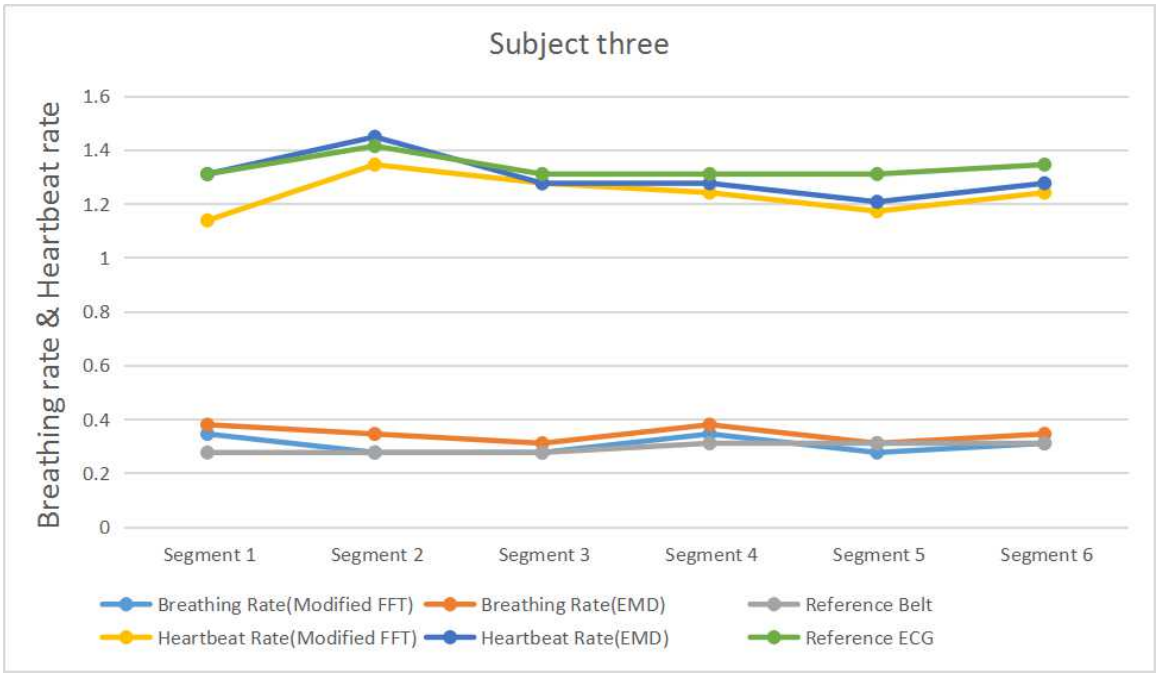

Figure 4.15: Comparison of breathing and heart rate estimation using modified FFT and EMD with reference belt and ECG signals of subject 3

Sitting with Normal breathing		Breathing rate		Heartbeat rate	
		Radar	Belt	Radar	ECG
Segment 1 with normal breathing	**Modified FFT**	0.2414	0.2414	1.103	1.379
	Error	0		0.276	
	Percentage	0.00%		20.01%	
	EMD	0.2414	0.2414	1.1379	1.379
	Error	0		0.2411	
	Percentage	0.00%		17.48%	
Segment 2 with normal breathing	**Modified FFT**	0.2069	0.3103	1.069	1.414
	Error	0.1034		0.345	
	Percentage	33.32%		24.39%	
	EMD	0.2414	0.3103	1.1379	1.414
	Error	0.0689		0.2761	
	Percentage	22.20%		19.52%	
Segment 3 with normal breathing	**Modified FFT**	0.2069	0.2069	1.172	1.379
	Error	0		0.207	
	Percentage	0.00%		15.01%	
	EMD	0.2069	0.2069	1.2069	1.379
	Error	0		0.1721	
	Percentage	0.00%		12.48%	
Segment 4 with normal breathing	**Modified FFT**	0.2414	0.2759	0.8965	1.483
	Error	0.0345		0.5865	
	Percentage	12.50%		39.54%	
	EMD	0.2414	0.2759	0.9655	1.483
	Error	0.0345		0.5175	
	Percentage	12.50%		34.90%	
Segment 5 with normal breathing	**Modified FFT**	0.1724	0.2069	1.069	1.517
	Error	0.0345		0.448	
	Percentage	16.67%		29.53%	
	EMD	0.2414	0.2069	1.1379	1.517
	Error	0.0345		0.3791	
	Percentage	16.67%		24.99%	
Segment 6 with normal breathing	**Modified FFT**	0.2069	0.2414	1.31	1.379
	Error	0.0345		0.069	
	Percentage	14.29%		5.00%	
	EMD	0.2069	0.2414	1.6551	1.379
	Error	0.0345		0.2761	
	Percentage	14.29%		20.02%	
Segment 7 with normal breathing	**Modified FFT**	0.2414	0.2759	1.103	1.103
	Error	0.0345		0	
	Percentage	12.50%		0.00%	
	EMD	0.2759	0.2759	1.1379	1.103
	Error	0		0.0349	
	Percentage	0.00%		3.16%	
Segment 8 with normal breathing	**Modified FFT**	0.2759	0.2414	1.345	1.172
	Error	0.0345		0.173	
	Percentage	14.29%		14.76%	
	EMD	0.2069	0.2414	1.3793	1.172
	Error	0.0345		0.2073	
	Percentage	14.29%		17.68%	

Figure 4.16: Comparison of breathing and heart rate estimation using modified FFT and EMD with reference belt and ECG signals

Segment 9 with normal breathing	**Modified FFT**	**0.2414**	**0.2414**	**1.207**	**1.241**
	Error	**0**		**0.034**	
	Percentage	**0.00%**		**2.74%**	
	EMD	**0.2759**	**0.2414**	**1.2413**	**1.241**
	Error	**0.0345**		**0.0003**	
	Percentage	**14.29%**		**0.02%**	
Segment 10 with normal breathing	**Modified FFT**	**0.2414**	**0.2632**	**1.552**	**1.421**
	Error	**0.0218**		**0.131**	
	Percentage	**8.28%**		**9.22%**	
	EMD	**0.2759**	**0.2632**	**1.5862**	**1.421**
	Error	**0.0127**		**0.1652**	
	Percentage	**4.82%**		**11.62%**	
Segment 11 with normal breathing	**Modified FFT**	**0.2069**	**0.2414**	**1.448**	**1.276**
	Error	**0.0345**		**0.172**	
	Percentage	**12.29%**		**13.48%**	
	EMD	**0.2414**	**0.2414**	**1.4827**	**1.276**
	Error	**0**		**0.2067**	
	Percentage	**0.00%**		**16.20%**	
Segment 12 with normal breathing	**Modified FFT**	**0.2414**	**0.25**	**1.241**	**1.312**
	Error	**0.0086**		**0.071**	
	Percentage	**3.44%**		**5.41%**	
	EMD	**0.1875**	**0.25**	**1.2758**	**1.312**
	Error	**0.0625**		**0.0362**	
	Percentage	**25.00%**		**2.76%**	
Segment 13 with normal breathing	**Modified FFT**	**0.3448**	**0.2759**	**1.138**	**1.31**
	Error	**0.0689**		**0.172**	
	Percentage	**24.97%**		**13.13%**	
	EMD	**0.3793**	**0.2759**	**1.3103**	**1.31**
	Error	**0.1034**		**0.0003**	
	Percentage	**37.47%**		**0.02%**	
Segment 14 with normal breathing	**Modified FFT**	**0.2759**	**0.2759**	**1.345**	**1.414**
	Error	**0**		**0.069**	
	Percentage	**0.00%**		**4.88%**	
	EMD	**0.3448**	**0.2759**	**1.4482**	**1.414**
	Error	**0.0689**		**0.0342**	
	Percentage	**24.97%**		**2.42%**	
Segment 15 with normal breathing	**Modified FFT**	**0.2759**	**0.2759**	**1.276**	**1.31**
	Error	**0**		**0.034**	
	Percentage	**0.00%**		**2.60%**	
	EMD	**0.3103**	**0.2759**	**1.2758**	**1.31**
	Error	**0.0344**		**0.0342**	
	Percentage	**12.46%**		**2.61%**	
Segment 16 with normal breathing	**Modified FFT**	**0.3448**	**0.3103**	**1.241**	**1.31**
	Error	**0.0345**		**0.069**	
	Percentage	**11.12%**		**5.27%**	
	EMD	**0.3793**	**0.3103**	**1.2758**	**1.31**
	Error	**0.069**		**0.0342**	
	Percentage	**22.25%**		**2.61%**	

Figure 4.17: Comparison of breathing and heart rate estimation using modified FFT and EMD with reference belt and ECG signals

Segment 17 with normal breathing	Modified FFT	0.2759	0.3103	1.172	1.31
	Error	0.0344		0.138	
	Percentage	11.08%		10.53%	
	EMD	0.3103	0.3103	1.2069	1.31
	Error	0		0.1031	
	Percentage	0.00%		7.87%	
Segment 18 with normal breathing	Modified FFT	0.3103	0.3103	1.241	1.345
	Error	0		0.104	
	Percentage	0.00%		7.73%	
	EMD	0.3448	0.3103	1.2758	1.345
	Error	0.0345		0.0692	
	Percentage	11.12%		5.14%	
Modified FFT	average error	0.026588889		0.172138889	
	avg percentage	9.71%		12.40%	
	median error	0.03445		0.1345	
	edian percentag	11.10%		9.88%	
EMD	average error	0.034822222		0.154877778	
	avg percentage	12.91%		11.19%	
	median error	0.0345		0.13415	
	edian percentag	13.40%		9.75%	

Figure 4.18: Comparison of breathing and heart rate estimation using modified FFT and EMD with reference belt and ECG signals

reference signals from the belt and ECG. Because the reference breathing and heartbeat signal are periodic, using FFT is enough to get the reference breathing rate and reference heart rate. Errors are measured using the absolute error between the estimate rate and the reference rate. Percentages are calculated by simply dividing the error by the reference rate.

In conclusion, both modified FFT and EMD with the Minkowski distance work for radar signal processing. The average error and median error between the two algorithms are small.

For the estimation of breathing rates of three subjects, the average error between the estimate breathing rate and reference breathing rate when using modified FFT is about 9.71% off from the reference breathing rate. The average error between the estimate breathing rate and reference breathing rate when using EMD is about 12.91% off from the reference breathing rate; The median error using modified FFT is about 11.10% off from the reference breathing rate. The median error using EMD is about 13.40% off from the reference breathing rate. With this data, we can conclude that to estimate the breathing rate, both of these algorithms produce good results.

For the estimation of the heartbeat rates of three subjects, the average error between the estimate heartbeat rate and the reference heartbeat rate when using modified FFT is about 12.40% off from the reference heartbeat rate. The average error between the estimate heartbeat rate and the reference heartbeat rate when using EMD is about 11.19% off from the reference heartbeat rate; The median error using modified FFT is about 9.88% off from the reference heartbeat rate. The median error using EMD is about 9.75% off from the

reference heartbeat rate. With this data, we can conclude that to estimate heartbeat rate, both of these two algorithms produce good results.

Chapter 5

Breathing rate and heart rate estimation of stationary subjects in standing, sitting and lying postures

The objective of this chapter is to analyze how different postures affect breathing and heart rate estimation. The data was collected from three subjects breathing normally in standing, sitting and right lateral recumbent (RLR) posture facing the radar. RLR posture means that the subject is lying on their right side. The experiments were set up in the lab at Carleton University as shown in Figure 2.6. These experiments allow us to detect bio-signals when the subject is in a mock-up "prison cell". Same as in Chapter 4, the radar was placed on the wall in the corner of the room, and the radar is facing the room at an angle. The room is closed with windows on one wall. There are three marks on the floor: mark A, B and C. These experiments were done on October 21st, Nov 3rd, and Nov 17th, 2016.

In these experiments, subjects are standing, sitting, and lying down at mark A shown in Figure 2.6.

We also used modified FFT and EMD algorithms to extract breathing and heart rate. The signal was divided into segments where each segment is 30 seconds and each experiment of one subject lasts approximately three minutes. This means that there are 18 segments for one subject, and 54 segments in total. Because an example of reference signals as well as raw and processed radar data in sitting posture were explained in chapter four, here we will show only examples of a 30 second data segment for a subject in lying down and standing postures.

5.1 Breathing and heart rate estimation when the subject is lying

In this section, we will discuss data collected when the subject is lying down on the bed in front of radar shown in Figure 2.6.

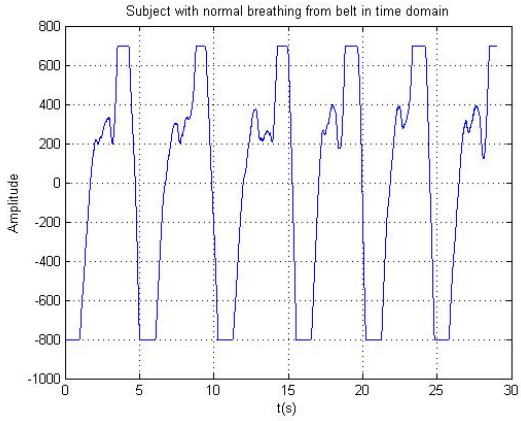

Figure 5.1: Signal from the belt when the subject is lying down and is breathing normally

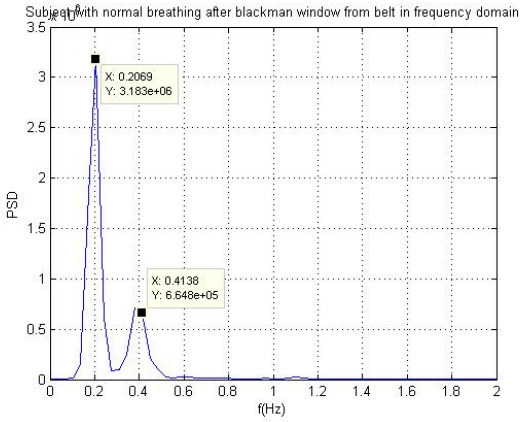

Figure 5.2: Signal from the belt in frequency domain after applying Blackman window when the subject is lying down and is breathing normally

5.1.1 Reference signals from belt and ECG

The reference breathing signal from the belt is shown in Figure 5.1 and its spectrum is shown in Figure 5.2. The reference heartbeat signal from ECG sensors are shown in Figure 5.3 and its spectrum in Figure 5.4.

From Figure 5.2, we can see that the reference breathing rate estimated from the belt is 0.2069 Hz. In addition, we can find its second harmonic which is at 0.4138 Hz. From Figure 5.4, we can find the reference heart rate from ECG sensors, which is 1.138 Hz.

5.1.2 Radar signals for breathing rate estimation

This subsection deals with breathing rate estimation using modified FFT as well as EMD when the subject is lying down on the bed in front of radar and breathing normally. The 30 seconds data in Figure 5.5 is from zone number 9.

After using modified FFT and finding the frequency of the maximum peak in the spectrum, we can clearly find that the estimated breathing rate is about 0.2069 Hz, as shown in Figure 5.6. Comparing with the reference breathing rate obtained from the belt which is 0.2069 Hz, we can calculate that the error is 0 Hz.

Next, we applied EMD on the same data collected from radar system. The IMFs is shown in Figure 5.7.

After finding the frequency of the maximum peak of the FFT of each IMF, the rate of each IMF is:

breathing_rate_of_imf 1 = [312.6500];

breathing_rate_of_imf 2 = [125.0669];

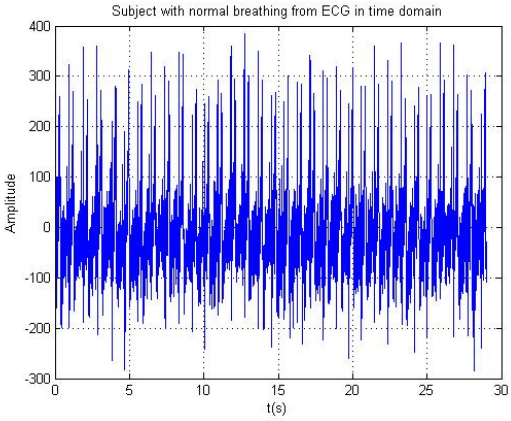

Figure 5.3: Signal from the ECG when the subject is lying down and is breathing normally

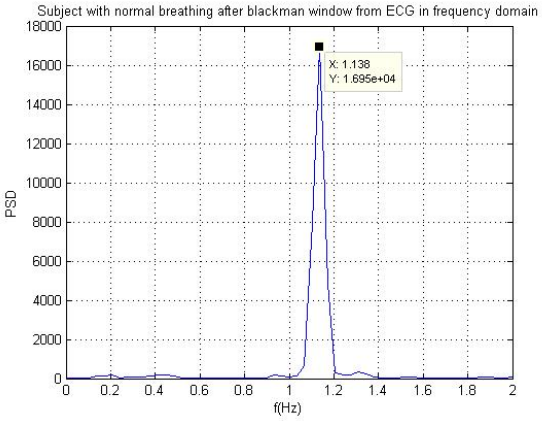

Figure 5.4: Signal from the ECG in frequency domain after applying Blackman window when the subject is lying down and is breathing normally

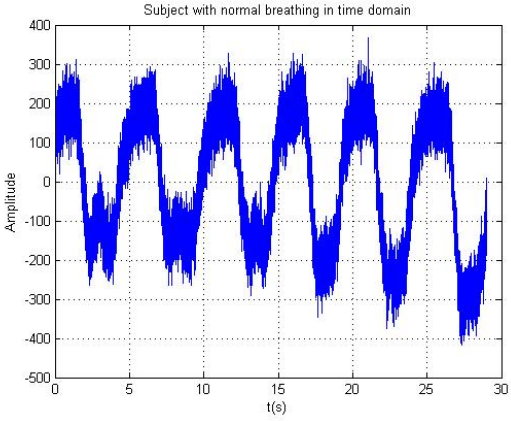

Figure 5.5: Signal from the radar in time domain when the subject is lying down and is breathing normally

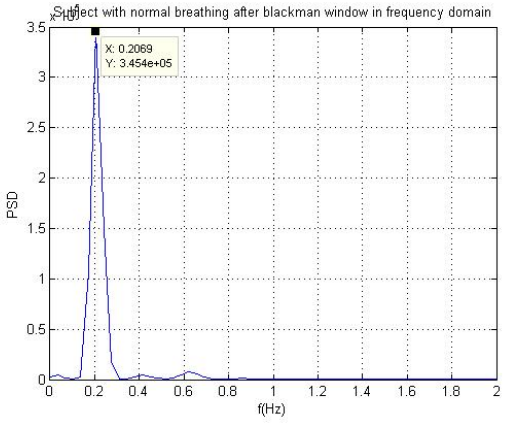

Figure 5.6: Signal from zone 9 of the radar in frequency domain after applying Blackman window when the subject is lying down and is breathing normally

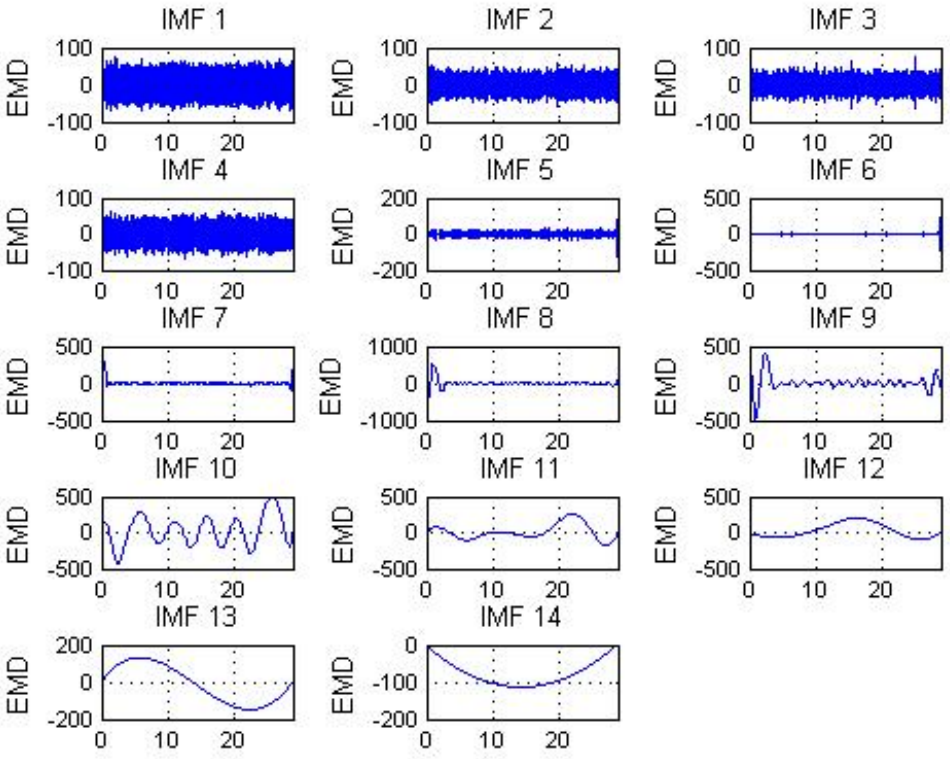

Figure 5.7: The IMFs of radar signal

breathing_rate_of_imf 3 = [57.4473];

breathing_rate_of_imf 4 = [30.6891];

breathing_rate_of_imf 5 = [19.0342];

breathing_rate_of_imf 6 = [5.1723];

breathing_rate_of_imf 7 = [2.6551];

breathing_rate_of_imf 8 = [0.4138];

breathing_rate_of_imf 9 = [0.6552];

breathing_rate_of_imf 10 = [0.2414];

breathing_rate_of_imf 11 = [0.1379];

breathing_rate_of_imf 12 = [0.0690];

breathing_rate_of_imf 13 = [0.0690];

breathing_rate_of_imf 14 = [0.0345];

After applying the Minkowski distance on each IMF, we get the results shown in Figure 5.8, and find the IMF that contains the breathing components. In this case, it is IMF 10 and the estimated breathing rate is 0.2414 Hz. Comparing with the reference breathing rate 0.2069 Hz which we get from belt, the error is 0.0345 per second, which is 16.67% off from the reference breathing rate while lying down.

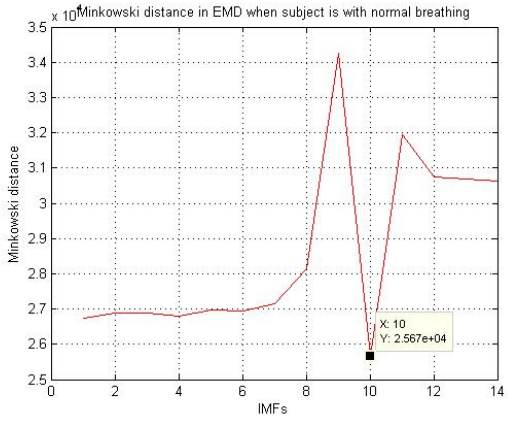

Figure 5.8: The Minkowski distance for the IMFs shown in Figure 5.7

The summary of the results is shown in Table 5.9. Comparing with reference breathing rate, the error between the reference breathing rate and the estimate breathing rate from the radar signal while using modified FFT is 0. Also, the error between reference breathing rate and the estimate breathing rate while using EMD is 0.0345. It shows us that in this 30 second segment case method, modified FFT is better than EMD while the subject is lying down on the bed in front of the radar system.

Lying down with Normal breathing		Breathing rate	
		Radar	Belt
30 seconds segment with normal breathing	**Modified FFT**	**0.2069**	**0.2069**
	Error	**0**	
	Percentage	**0.00%**	
	EMD	**0.2414**	**0.2069**
	Error	**0.0345**	
	Percentage	**16.67%**	

Figure 5.9: The comparison of Modified FFT and EMD applied on the radar signal while the subject is lying down

5.1.3 Radar signals for heartbeat rate estimation

This subsection addresses heart rate estimation when the subject is lying down on the bed facing the radar. The 30 second segment data to be analyzed is the same as in Section 5.1.2.

Figure 5.10 shows 30 seconds of data collected from the radar system when the subject is lying down facing the radar and breathing normally. From section 5.1.2, we already know the estimated breathing rate. Here we can use a notch filter obtain a radar signal that does not include breathing, as shown in Figure 5.10.

After applying the modified FFT, we found that the estimate heartbeat rate is approximately 0.8621 Hz, as shown in Figure 5.11. When Compared with the reference heart rate from the ECG which is 1.138 Hz, we can calculate that the error is 0.2759 Hz, which is 24.24% off from the reference heartbeat rate.

Next, we apply the EMD on the same signal after removing the breathing components. The IMFs are shown in Figure 5.12.

The rate of each IMF is computed after finding the frequency of the maximum peak in the spectrum of that IMF. The rates are:

breathing_rate_of_imf 1 = [1.5862];

breathing_rate_of_imf 2 = [1.5517];

breathing_rate_of_imf 3 = [0.8965];

breathing_rate_of_imf 4 = [0.6207];

breathing_rate_of_imf 5 = [0.2414];

breathing_rate_of_imf 6 = [0.1379];

breathing_rate_of_imf 7 = [0.0690];

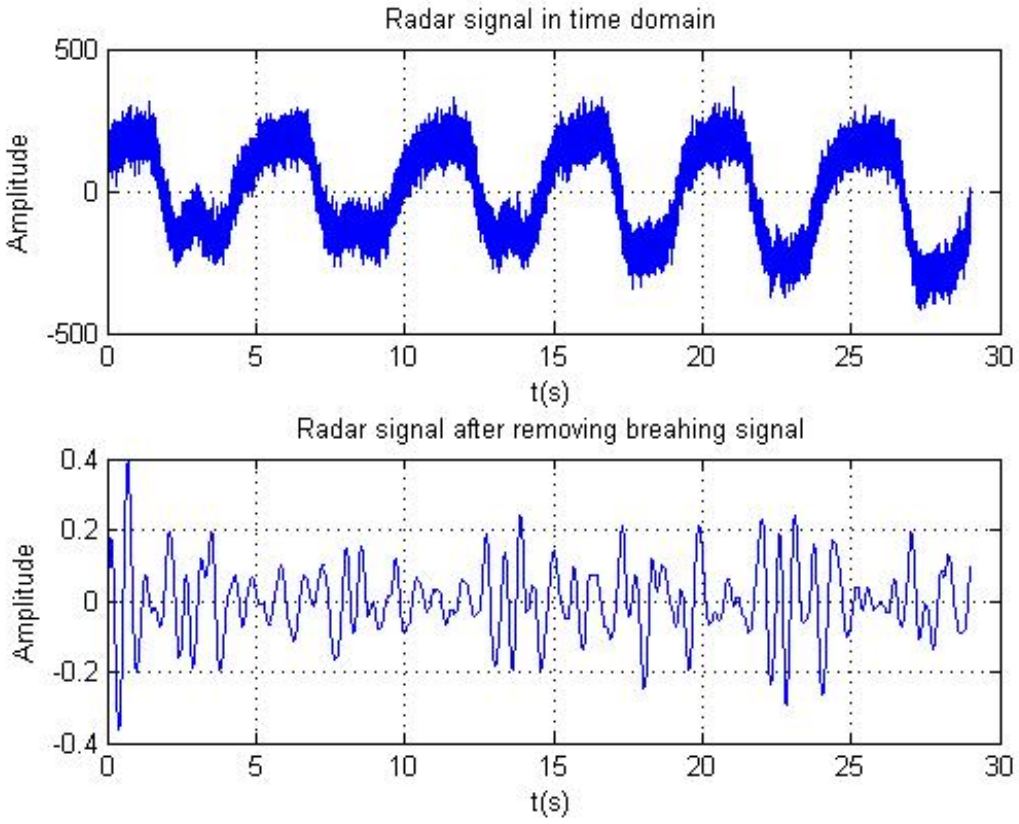

Figure 5.10: The comparison of the raw radar signal and the signal with removed breathing signal from the subject in RLR posture

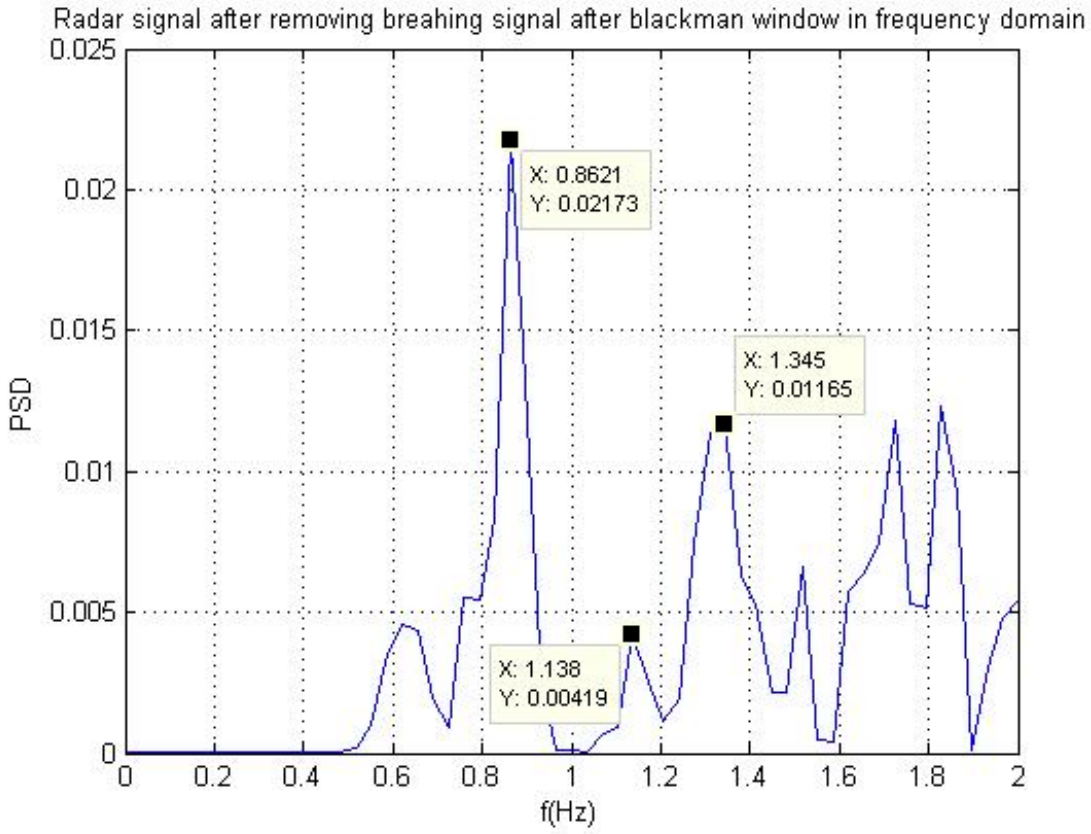

Figure 5.11: Signal after removing breathing components in the frequency domain and applying the Blackman window when the subject is lying down and is breathing normally

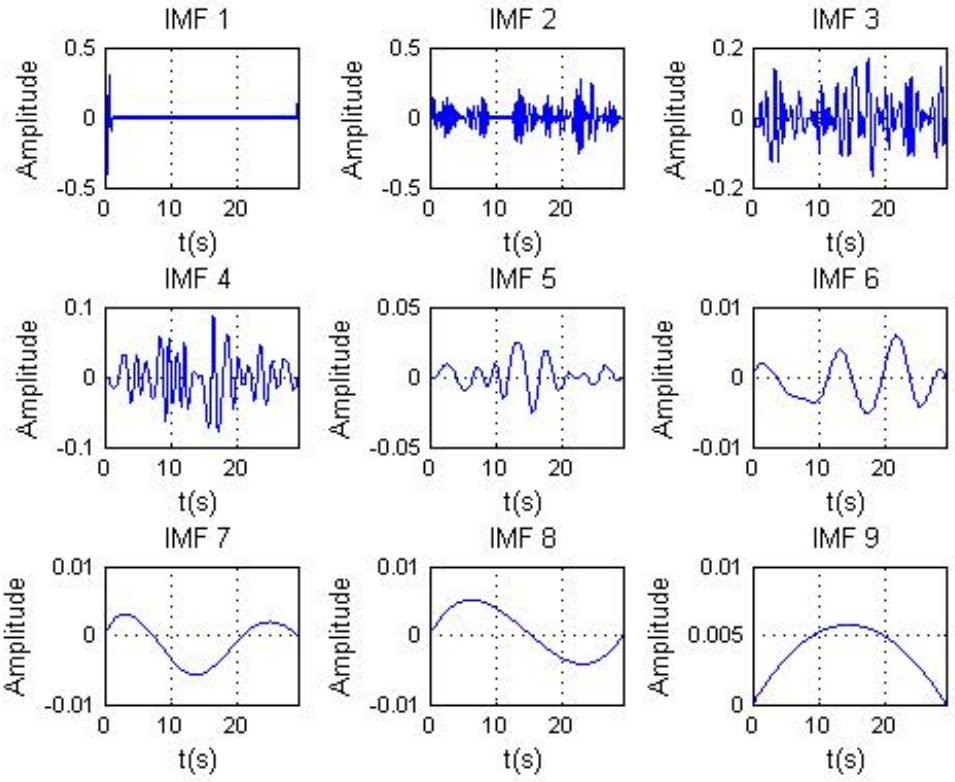

Figure 5.12: The IMFs of the radar signal after removing breathing components

breathing_rate_of_imf 8 = [0.0690];

breathing_rate_of_imf 9 = [0.0345];

After applying the Minkowski distance on each IMF, we get the results shown in Figure 5.13, so that we can find that the estimate of heartbeat signal is in IMF 2 which is 1.5517 Hz. When compared with the reference heartbeat rate of 1.138 Hz obtained from ECG, the error is 0.4137 Hz, which is 36.35% off from the reference heartbeat rate.

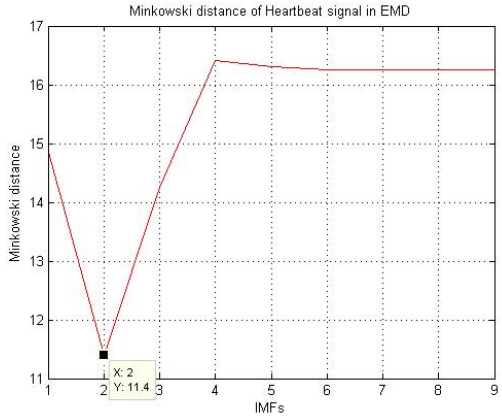

Figure 5.13: The Minkowski distance for the IMFs shown in Figure 5.12

A summary of the results is shown in Table 5.14. Compared with the reference heartbeat rate, the error between the reference heartbeat rate and the estimate heartbeat rate from the radar while using modified FFT is 0.2759. Also, the error between reference heartbeat rate and the estimate heartbeat rate from the radar while using EMD is 0.4137. It shows us that in this 30 second segment case modified FFT is better than the EMD method.

Lying down with Normal breathing		Breathing rate		Heartbeat rate	
		Radar	Belt	Radar	ECG
30 seconds segment with normal breathing	**Modified FFT**	**0.2069**	**0.2069**	**0.8621**	**1.138**
	Error	**0**		**0.2759**	
	Percentage	**0.00%**		**24.24%**	
	EMD	**0.2414**	**0.2069**	**1.5517**	**1.138**
	Error	**0.0345**		**0.4137**	
	Percentage	**16.67%**		**36.35%**	

Figure 5.14: The comparison of heart rate errors using Modified FFT and EMD applied on the radar signal from the subject in lying posture

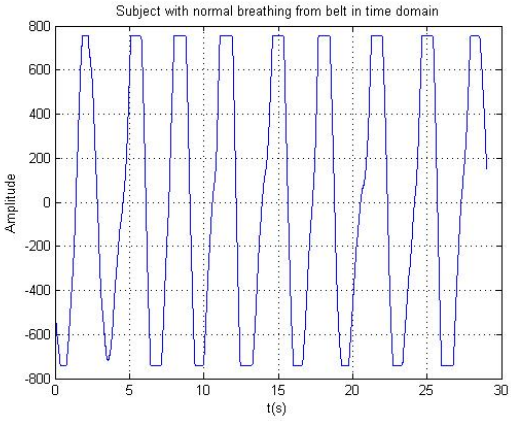

Figure 5.15: Signal from the belt when the subject is standing and is breathing normally

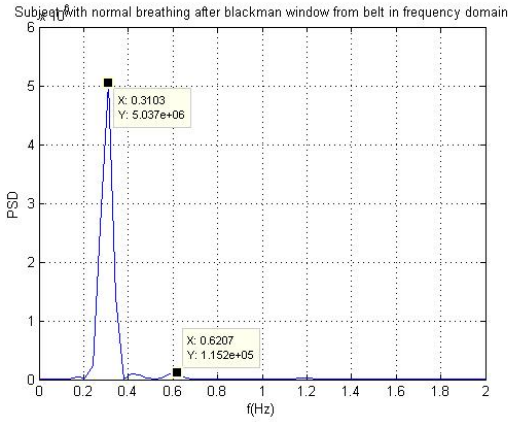

Figure 5.16: Signal from the belt in frequency domain after applying the Blackman window when the subject is standing and is breathing normally

5.2 Breathing and heart rate estimation when the subject is standing

In this section, we will discuss the data collected when the subject is standing in front of the radar.

5.2.1 Reference signals from belt and ECG

The reference breathing signal from the belt is shown in Figure 5.15 and its spectrum is shown in Figure 5.16. The reference heartbeat signal from ECG sensors is shown in Figure 5.17 and its spectrum in Figure 5.18.

From Figure 5.16, we can see that the reference breathing rate estimated from the belt is 0.3103 Hz. In addition, we can find its second harmonic which is at 0.6207 Hz. From Figure 5.18, we can find the reference heartbeat rate from ECG sensors, which is 1.448 Hz.

5.2.2 Radar signals for breathing rate estimation

This subsection deals with the breathing rate estimation using modified FFT as well as EMD when the subject is standing in front of the radar and breathing normally. The 30 second data in Figure 5.19 is from zone number 8.

After using modified FFT and finding the frequency of the maximum peak in the spectrum, we can clearly find that the estimated breathing rate is about 0.2069 Hz, as shown in Figure 5.20. Compared with the reference breathing rate obtained from the belt which is 0.3103 Hz, we can calculate that the error is 0.1034 per second, which is 33.32% off from the reference breathing rate.

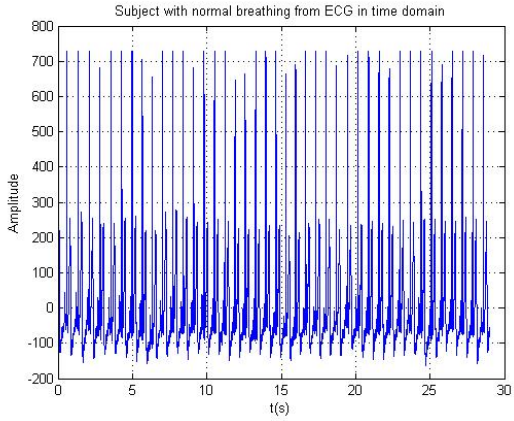

Figure 5.17: Signal from the ECG when the subject is standing and is breathing normally

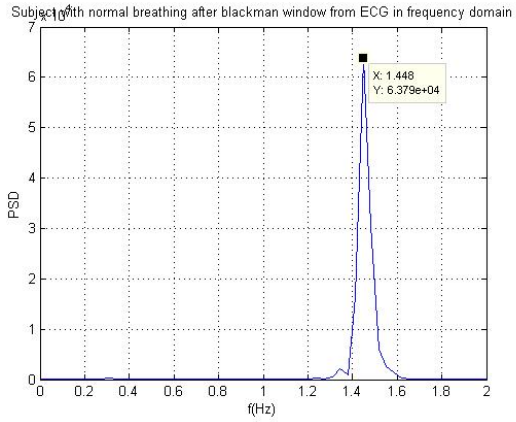

Figure 5.18: Signal from the ECG in frequency domain after applying Blackman window when the subject is standing and is breathing normally

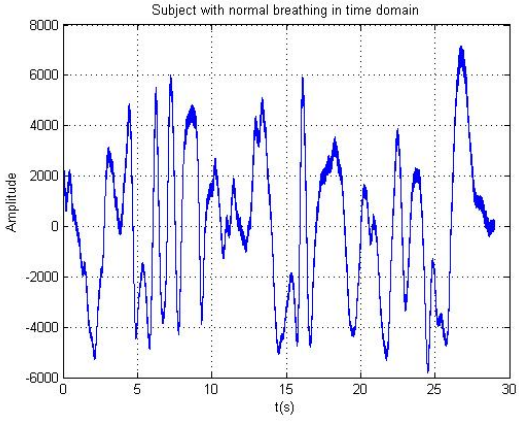

Figure 5.19: Signal from the radar in time domain when the subject is standing and is breathing normally

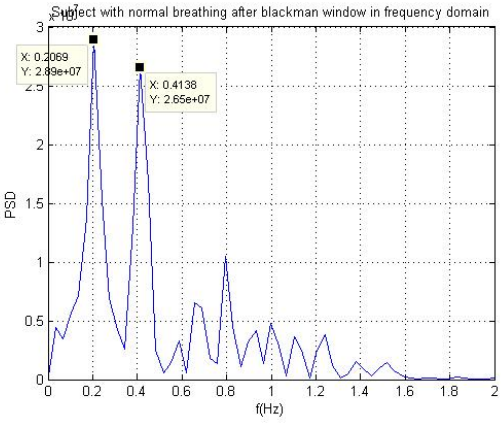

Figure 5.20: Signal from zone 8 of the radar in frequency domain after applying the Blackman window when the subject is standing and is breathing normally

Next, we applied EMD on the same data collected from the radar system. The IMFs is shown in Figure 5.21.

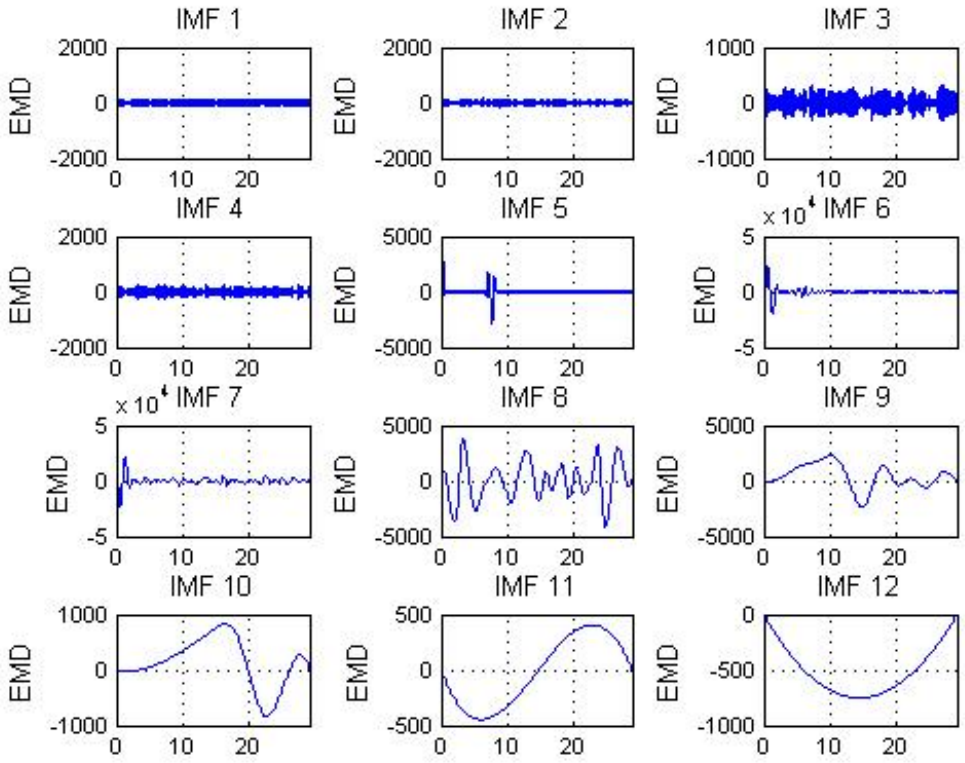

Figure 5.21: The IMFs of radar signal

After finding the frequency of the maximum peak of the FFT of each IMF, the rate of each IMF is:

breathing_rate_of_imf 1 = [415.0882];

breathing_rate_of_imf 2 = [124.5127];

breathing_rate_of_imf 3 = [42.3778];

breathing_rate_of_imf 4 = [41.7226];

breathing_rate_of_imf 5 = [1.0344];

breathing_rate_of_imf 6 = [1.1379];

breathing_rate_of_imf 7 = [0.4483];

breathing_rate_of_imf 8 = [0.2414];

breathing_rate_of_imf 9 = [0.1379];

breathing_rate_of_imf 10 = [0.0690];

breathing_rate_of_imf 11 = [0.0690];

breathing_rate_of_imf 12 = [0.0345];

After applying the Minkowski distance on each IMF, we get the results shown in Figure 5.22, so that we find the IMF that contains the breathing components. In this case, it happens to be IMF 8 and the estimated breathing rate is 0.2414 Hz. Compared with the reference breathing rate 0.3103 which we get from belt, the error is 0.0689 per second, which is 22.20% off from the reference breathing rate, in this case while standing.

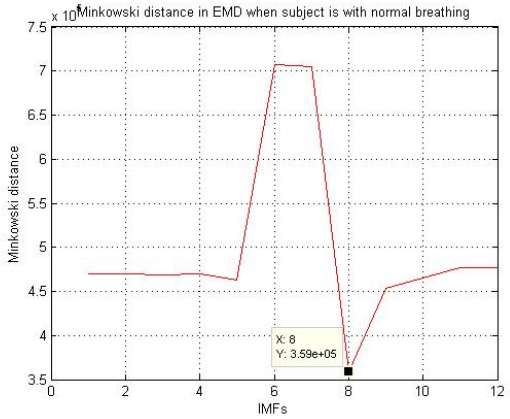

Figure 5.22: The Minkowski distance for the IMFs shown in Figure 5.21

The summary of the results is shown in Table 5.23. Compared with the reference breathing rate, the error between the reference breathing rate and the estimate breathing rate from the radar while using modified FFT is 0.1034. Also, the error between the reference breathing rate and the estimate breathing rate from radar while using EMD is 0.0689. It shows us that in this 30 second segment case method, EMD is better than modified FFT while the subject is standing in front of radar.

5.2.3 Radar signals for heartbeat rate estimation

This subsection addresses heart rate estimation when the subject is standing and facing the radar. The 30 second segment data to be analyzed is the same as in Section 5.2.2.

Figure 5.19 shows 30 seconds of data collected from the radar system when the subject is standing and facing the radar while breathing normally. From section 5.2.2, we already know the estimated breathing rate. Here we can use notch filter to remove the breathing signal, so that we can get the radar signal without breathing signals as shown in Figure 5.24.

Standing with Normal breathing		Breathing rate	
		Radar	Belt
30 seconds segment with normal breathing	**Modified FFT**	**0.2069**	**0.3103**
	Error	**0.1034**	
	Percentage	**33.32%**	
	EMD	**0.2414**	**0.3103**
	Error	**0.0689**	
	Percentage	**22.20%**	

Figure 5.23: The comparison of Modified FFT and EMD applied on the radar signal while the subject is standing

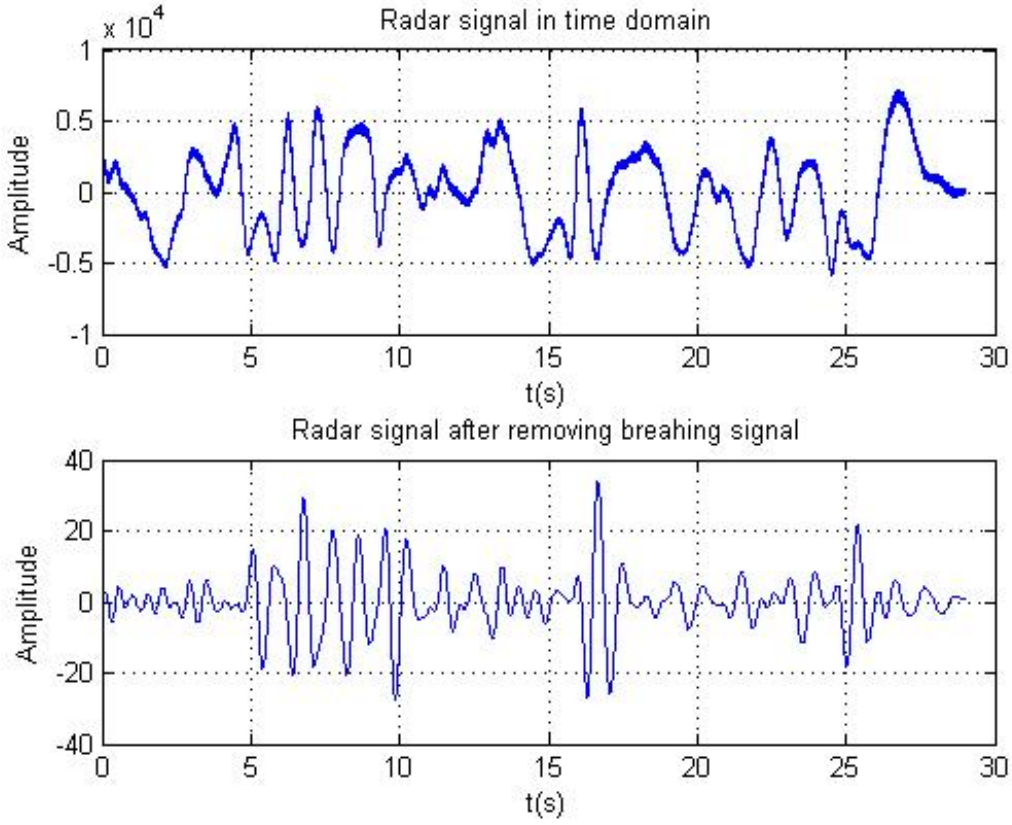

Figure 5.24: The comparison of the raw radar signal and the signal with removed breathing signal from the subject while standing

After applying the modified FFT, we found that the estimate heartbeat rate is approximately 1.241 Hz, as shown in Figure 5.25. Compared with the reference heart rate from the ECG which is 1.448 Hz, we can calculate that the error is 0.207 Hz, which is 14.30% off from the reference heartbeat rate.

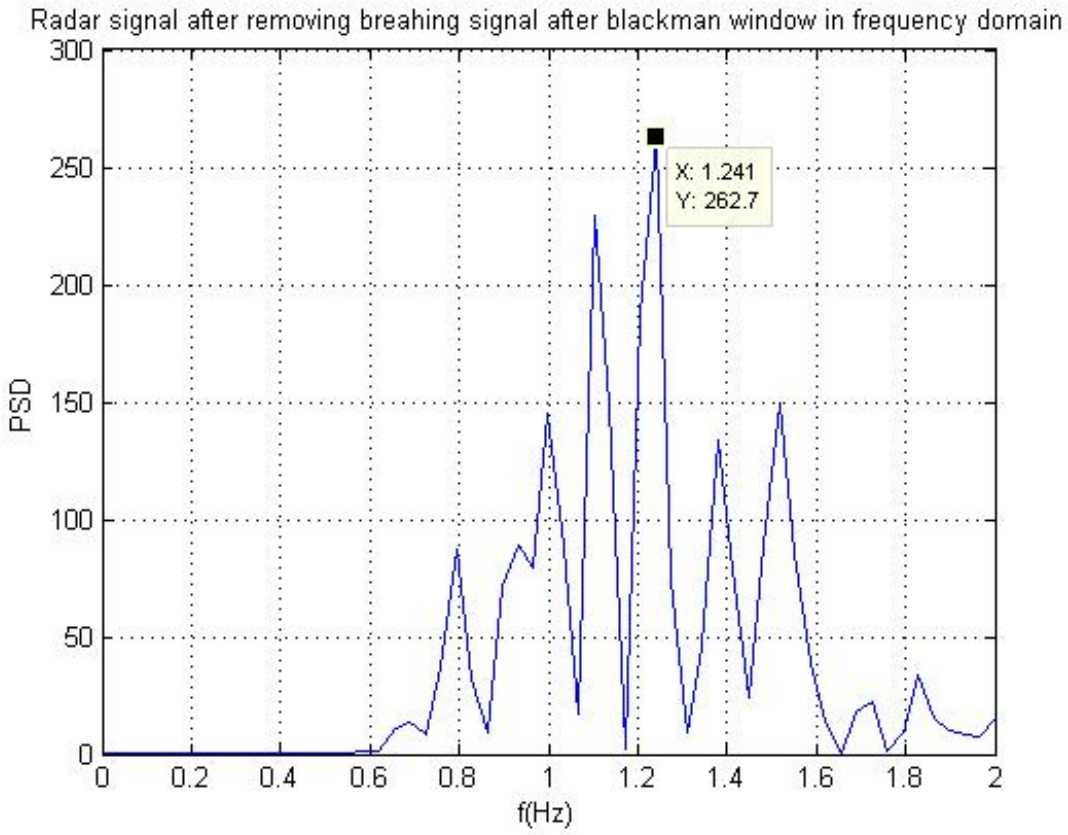

Figure 5.25: Signal after removing the breathing components in the frequency domain and applying Blackman window, while the subject is standing and is breathing normally

Next, we will applied EMD on the same signal after removing breathing components. The IMFs are shown in Figure 5.26.

The rate of each IMF is computed after finding the frequency of the maximum peak in the spectrum of that IMF. The rates are:

breathing_rate_of_imf 1 = [1.1379];

breathing_rate_of_imf 2 = [0.5172];

breathing_rate_of_imf 3 = [0.2414];

breathing_rate_of_imf 4 = [0.1379];

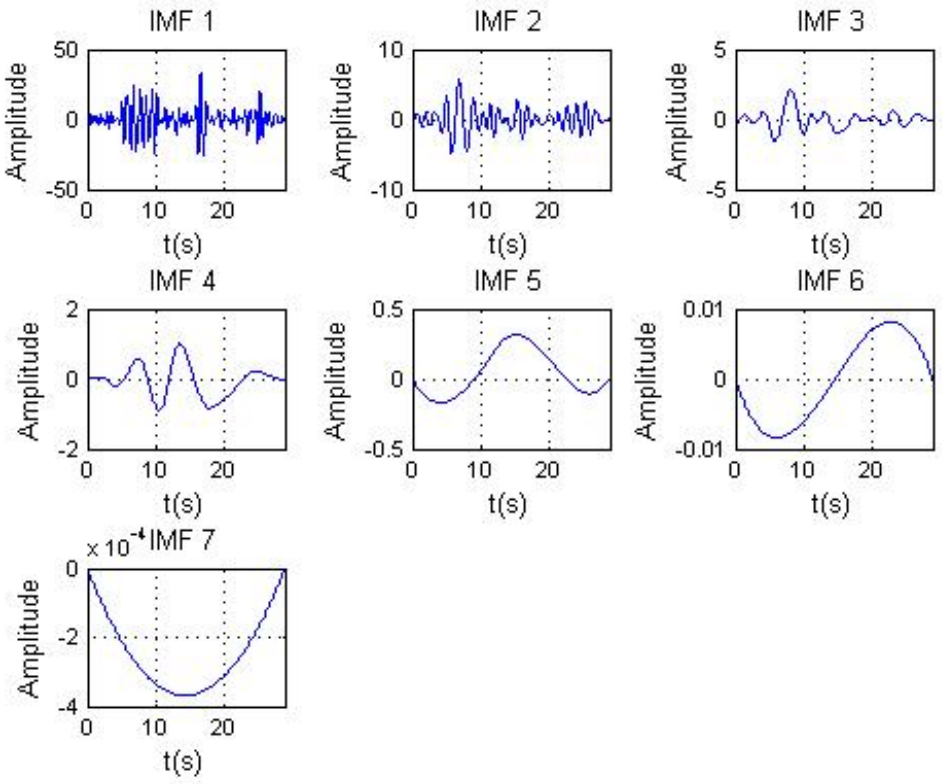

Figure 5.26: The IMFs of the radar signal after removing breathing components

breathing_rate_of_imf 5 = [0.0690];

breathing_rate_of_imf 6 = [0.0690];

breathing_rate_of_imf 7 = [0.0345];

After applying the Minkowski distance from each IMF, we get the results shown in Figure 5.27, so that we can find that the estimate of the heartbeat signal is in IMF 1 which is 1.1379 Hz. Compared with the reference heartbeat rate of 1.448 Hz obtained from ECG, the error is 0.3103 Hz, which is 21.42% off from the reference heartbeat rate.

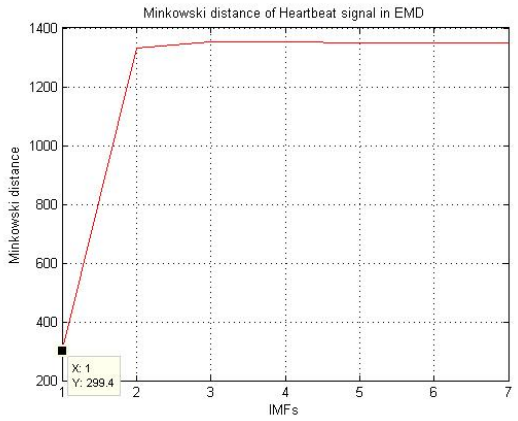

Figure 5.27: The Minkowski distance for the IMFs shown in Figure 5.26

Standing with Normal breathing		Breathing rate		Heartbeat rate	
		Radar	Belt	Radar	ECG
30 seconds segment with normal breathing	**Modified FFT**	**0.2069**	**0.3103**	**1.241**	**1.448**
	Error	**0.1034**		**0.207**	
	Percentage	**33.32%**		**14.30%**	
	EMD	**0.2414**	**0.3103**	**1.1379**	**1.448**
	Error	**0.0689**		**0.3103**	
	Percentage	**22.20%**		**21.42%**	

Figure 5.28: The comparison of heart rate errors using Modified FFT and EMD applied on the radar signal from the subject in standing posture

A summary of the results is shown in Table 5.28. Compared with the reference heartbeat rate, the error between the reference heartbeat rate and the estimate heartbeat rate from radar while using modified FFT is 0.207. Also, the error between the reference heartbeat rate and the estimate heartbeat rate from the radar while using EMD is 0.3103. It shows us that in this 30 second segment case method modified FFT is better than EMD while standing.

5.3 Discussion

In this section, we compare the results of 18 segments for each posture (standing, sitting, and lying down). The comparisons of breathing rate estimation and heartbeat rate estimation using two methods for the three postures (sitting, standing and lying down) are shown in Figure 5.29, Figure 5.30, Figure 5.31 and Figure 5.32. The details for each segment are shown for sitting (Figure 4.16, Figure 4.17, Figure 4.18), lying down (Figure 5.33, Figure 5.34, Figure 5.35), and standing (Figure 5.36, Figure 5.37 and Figure 5.38).

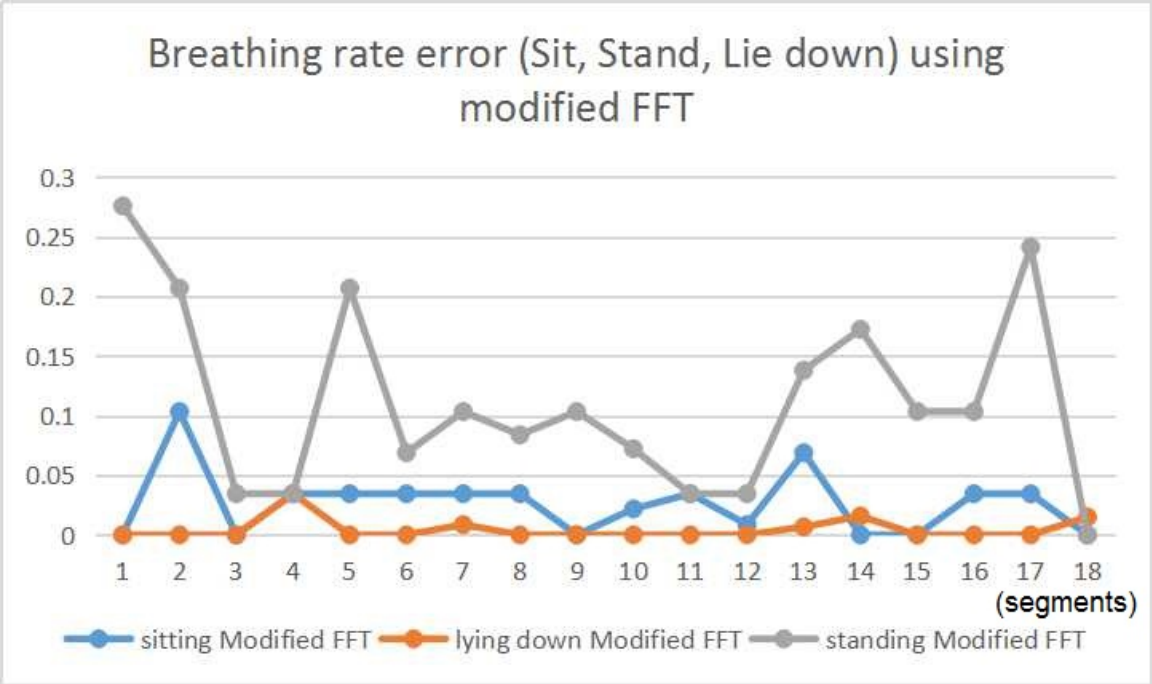

Figure 5.29: Comparing breathing rate error using modified FFT when subject is standing, sitting or lying down

From Figure 5.29 and Figure 5.30, we can find that for the breathing rate estimation, the error is lowest when the subject is lying down on the bed facing the radar; the error is highest when the subject is standing facing the radar.

From Figure 5.31 and Figure 5.32, we can find that for heart rate estimation, the error is lowest when the subject is lying down on the bed facing the radar; the error is highest when the subject is standing facing the radar, too. The reason is that when the subject is standing, their body will be swinging back and forth subconsciously, which increases the error. However, when the subject is sitting or lying down, the chair or bed can support their body, preventing it from swinging back and forth.

The table above shows estimated breathing and heart rates while the subject is standing and lying down. The estimated breathing rate and heart rate are compared with the

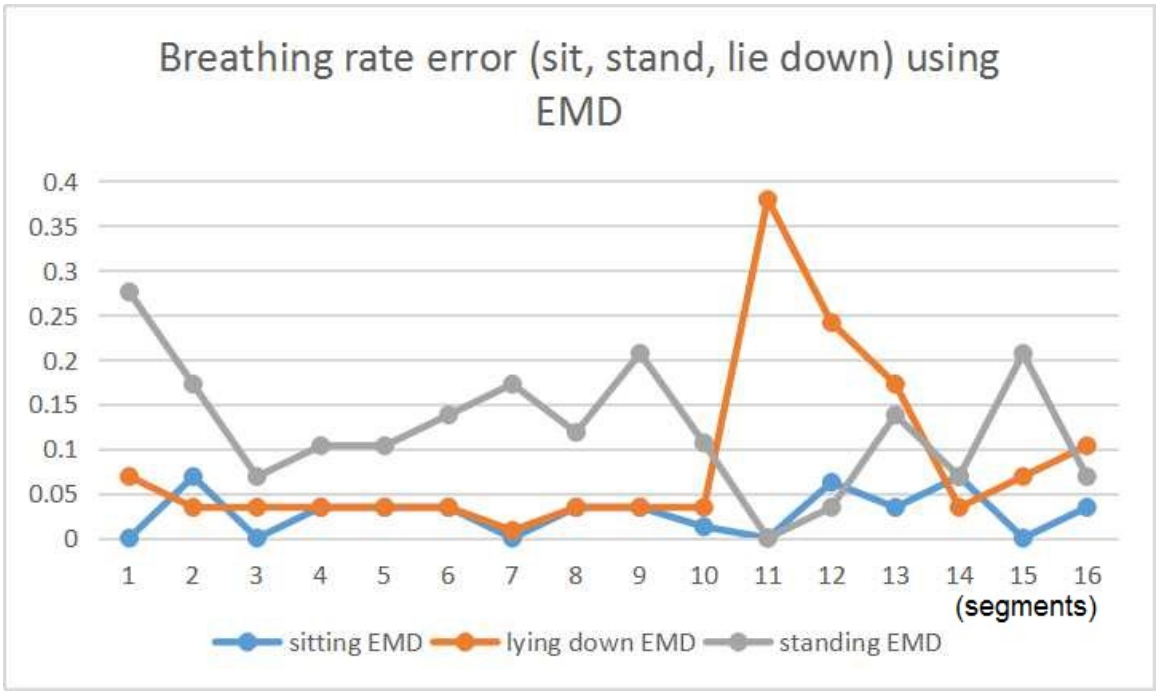

Figure 5.30: Comparing breathing rate error using EMD when subject is standing, sitting or lying down

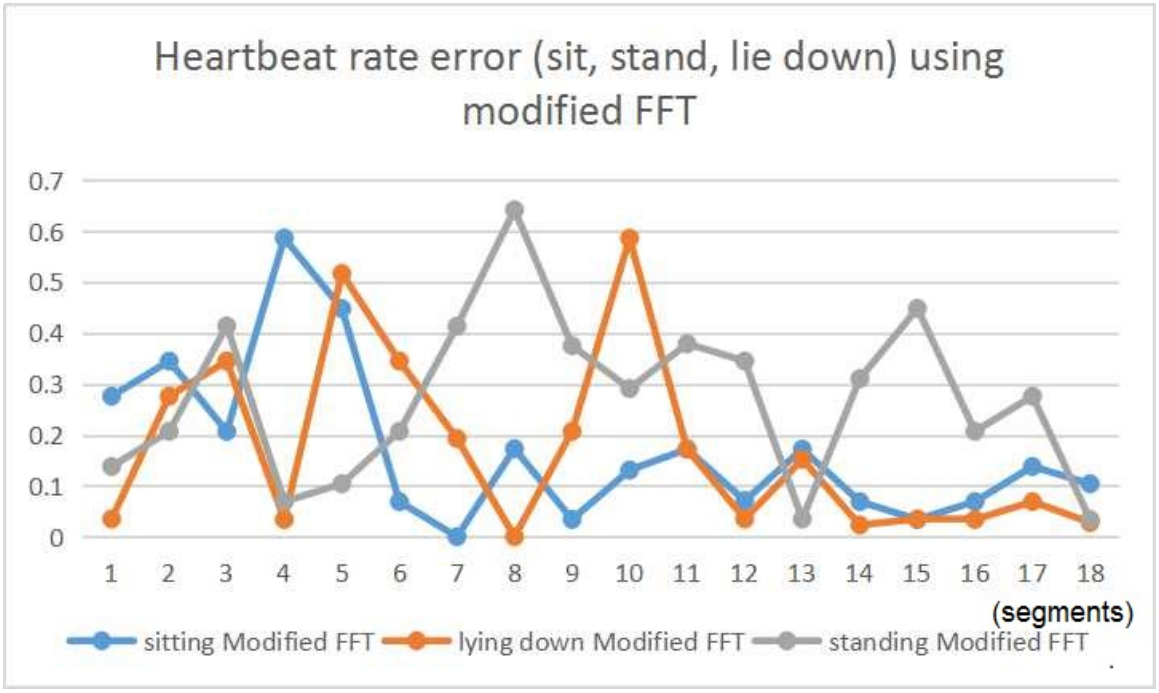

Figure 5.31: Comparing heart rate error using modified FFT when subject is standing, sitting or lying down

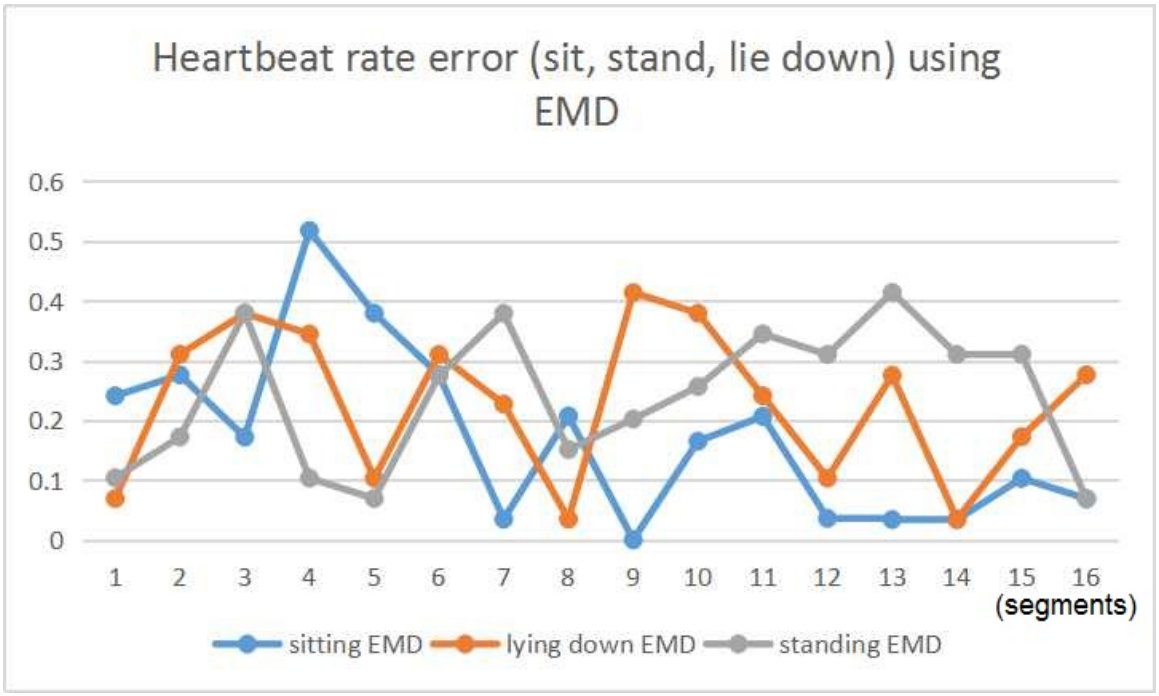

Figure 5.32: Comparing heart rate error using EMD when subject is standing, sitting or lying down

reference signals from the belt and ECG. Error is computed as the absolute error between the estimated rate and the reference rate. Percentages are obtained as a result of dividing the error by the reference breathing or heart rates.

From Figure 5.38, we can find that when the subject is standing, the average breathing rate error is approximately 42.55% when using modified FFT, and 49.36% when using EMD. The average heart rate error is approximately 18.54% when using modified FFT, and 15.66% when using EMD;

From Figure 5.35, we can find that when the subject is lying down, the average breathing rate error is approximately 1.74% when using modified FFT, and 34.43% when using EMD. The average heart rate error is approximately 13.67% when using modified FFT, and 17.05% when using EMD;

From Figure 4.18, we can find that when the subject is lying down, the average breathing rate error is approximately 9.71% when using modified FFT, and 12.91% when using EMD. The average heartbeat rate error is approximately 12.40% when using modified FFT, and 11.19% when using EMD.

In conclusion, for the breathing rate estimation, the error when the subject is lying down is lesser than when the subject is sitting, which in turn is lesser than when the subject is standing. For the heart rate estimation, the error when the subject is sitting is lesser than the error when the subject is lying down, which in turn is lesser than the error when the subject is standing.

Lying down with Normal breathing		Breathing rate		Heartbeat rate	
		Radar	Belt	Radar	ECG
Segment 1 with normal breathing	**Modified FFT**	0.2069	0.2069	1.345	1.31
	Error	0		0.035	
	Percentage	0.00%		2.67%	
	EMD	0.1379	0.2069	1.3793	1.31
	Error	0.069		0.0693	
	Percentage	33.35%		5.29%	
Segment 2 with normal breathing	**Modified FFT**	0.2759	0.2759	1.724	1.448
	Error	0		0.276	
	Percentage	0.00%		19.06%	
	EMD	0.3103	0.2759	1.7586	1.448
	Error	0.0344		0.3106	
	Percentage	12.47%		21.45%	
Segment 3 with normal breathing	**Modified FFT**	0.2414	0.2414	1.034	1.379
	Error	0		0.345	
	Percentage	0.00%		25.02%	
	EMD	0.2759	0.2414	1	1.379
	Error	0.0345		0.379	
	Percentage	14.29%		27.48%	
Segment 4 with normal breathing	**Modified FFT**	0.2069	0.2414	1.345	1.379
	Error	0.0345		0.034	
	Percentage	14.29%		2.46%	
	EMD	0.2759	0.2414	1.0345	1.379
	Error	0.0345		0.3445	
	Percentage	14.29%		24.98%	
Segment 5 with normal breathing	**Modified FFT**	0.2414	0.2414	0.931	1.448
	Error	0		0.517	
	Percentage	0.00%		35.70%	
	EMD	0.2759	0.2414	1.3448	1.448
	Error	0.0345		0.1032	
	Percentage	14.29%		7.13%	
Segment 6 with normal breathing	**Modified FFT**	0.2414	0.2414	1	1.345
	Error	0		0.345	
	Percentage	0.00%		25.65%	
	EMD	0.2759	0.2414	1.6551	1.345
	Error	0.0345		0.3101	
	Percentage	14.29%		23.06%	
Segment 7 with normal breathing	**Modified FFT**	0.2414	0.25	1.276	1.083
	Error	0.0086		0.193	
	Percentage	3.44%		17.82%	
	EMD	0.2414	0.25	1.3103	1.083
	Error	0.0086		0.2273	
	Percentage	3.44%		20.99%	
Segment 8 with normal breathing	**Modified FFT**	0.2069	0.2069	1.034	1.034
	Error	0		0	
	Percentage	0.00%		0.00%	
	EMD	0.1724	0.2069	1.0689	1.034
	Error	0.0345		0.0349	
	Percentage	16.67%		3.38%	

Figure 5.33: Estimation of breathing rate and heartbeat rate from radar system while lying down-1

Segment 9 with normal breathing	**Modified FFT**	0.2069	0.2069	0.8621	1.138
	Error	0		0.2759	
	Percentage	0.00%		24.24%	
	EMD	0.2414	0.2069	1.5517	1.138
	Error	0.0345		0.4137	
	Percentage	16.67%		36.35%	
Segment 10 with normal breathing	**Modified FFT**	0.2414	0.2414	1.724	1.138
	Error	0		0.586	
	Percentage	0.00%		51.49%	
	EMD	0.2759	0.2414	1.5172	1.138
	Error	0.0345		0.3792	
	Percentage	14.29%		33.32%	
Segment 11 with normal breathing	**Modified FFT**	0.2069	0.2069	1.379	1.207
	Error	0		0.172	
	Percentage	0.00%		14.25%	
	EMD	0.5862	0.2069	1.4483	1.207
	Error	0.3793		0.2413	
	Percentage	183.32%		19.99%	
Segment 12 with normal breathing	**Modified FFT**	0.2069	0.2069	1.103	1.138
	Error	0		0.035	
	Percentage	0.00%		3.08%	
	EMD	0.4483	0.2069	1.2414	1.138
	Error	0.2414		0.1034	
	Percentage	116.67%		9.09%	
Segment 13 with normal breathing	**Modified FFT**	0.2759	0.2692	1.31	1.462
	Error	0.0067		0.152	
	Percentage	2.49%		10.40%	
	EMD	0.2414	0.2692	1.6206	1.462
	Error	0.0278		0.1586	
	Percentage	10.33%		10.85%	
Segment 14 with normal breathing	**Modified FFT**	0.2759	0.2917	1.31	1.333
	Error	0.0158		0.023	
	Percentage	5.42%		1.72%	
	EMD	0.2759	0.2917	1.3448	1.333
	Error	0.0158		0.0118	
	Percentage	5.42%		0.88%	
Segment 15 with normal breathing	**Modified FFT**	0.2759	0.2759	1.31	1.345
	Error	0		0.035	
	Percentage	0.00%		2.60%	
	EMD	0.1034	0.2759	1.6206	1.345
	Error	0.1725		0.2756	
	Percentage	62.52%		20.49%	
Segment 16 with normal breathing	**Modified FFT**	0.2759	0.2759	1.276	1.31
	Error	0		0.034	
	Percentage	0.00%		2.60%	
	EMD	0.3103	0.2759	1.3448	1.31
	Error	0.0344		0.0348	
	Percentage	12.47%		2.66%	

Figure 5.34: Estimation of breathing rate and heartbeat rate from radar system while lying down-2

Segment 17 with normal breathing	Modified FFT	0.2759	0.2759	1.276	1.345
	Error	0		0.069	
	Percentage	0.00%		5.13%	
	EMD	0.2069	0.2759	1.1724	1.345
	Error	0.069		0.1726	
	Percentage	25.01%		12.83%	
Segment 18 with normal breathing	Modified FFT	0.2759	0.2609	1.276	1.304
	Error	0.015		0.028	
	Percentage	5.75%		2.15%	
	EMD	0.3103	0.2069	1.3103	1.034
	Error	0.1034		0.2763	
	Percentage	49.98%		26.72%	
Modified FFT	average error	0.004477778		0.175272222	
	avg percentage	1.74%		13.67%	
	median error	0		0.1105	
	edian percentag	0.00%		7.77%	
EMD	average error	0.077616667		0.213677778	
	avg percentage	34.43%		17.05%	
	median error	0.0345		0.2343	
	edian percentag	14.29%		20.24%	

Figure 5.35: Estimation of breathing rate and heartbeat rate from radar system while lying down-3

Standing with Normal breathing		Breathing rate		Heartbeat rate	
		Radar	Belt	Radar	ECG
Segment 1 with normal breathing	**Modified FFT**	0.5172	0.2414	1.552	1.69
	Error	0.2758		0.138	
	Percentage	114.25%		8.16%	
	EMD	0.5172	0.2414	1.5861	1.69
	Error	0.2758		0.1039	
	Percentage	114.25%		6.15%	
Segment 2 with normal breathing	**Modified FFT**	0.069	0.2759	1.517	1.724
	Error	0.2069		0.207	
	Percentage	74.99%		12.01%	
	EMD	0.1034	0.2759	1.5517	1.724
	Error	0.1725		0.1723	
	Percentage	62.52%		9.99%	
Segment 3 with normal breathing	**Modified FFT**	0.2759	0.2414	1.241	1.655
	Error	0.0345		0.414	
	Percentage	14.29%		25.02%	
	EMD	0.3103	0.2414	1.2758	1.655
	Error	0.0689		0.3792	
	Percentage	28.54%		22.91%	
Segment 4 with normal breathing	**Modified FFT**	0.2414	0.2069	1.793	1.724
	Error	0.0345		0.069	
	Percentage	16.67%		4.00%	
	EMD	0.1034	0.2069	1.8275	1.724
	Error	0.1035		0.1035	
	Percentage	50.02%		6.00%	
Segment 5 with normal breathing	**Modified FFT**	0.4483	0.2414	1.586	1.69
	Error	0.2069		0.104	
	Percentage	85.71%		6.15%	
	EMD	0.3448	0.2414	1.6206	1.69
	Error	0.1034		0.0694	
	Percentage	42.83%		4.11%	
Segment 6 with normal breathing	**Modified FFT**	0.3448	0.2759	1.931	1.724
	Error	0.0689		0.207	
	Percentage	24.97%		12.01%	
	EMD	0.1379	0.2759	1.9999	1.724
	Error	0.138		0.275	
	Percentage	50.02%		15.59%	
Segment 7 with normal breathing	**Modified FFT**	0.3793	0.2759	0.9655	1.379
	Error	0.1034		0.4135	
	Percentage	37.48%		29.98%	
	EMD	0.1034	0.2759	1	1.379
	Error	0.1725		0.379	
	Percentage	62.52%		27.48%	
Segment 8 with normal breathing	**Modified FFT**	0.3448	0.2609	0.7931	1.435
	Error	0.0839		0.6419	
	Percentage	32.16%		44.73%	
	EMD	0.3793	0.2609	1.5862	1.435
	Error	0.1184		0.1512	
	Percentage	45.38%		10.54%	

Figure 5.36: Estimation of breathing rate and heartbeat rate from radar system while standing-1

Segment 9 with normal breathing	**Modified FFT**	**0.3448**	**0.2414**	**1.103**	**1.478**
	Error	**0.1034**		**0.375**	
	Percentage	42.83%		25.37%	
	EMD	**0.4483**	**0.2414**	**1.2758**	**1.478**
	Error	**0.2069**		**0.2022**	
	Percentage	85.71%		13.68%	
Segment 10 with normal breathing	**Modified FFT**	**0.3103**	**0.2381**	**1.138**	**1.429**
	Error	**0.0722**		**0.291**	
	Percentage	30.32%		20.36%	
	EMD	**0.3448**	**0.2381**	**1.1724**	**1.429**
	Error	**0.1067**		**0.2566**	
	Percentage	44.81%		17.96%	
Segment 11 with normal breathing	**Modified FFT**	**0.2069**	**0.2414**	**1.069**	**1.448**
	Error	**0.0345**		**0.379**	
	Percentage	14.29%		26.17%	
	EMD	**0.2414**	**0.2414**	**1.1034**	**1.448**
	Error	**0**		**0.3446**	
	Percentage	0.00%		23.80%	
Segment 12 with normal breathing	**Modified FFT**	**0.2759**	**0.2414**	**1.103**	**1.448**
	Error	**0.0345**		**0.345**	
	Percentage	14.29%		23.82%	
	EMD	**0.2069**	**0.2414**	**1.1379**	**1.448**
	Error	**0.0345**		**0.3101**	
	Percentage	14.29%		21.42%	
Segment 13 with normal breathing	**Modified FFT**	**0.4483**	**0.3103**	**1.483**	**1.448**
	Error	**0.138**		**0.035**	
	Percentage	44.47%		2.42%	
	EMD	**0.4827**	**0.3103**	**1.5172**	**1.448**
	Error	**0.1724**		**0.0692**	
	Percentage	55.56%		4.78%	
Segment 14 with normal breathing	**Modified FFT**	**0.1379**	**0.3103**	**0.9655**	**1.276**
	Error	**0.1724**		**0.3105**	
	Percentage	55.56%		24.33%	
	EMD	**0.1379**	**0.3103**	**1.5172**	**1.276**
	Error	**0.1724**		**0.2412**	
	Percentage	55.56%		18.90%	
Segment 15 with normal breathing	**Modified FFT**	**0.1379**	**0.2414**	**0.8965**	**1.345**
	Error	**0.1035**		**0.4485**	
	Percentage	42.87%		33.34%	
	EMD	**0.3793**	**0.2414**	**0.931**	**1.345**
	Error	**0.1379**		**0.414**	
	Percentage	57.12%		30.78%	
Segment 16 with normal breathing	**Modified FFT**	**0.2069**	**0.3103**	**1.241**	**1.448**
	Error	**0.1034**		**0.207**	
	Percentage	33.32%		14.30%	
	EMD	**0.2414**	**0.3103**	**1.1379**	**1.448**
	Error	**0.0689**		**0.3103**	
	Percentage	22.20%		21.42%	

Figure 5.37: Estimation of breathing rate and heartbeat rate from radar system while standing-2

Segment 17 with normal breathing	Modified FFT	0.5172	0.2759	1.724	1.448
	Error	0.2413		0.276	
	Percentage	87.46%		19.06%	
	EMD	0.4827	0.2759	1.7586	1.448
	Error	0.2068		0.3106	
	Percentage	74.95%		21.45%	
Segment 18 with normal breathing	Modified FFT	0.3103	0.3103	1.448	1.414
	Error	0		0.034	
	Percentage	0.00%		2.40%	
	EMD	0.2414	0.3103	1.4827	1.414
	Error	0.0689		0.0687	
	Percentage	22.20%		4.86%	
Modified FFT	average error	0.112111111		0.271966667	
	avg percentage	42.55%		18.54%	
	median error	0.1304		0.2835	
	edian percentag	35.40%		19.71%	
EMD	average error	0.129355556		0.231166667	
	avg percentage	49.36%		15.66%	
	median error	0.12815		0.2489	
	edian percentag	50.02%		16.78%	

Figure 5.38: Estimation of breathing rate and heartbeat rate from radar system while standing-3

Chapter 6

Breathing and heart rate estimation of subjects oriented at different angles relative to the radar

The goal of this chapter is to estimate the heartbeat and breathing rates when the subject is not moving and is oriented towards the radar at different angles. Two algorithms were compared: modified FFT algorithm and EMD with Minkowski distance.

These experiments were performed on Dec 17th, 2015 at the University of Ottawa, SITE building, room 3013. Figure 2.3 shows that the radar is placed on the edge of a desk, facing the door, and that the room is closed with no windows. There are three marks on the floor: mark A, B and C. The approximate distances to the radar from points A, B and C are 7 meters, 4.5 meters, and 2 meters, respectively. In these experiments, the subject is sitting at mark B, shown in Figure 2.3. Each experiment lasts one minute and includes:

1. Subject is oriented away from the radar and breathes normally - this is described in Section 6.1.
2. Subject is oriented 90 degrees relative to the radar and breathes normally - this is described in Section 6.2.
3. Subject is facing the radar and breathes normally.

In this chapter, we divide the data into 10 second segments so that we get 6 segments of data per experiment. Because we already analyzed the signal when the subject is facing the radar, here we will only present one segment of each experiment when the radar is behind the subject and when the radar is on the left of the subject.

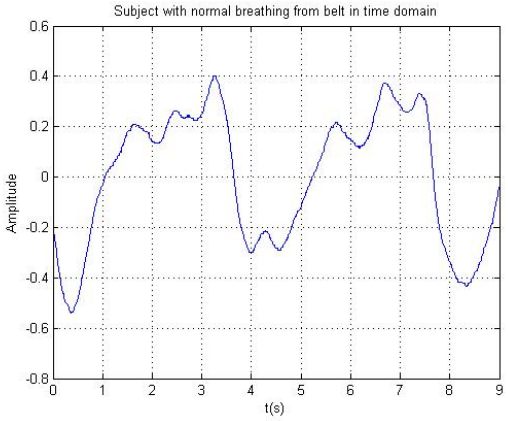

Figure 6.1: Signal from the belt when the subject is oriented 180 degrees relative to the radar with normal breathing.

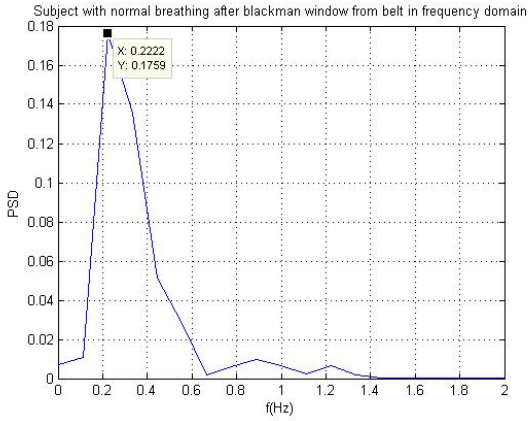

Figure 6.2: Signal from the belt in frequency domain after applying the Blackman window when the subject is oriented 180 degrees relative to the radar with normal breathing.

6.1 Breathing and heart rate estimation when the subject is oriented 180 degrees relative to the radar

6.1.1 Reference data from belt and ECG sensors

Figure 6.1 shows 10 seconds of the reference breathing signal from the belt. After applying FFT on it, we can see from Figure 6.2 the reference breathing rate which is 0.2222 Hz.

Figure 6.3 shows 10 seconds of the reference heartbeat signal from ECG sensors. After applying FFT on it, we can see from Figure 6.4 the reference heartbeat rate which is 1.222 Hz.

6.1.2 Breathing rate estimation from the radar signal

Figure 6.5 shows one segment of the radar signal when the subject is sitting in front of the radar and is turned away from it. Based on our analysis, a signal from zone four was chosen to extract the breathing signal.

After applying modified FFT (Section 3.2) on it, we estimate the breathing rate to be 0.2222 Hz as shown in Figure 6.6. Compared with the reference breathing rate of 0.2222 Hz obtained from belt, the error is 0 Hz.

Next, we applied EMD on the same 10 seconds of data from the radar system. The IMFs are shown in Figure 6.7.

After applying FFT on each IMF and finding the frequency of maximum peaks, the rate of each IMF is in Hz:

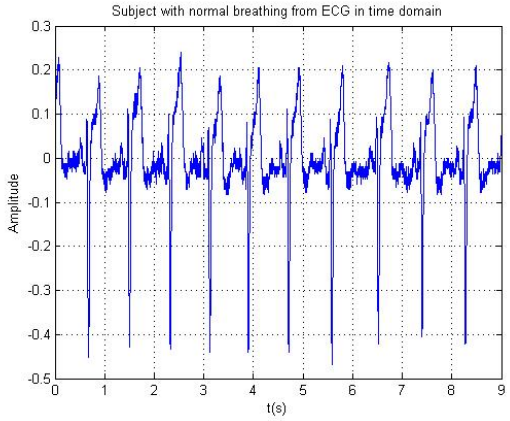

Figure 6.3: Signal from the ECG when the subject is oriented 180 degrees relative to the radar with normal breathing.

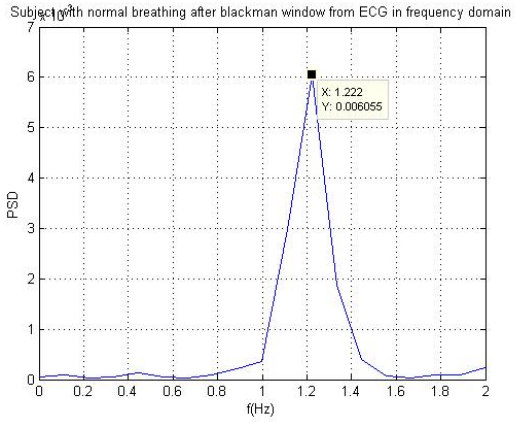

Figure 6.4: Signal from the ECG in frequency domain after applying the Blackman window when the subject is oriented 180 degrees relative to the radar with normal breathing.

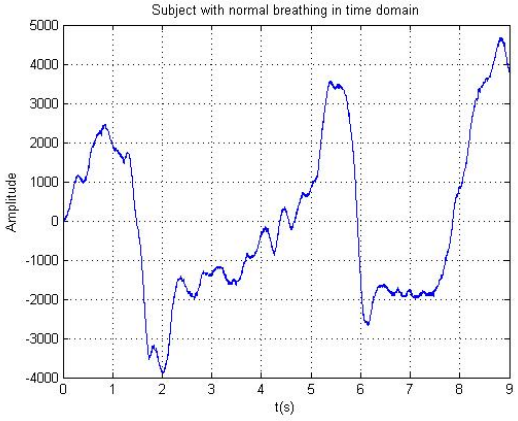

Figure 6.5: Signal from the radar when the subject is oriented 180 degrees relative to the radar with normal breathing.

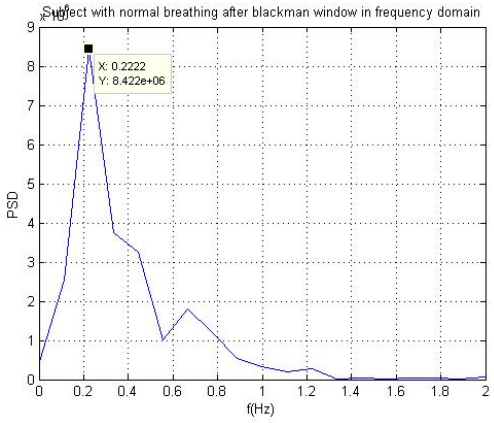

Figure 6.6: Signal from the radar in frequency domain after applying the Blackman window when the subject is oriented 180 degrees relative to the radar with normal breathing.

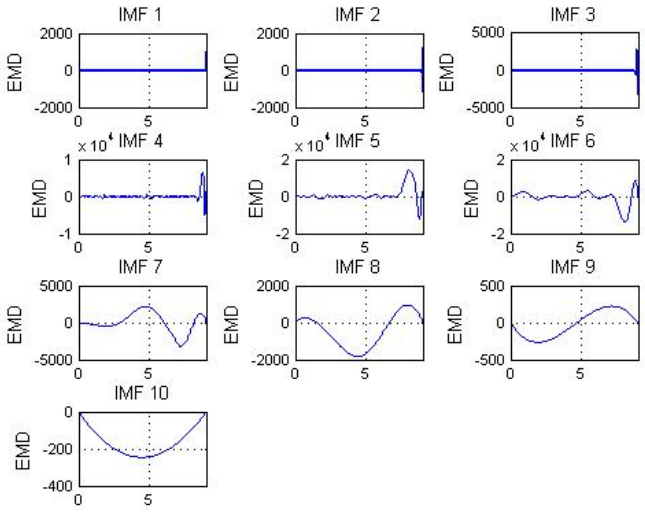

Figure 6.7: IMFs of 10 seconds of radar signals when the subject is oriented 180 degrees relative to the radar while breathing normally.

breathing_rate_of_imf 1 = [108.4371];

breathing_rate_of_imf 2 = [68.1065];

breathing_rate_of_imf 3 = [6.7773];

breathing_rate_of_imf 4 = [2.2221];

breathing_rate_of_imf 5 = [0.2222];

breathing_rate_of_imf 6 = [0.3333];

breathing_rate_of_imf 7 = [0.3333];

breathing_rate_of_imf 8 = [0.2222];

breathing_rate_of_imf 9 = [0.2222];

breathing_rate_of_imf 10 = [0.1111];

To figure out which IMF corresponds to the estimated breathing signal, we use the Minkowski distance which is explained in Chapter 3.3.1.

After applying the Minkowski distance on each IMF, we get the results shown in Figure 6.8. The minimum is IMF 7 which has breathing rate of 0.3333 Hz. Compared with the reference breathing rate of 0.2222 Hz obtained from the belt, the error is 0.1111 Hz, which is 50.00% off from the reference breathing rate.

6.1.3 Heart rate estimation from the radar signal

Figure 6.9 above shows a 10 seconds signal collected from the radar system. The bottom figure shows the radar signal after removing breathing signal. Since we already found the

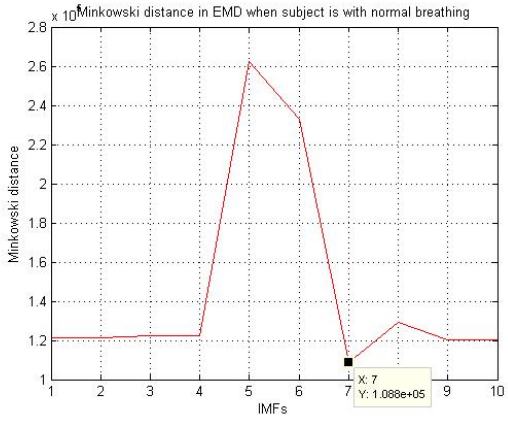

Figure 6.8: Minkowski distance of each IMF from Figure 6.7 when the subject is oriented 180 degrees relative to the radar while breathing normally.

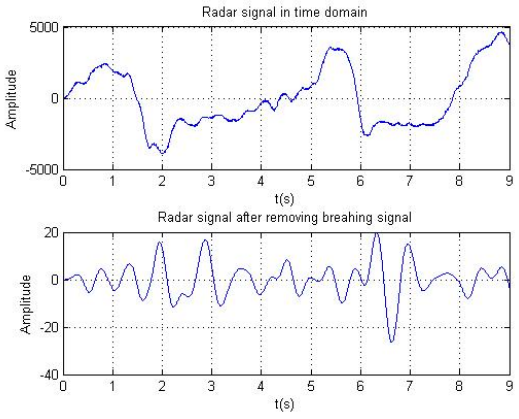

Figure 6.9: Signal from the radar before and after removing the breathing signal from it when the subject is oriented 180 degrees relative to the radar and breathing normally

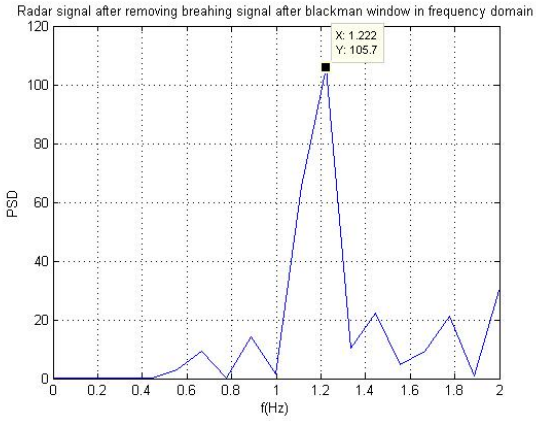

Figure 6.10: Signal from the radar after removing breathing in frequency domain after applying the Blackman window when the subject is oriented 180 degrees relative to the radar

breathing rate from Section 6.1.2, we can use a notch filter to remove our breathing signal and use the remaining signal to estimate the heart rate.

After applying modified FFT (Section 3.2) on the signal and finding the frequency of the maximum peak in the spectrum, the estimated heart rate is 1.222 beat per second as shown in Figure 6.10. Compared with the reference heartbeat rate 1.222 Hz from ECG sensors, we obtain the error of 0 Hz.

Next, we applied EMD on the same 10 seconds of data from the radar system. The IMFs are shown in Figure 6.11.

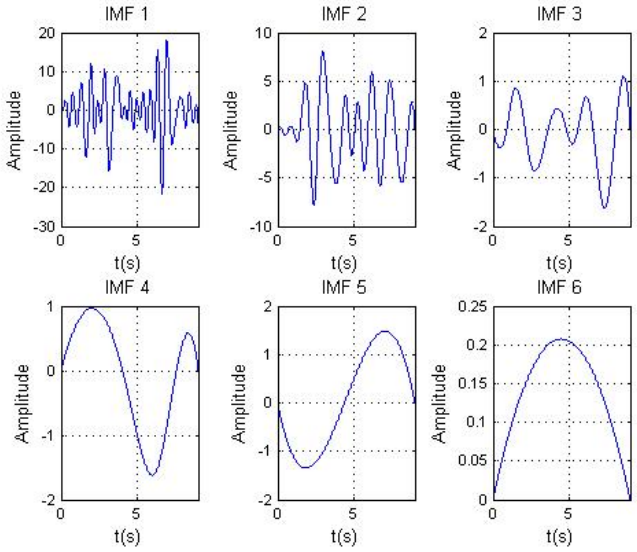

Figure 6.11: IMFs of 10 seconds of radar signals with removed breathing component when the subject is oriented 180 degrees relative to the radar while breathing normally

After applying FFT on each IMF and finding the frequency of the maximum peak of each IMF, we obtain the following:

breathing_rate_of_imf 1 = [1.3332];

breathing_rate_of_imf 2 = [0.7777];

breathing_rate_of_imf 3 = [0.5555];

breathing_rate_of_imf 4 = [0.2222];

breathing_rate_of_imf 5 = [0.2222];

breathing_rate_of_imf 6 = [0.1111];

To figure out which IMF is our estimate heartbeat signal, we use the Minkowski distance which is shown in Chapter 3.3.1.

After applying the Minkowski distance on each IMF, we get the results shown in Figure 6.12. The minimum Minkowski distance is for IMF 1, so the heart rate is 1.3332 Hz. Compared with the reference heartbeat rate of 1.222 Hz which we get from ECG sensors, the error is 0.1112 Hz, which is 9.10% off from the reference heart rate.

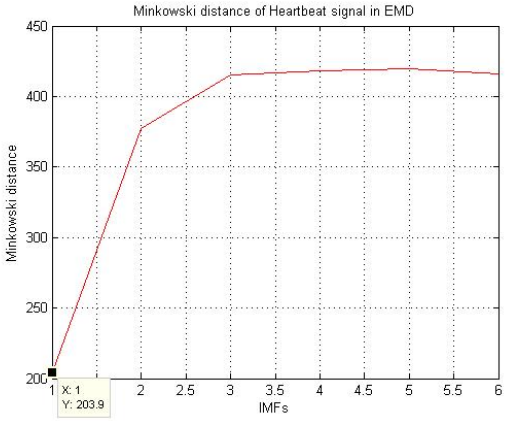

Figure 6.12: Minkowski distance of each IMF from Figure 6.11 when Subject is oriented 180 degrees relative to the radar with normal breathing

6.2 Breathing and heart rate estimation when the subject is oriented 90 degrees relative to the radar

6.2.1 Reference data from belt and ECG sensors

From Figure 6.13, we can find the 10 seconds reference breathing signal from belt. After applying FFT on it, we can find the reference breathing rate, which is 0.2222 from Figure 6.14.

From Figure 6.15, we can find the 10 seconds reference heartbeat signal from ECG sensors. After applying FFT on it, we can find the reference heartbeat rate, which is 1.111 from Figure 6.16.

6.2.2 Radar signal to estimate breathing rate

Figure 6.17 shows us 10 seconds signal collected from the radar system.

After applying modified FFT (Section 3.2) on it, we can get our estimated breathing rate which is 0.1111 beat per second, as shown in Figure 6.18. Compared with the reference breathing rate 0.2222 which we get from the belt, the error is 0.1111, which is 50% off.

Comparing with EMD: after applying EMD on the same 10 seconds data from the radar system, the IMFs is shown in Figure 6.19

After applying FFT on each IMF and finding the frequency of maximum peaks, the rate of each IMF is in Hz:

breathing_rate_of_imf 1 = [175.4371];

breathing_rate_of_imf 2 = [57.5531];

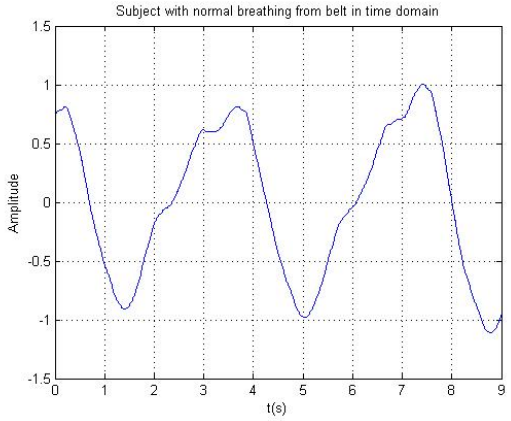

Figure 6.13: Subject is oriented 90 degrees relative to the radar with normal breathing from belt

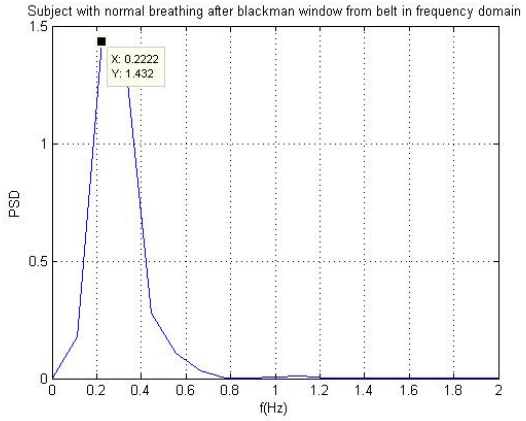

Figure 6.14: Subject is oriented 90 degrees relative to the radar with normal breathing from the belt in frequency domain after the Blackman window

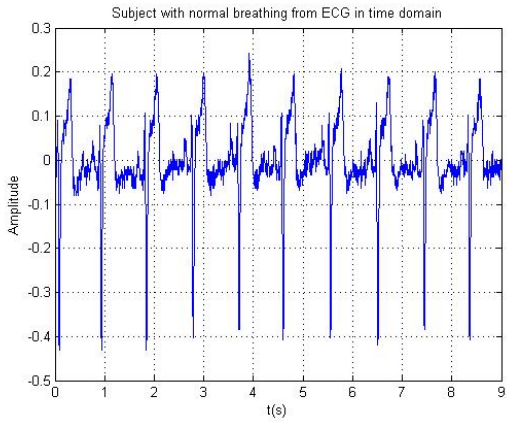

Figure 6.15: Subject is oriented 90 degrees relative to the radar with normal breathing from ECG sensors

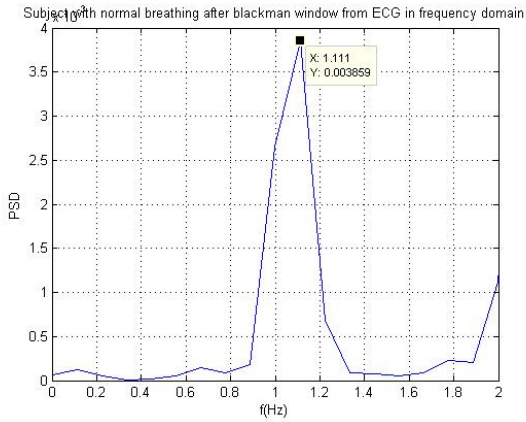

Figure 6.16: Subject is oriented 90 degrees relative to the radar with normal breathing from ECG sensors in frequency domain after the Blackman window

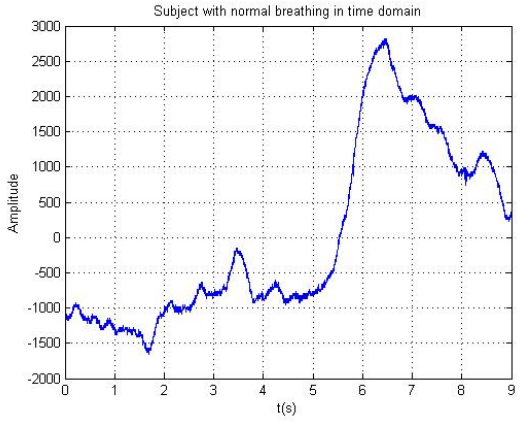

Figure 6.17: Subject is oriented 90 degrees relative to the radar with normal breathing from the radar system

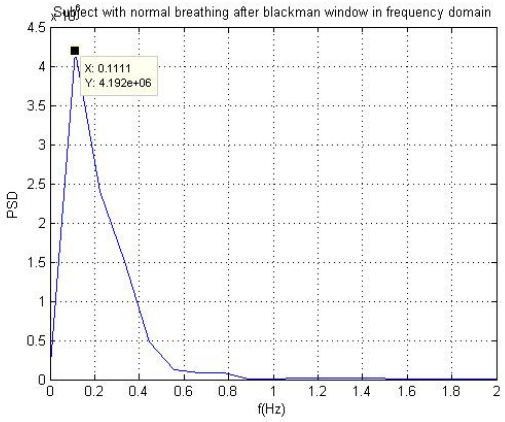

Figure 6.18: Subject is oriented 90 degrees relative to the radar with normal breathing from the radar system in frequency domain after the Blackman window

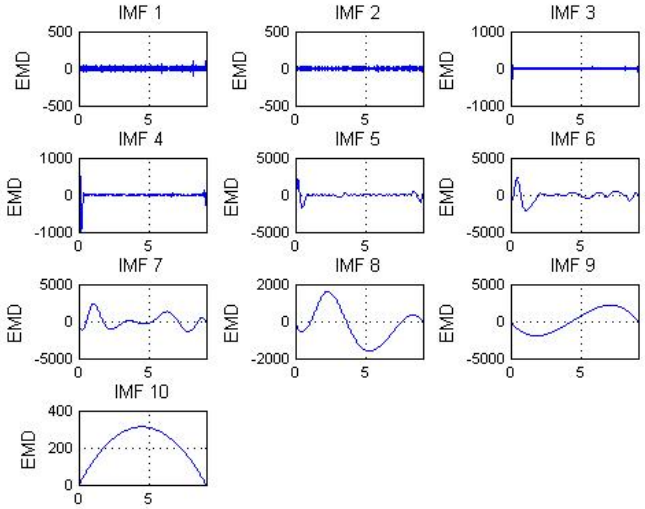

Figure 6.19: IMFs of 10 seconds radar signals when the subject is oriented 90 degrees relative to the radar with normal breathing

breathing_rate_of_imf 3 = [30.8876];

breathing_rate_of_imf 4 = [7.8886];

breathing_rate_of_imf 5 = [1.3333];

breathing_rate_of_imf 6 = [0.5555];

breathing_rate_of_imf 7 = [0.3333];

breathing_rate_of_imf 8 = [0.2222];

breathing_rate_of_imf 9 = [0.2222];

breathing_rate_of_imf 10 = [0.1111];

To figure out which IMF is our estimate breathing signal, we use the Minkowski distance shown in Chapter 3.3.1.

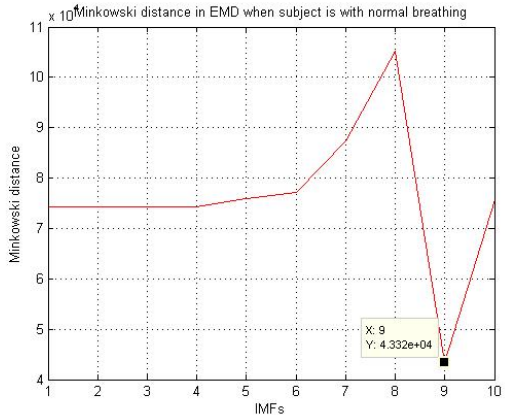

Figure 6.20: Minkowski distance of each IMF from Figure 6.19 when the subject is oriented 90 degrees relative to the radar with normal breathing

After applying the Minkowski distance on each IMF, we get the results shown in Figure 6.20, to fins that the estimate breathing signal is in IMF 9 which is 0.2222 per second. Compared with the reference breathing rate 0.2222 which we get from belt, the error is 0 per second in this case while the subject is oriented 90 degrees relative to the radar.

6.2.3 Radar signal to estimate heartbeat rate

Figure 6.21 shows two figures: the top one shows a 10 seconds signal collected from the radar system, while the bottom one shows us the radar signal after removing the breathing signal. Because we already found the breathing rate from section 6.2.2, we can use a notch filter to remove our breathing signal and use the remaining signal to estimate the heartbeat rate.

After applying modified FFT (Section 3.2) on it, we can get our estimated heartbeat rate which is 1.333 beat per second shown in Figure 6.22. Comparing with the reference

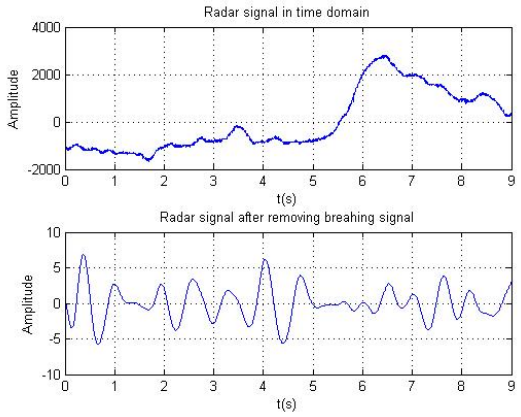

Figure 6.21: Subject is oriented 90 degrees relative to the radar with normal breathing from the radar system

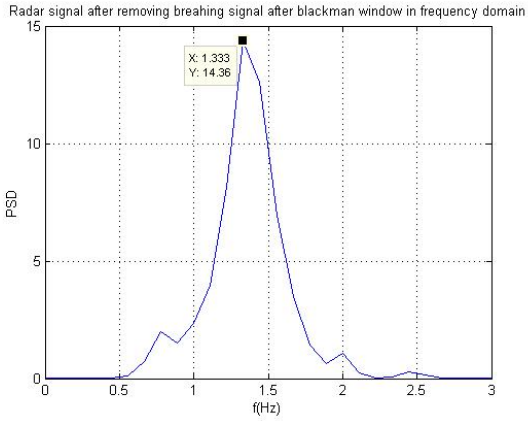

Figure 6.22: Subject is oriented 90 degrees relative to the radar with normal breathing from the radar system in the frequency domain after the Blackman window

heartbeat rate 1.111 which we get from ECG sensors, the error is 0.222, which is 19.98% of reference heartbeat rate from ECG sensors in this case when Subject is oriented 90 degrees relative to the radar.

Comparing with EMD: after applying EMD on the same 10 second data from the radar system, the IMFs is shown in Figure 6.23

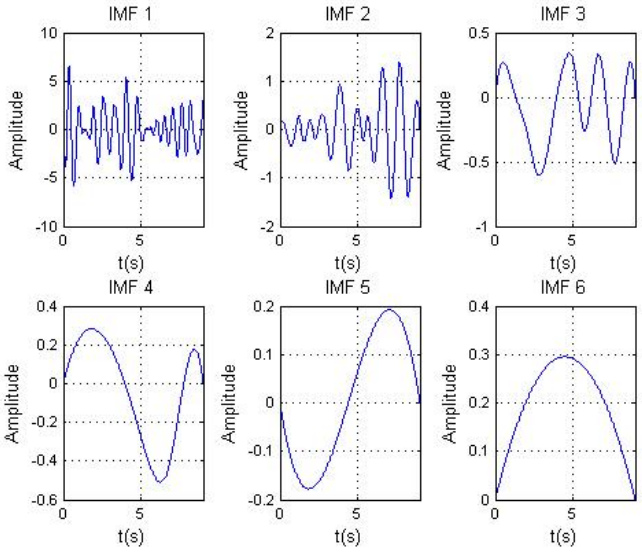

Figure 6.23: IMFs of 10 second radar signals when the subject is oriented 90 degrees relative to the radar with normal breathing

After applying FFT on each IMF and finding the frequency of maximum peaks, the rate of each IMF is in Hz:

breathing_rate_of_imf 1 = [1.4444];

breathing_rate_of_imf 2 = [0.8889];

breathing_rate_of_imf 3 = [0.3333];

breathing_rate_of_imf 4 = [0.2222];

breathing_rate_of_imf 5 = [0.2222];

breathing_rate_of_imf 6 = [0.1111];

To figure out which IMF is our estimate heartbeat signal, we use the Minkowski distance as seen in Chapter 3.3.1.

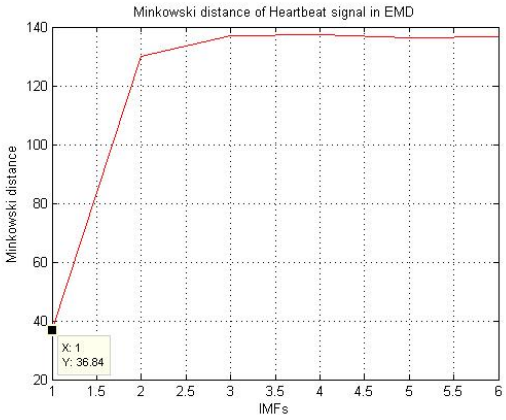

Figure 6.24: Minkowski distance of each IMF from Figure 6.23 when the subject is oriented 90 degrees relative to the radar with normal breathing

After applying the Minkowski distance on each IMF, we get the results shown in Figure 6.24 and find that the estimated heartbeat signal is in IMF 1, which is 1.4444 per second. Compared with the reference heartbeat rate 1.111 obtained from ECG sensors, the error is 0.3334 per second, which is 30.01% 0ff from reference heartbeat rate when the subject is oriented 90 degrees relative to the radar.

6.3 Discussion

Figure 6.25 shows the breathing rate errors using modified FFT, which is relative to the reference breathing rate estimated from the belt when the subject is at different orientations relative to the radar. Figure 6.26 shows the breathing rate errors using EMD method for the same experiment. Similarly, Figure 6.27 and Figure 6.28 show the heart rate errors for FFT-based and for EMD-based methods for the same experiment.

Tables 6.29 and 6.30 show estimated breathing rate and heart rate. Errors are the absolute errors between the estimated rate and the reference rate. Percentages are calculated by: error divide by reference rate. So, to summarize:

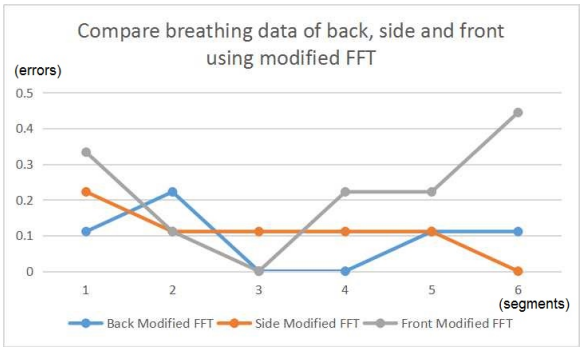

Figure 6.25: Comparison of breathing rate errors when the subject is sitting oriented at 0, 90 and 180 degrees relative to the radar using modified FFT

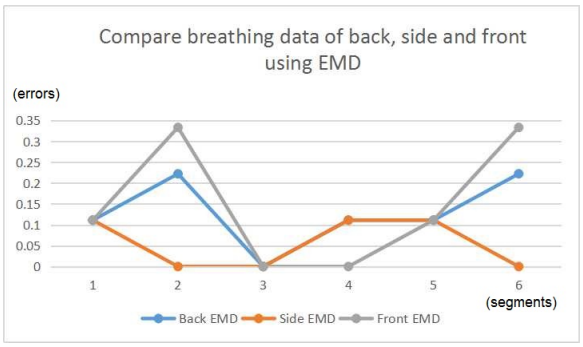

Figure 6.26: Comparison of breathing rate errors when the subject is sitting oriented at 0, 90 and 180 degrees relative to the radar using EMD

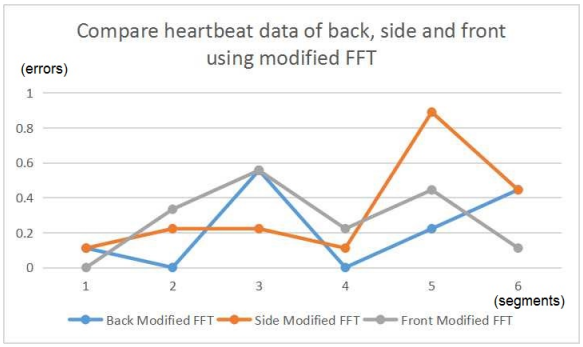

Figure 6.27: Comparison of heart rate errors when the subject is sitting oriented at 0, 90 and 180 degrees relative to the radar using modified FFT

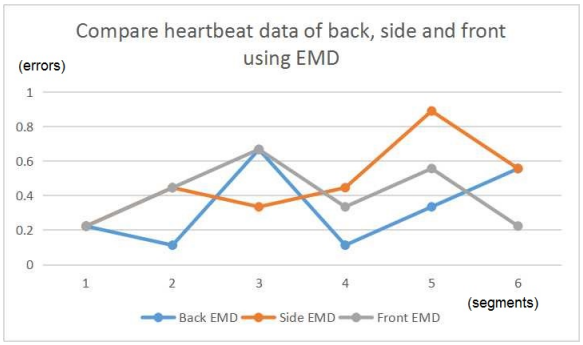

Figure 6.28: Comparison of heart rate errors when the subject is sitting oriented at 0, 90 and 180 degrees relative to the radar using EMD

Normal breathing Rate		Back		Side		Front	
		Radar	Belt	Radar	Belt	Radar	Belt
Segment 1 with normal breathing	Modified FFT	0.3333	0.2222	0.1111	0.3333	0.5555	0.2222
	Error	0.1111		0.2222		0.3333	
	Percentage	50.00%		66.67%		150.00%	
	EMD	0.3333	0.2222	0.2222	0.3333	0.3333	0.2222
	Error	0.1111		0.1111		0.1111	
	Percentage	50.00%		33.33%		50.00%	
Segment 2 with normal breathing	Modified FFT	0.1111	0.3332	0.3333	0.2222	0.3333	0.2222
	Error	0.2221		0.1111		0.1111	
	Percentage	66.66%		50.00%		50.00%	
	EMD	0.1111	0.3332	0.2222	0.2222	0.5555	0.2222
	Error	0.2221		0		0.3333	
	Percentage	66.66%		0.00%		150.00%	
Segment 3 with normal breathing	Modified FFT	0.2222	0.2222	0.1111	0.2222	0.2222	0.2222
	Error	0		0.1111		0	
	Percentage	0.00%		50.00%		0.00%	
	EMD	0.2222	0.2222	0.2222	0.2222	0.2222	0.2222
	Error	0		0		0	
	Percentage	0.00%		0.00%		0.00%	
Segment 4 with normal breathing	Modified FFT	0.2222	0.2222	0.2222	0.3333	0.1111	0.3333
	Error	0		0.1111		0.2222	
	Percentage	0.00%		33.33%		66.67%	
	EMD	0.3333	0.2222	0.2222	0.3333	0.3333	0.3333
	Error	0.1111		0.1111		0	
	Percentage	50.00%		33.33%		0.00%	
Segment 5 with normal breathing	Modified FFT	0.1111	0.2222	0.2222	0.3333	0.1111	0.3333
	Error	0.1111		0.1111		0.2222	
	Percentage	50.00%		33.33%		66.67%	
	EMD	0.3333	0.2222	0.2222	0.3333	0.2222	0.3333
	Error	0.1111		0.1111		0.1111	
	Percentage	50.00%		33.33%		33.33%	
Segment 6 with normal breathing	Modified FFT	0.3333	0.2222	0.2222	0.2222	0.6666	0.2222
	Error	0.1111		0		0.4444	
	Percentage	50.00%		0.00%		200.00%	
	EMD	0.4444	0.2222	0.2222	0.2222	0.5555	0.2222
	Error	0.2222		0		0.3333	
	Percentage	100.00%		0.00%		150.00%	
Modified FFT	average error	0.092566667		0.1111		0.2222	
	vg percentag	36.11%		38.89%		88.89%	
	median error	0.1111		0.1111		0.2222	
	dian percenta	50.00%		41.67%		66.67%	
EMD	average error	0.1296		0.05555		0.148133333	
	vg percentag	52.78%		16.67%		63.89%	
	median error	0.1111		0.05555		0.1111	
	dian percenta	50.00%		16.67%		41.67%	

Figure 6.29: Comparing breathing rate errors per 10-sec segment when the subject is sitting oriented at 0, 90 and 180 degrees relative to the radar

Heartbeat Rate		Back		Side		Front	
		Radar	ECG	Radar	ECG	Radar	ECG
Segment 1 with normal breathing	Modified FFT	1.333	1.222	1.222	1.111	1.222	1.222
	Error	0.111		0.111		0	
	Percentage	9.08%		9.99%		0.00%	
	EMD	1.4443	1.222	1.3333	1.111	1.4443	1.222
	Error	0.221		0.2223		0.221	
	Percentage	18.08%		20.01%		18.08%	
Segment 2 with normal breathing	Modified FFT	1.222	1.222	0.8889	1.111	1.555	1.222
	Error	0		0.2221		0.333	
	Percentage	0.00%		19.99%		27.25%	
	EMD	1.3332	1.222	1.5555	1.111	1.6665	1.222
	Error	0.111		0.4445		0.4445	
	Percentage	9.08%		40.01%		36.37%	
Segment 3 with normal breathing	Modified FFT	1.778	1.222	1.333	1.111	1.778	1.222
	Error	0.556		0.222		0.556	
	Percentage	45.50%		19.98%		45.50%	
	EMD	1.8888	1.222	1.4444	1.111	1.8887	1.222
	Error	0.666		0.3334		0.6667	
	Percentage	54.50%		30.01%		54.56%	
Segment 4 with normal breathing	Modified FFT	1.222	1.222	1.222	1.111	1.333	1.111
	Error	0		0.111		0.222	
	Percentage	0.00%		9.99%		19.98%	
	EMD	1.3332	1.222	1.5555	1.111	1.4443	1.111
	Error	0.1112		0.4445		0.3333	
	Percentage	9.10%		40.01%		30.00%	
Segment 5 with normal breathing	Modified FFT	1.444	1.222	2	1.111	1.555	1.111
	Error	0.222		0.889		0.444	
	Percentage	18.17%		80.02%		39.96%	
	EMD	1.5555	1.222	1.9999	1.111	1.6665	1.111
	Error	0.3335		0.8889		0.5555	
	Percentage	27.29%		80.01%		50.00%	
Segment 6 with normal breathing	Modified FFT	1.667	1.222	1.555	1.111	1.222	1.111
	Error	0.445		0.444		0.111	
	Percentage	36.42%		39.96%		9.99%	
	EMD	1.7777	1.222	1.6666	1.111	1.3332	1.111
	Error	0.555		0.5556		0.2222	
	Percentage	45.42%		50.01%		20.00%	
Modified FFT	average error	0.222333333		0.333183333		0.277666667	
	vg percentag	18.20%		29.99%		23.78%	
	median error	0.1665		0.22205		0.2775	
	dian percenta	13.63%		19.99%		23.62%	
EMD	average error	0.33295		0.481533333		0.4072	
	vg percentag	27.24%		43.34%		34.84%	
	median error	0.27725		0.4445		0.3889	
	dian percenta	22.69%		40.01%		33.19%	

Figure 6.30: Comparing heart rate errors per 10-sec segment when the subject is sitting oriented at 0, 90 and 180 degrees relative to the radar

1. For breathing rate estimation, the average estimated error when the subject is facing the radar is about 0.2222 Hz using modified FFT, and is 0.1481 Hz using EMD. The average error between the estimated breathing rate and the reference breathing rate when the subject is oriented 180 degrees relative to the radar is about 0.0925 Hz using modified FFT and 0.1296 using EMD. The errors when facing the radar are larger because in those cases, the radar picks up not only the chest movements, but also the movements of the abdomen, facial movement and so on. When the subject is facing away from the radar, most of the movements are related to the expansion of the chest. This might be a potential reason why the result of the estimated breathing rate when facing away from the radar is more accurate than that when facing the radar directly. In addition, we can still find the breathing rate when the subject is turned 90 degrees away from the radar.

2. For heart rate estimation, the average error between the estimated heart rate and the reference heart rate when the subject is facing the radar is about 0.2776 Hz using modified FFT, and about 0.4072 Hz using EMD. The average error is smaller again when the subject is oriented 180 degrees relative to the radar and it is about 0.2223 Hz using modified FFT and is 0.3329 Hz using EMD. We believe these reasons explain the difference in errors, and that the estimated heart rate from the subject's side is less accurate than in the two other cases.

Chapter 7

Non-stationary analysis in walking experiments

The goal of this chapter is to show that we are able to track a subject as the subject moves in the room. The algorithm for detecting the zone where the subject occupies is described in Section 3.4. The experiment is shown in Figure 2.3. Here we choose 11 zones shown in figure 7.1.

7.1 Results

For this experiment, the subject is in front of the radar. The subject started to slowly walk from mark A shown in Figure 2.3 towards the radar to mark C and then back to mark A.

In figure 7.1, the radar signal on the left is from KG application and it shows the signal in the time domain in all 11 zones. The estimated position is shown in the right figure. The time instants and the zones that are detected are colored in red. Each time segment of estimated signal is 5 seconds long. As for processing, we first divide the radar signal into 5 second segments in each zone. Secondly, we find the maximum energy in each segment for each zone and then select the zone for a particular segment with maximum energy. The zone, where the maximal energy is, is determined as the current estimated position. Then, we repeat the algorithm for each segment to estimate the positions as shown in the right of the Figure 7.1.

7.2 Discussion

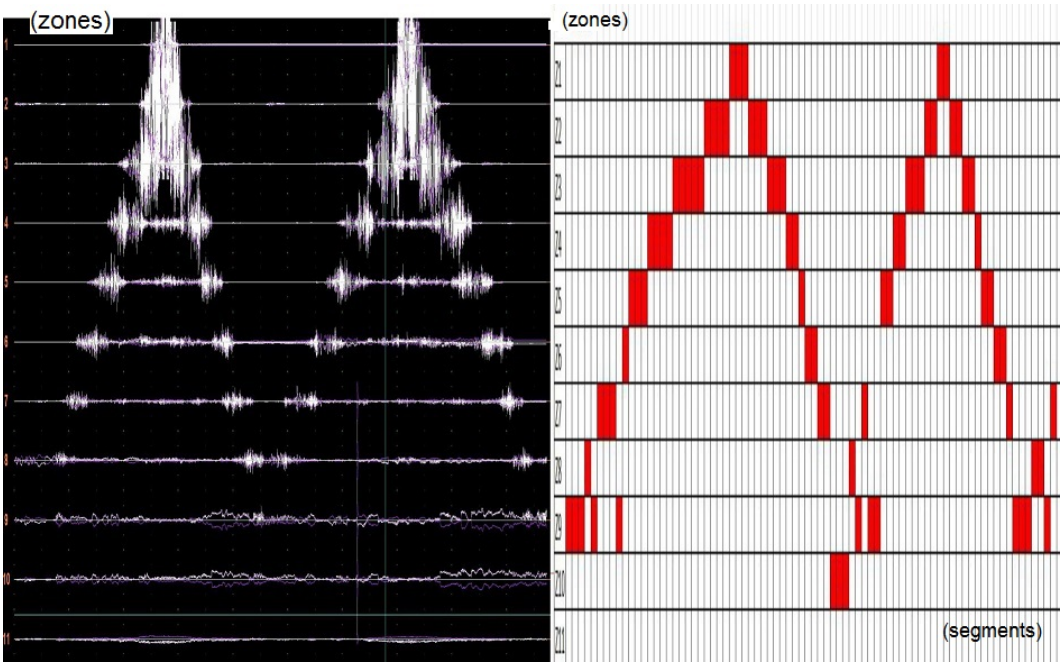

Figure 7.1: Figure on the left shows raw radar data per zone over time while the figure on the right shows zones divided into time segments. Red rectangles show estimates of current zone and time segment.

From Figure 7.1, we can see that there are errors in segment number 9, 43, 49, and 50. The total number of segments is 78 and, therefore, the error of estimating the walking position is about $\frac{4}{78} = 5.13\%$. This means that the method of estimating the correct position during the walk is about $1 - 5.13\% = 94.87\%$ in this case. We did five more experiments and found that the correct estimate of the position during the walk was about $1 - \frac{4}{48} = 91.67\%$, $1 - \frac{9}{61} = 85.25\%$, $1 - \frac{7}{73} = 90.41\%$, $1 - \frac{6}{32} = 81.25\%$, and $1 - \frac{11}{74} = 85.16\%$. So the average of all correct estimate of the position during the walk was approximately 88.1017%.

Chapter 8

Conclusion and future work

8.1 Conclusion

This project was based on the realistic detection of radar signals from subjects under different conditions and in different environments. It was part of a large project with the goal of detecting behavioral patterns of prison inmates in order to prevent any harm to their physical well-being.

In this study, we have developed two algorithms that allowed us to estimate the breathing rate of a subject without the need of physical contact. We developed algorithms called Modified Fast Fourier Transformation (FFT) and Minkowski distance after EMD which include a number of steps and sub-algorithms.

The work began by performing a large number of experiments in different real-life conditions using the radar system. Then, we used modified FFT and EMD based algorithms to detect more reliably the heartbeat and the breathing rates, which allowed us to evaluate the algorithms. This was done to find the algorithm that produced the lowest error between the estimated breathing rate and the reference breathing rate. We then extracted the breathing signal using the estimate breathing rate and filtering it out from the radar signal. Finally, we used the algorithm that produced the lowest error margin between the estimated heartbeat rate and the reference heart rate to extract a reliable estimates of the heart rate. In this case, modified FFT and EMD both worked well when the subject was sitting with a normal breathing pattern, as shown in section 4.3. At this point, we could tell that the average error and median error between these two algorithms were small. We also found that the breathing rate estimation when the subject was lying down was the most accurate, followed by the sitting down position. The estimation when the subject was in the standing position was the least accurate. These results are shown in section 6.3. We were also able to find the breathing signal and heartbeat signal when the subject looked to the opposite side to the radar or when the subject was oriented at 90 degrees relative to the radar as shown in section 5.3. We have noted that the former position yields slightly better data than when the subject was facing the radar. However, we were unable to detect a good heartbeat signal when the subject was oriented at 90 degrees relative to the radar

and therefore could not estimate a heart rate. Moreover, using so-called walking algorithm, we were able to detect the subject's position accurately as shown in section 7.2.

8.2 Future work

The radar signal collection was done using a radar device with four antennas. In the future, we would like to use all four antennas to scan the room to collect data, alternating from one antenna to the other automatically, each covering different angles. However, for the purpose of this project, only a single antenna was used to collect the data.

Another future direction includes monitoring more than one subject at a time.

In the future, we will not need to record the data and process it later. Instead, we will estimate the breathing rate and heartbeat rate in real-time.

Also, in the future, we will focus on extracting different features from the radar signal in order to classify the activities of the subject.

It is our hope that this original process of using the radar system may be used in the future to inexpensively and accurately detect and record the respiratory and cardiovascular activity of a human subject present in a closed room.

APPENDICES

Appendix A

MATLAB Code samples

A.1 Modified FFT and EMD for breathing rate estimation

```
clear all;
close all;
clc;

%%% modified FFT method for berathing rate estimation
%%% read radar data
x = csvread('C:\Users\Susie\Desktop\data\USE\thesis\New Radar
Data\November 3\XZ_NB_LY_F_A02_FR.csv',1);
%%% set sampling rate of raday system
fs=905.4333;
%%% select zone (where the subject is)
zone=9;
Ts= 1/fs;
%%% choose data in selected zone
L = (x(:,zone))';
%%% choose 30 sec data to analyze
signal1 = L(31*fs:60*fs);
%%% remove DC shift from radar signal
signal1 = signal1-mean(signal1);
t1 = 0:1/fs:(length(signal1)-1)/fs;
%%% plot radar signal in time domain
figure;
plot(t1(1:length(signal1)),signal1);
xlabel('t(s)');
ylabel('Amplitude');
title('Subject with normal breathing in time domain');
```

```
grid on;
%%%Apply IIR Butterworth bandpass filter
%%%using BPF applied for every range bin
nn=3;
s1=(0.2)/fs;
%normalized pass frequency
s2=(4)/fs;
%normalized pass frequency
[b11,a11] = butter(nn,[s1 s2],'bandpass');
signal1 = filter(b11,a11,(signal1));
%%% apply blackman window/hamming window
nfft = length(signal1);
% window = hamming(length(s));
window = blackman(length(signal1));
[p1,f1] = periodogram(signal1,window,nfft,fs);
%%% plot radar signal in frequency domain
figure;
plot(f1,abs(p1))
xlim([0 2]);
xlabel('f(Hz)');
ylabel('PSD');
title('Subject with normal breathing after blackman window in frequency domain');
grid on;

%%%%%
%%% EMD method for breathing rate estimation
xx = signal1;
t = t1;
%%% find IMFs of radar signal
imf=emd(xx);
for k = 1:length(imf)
b(k)=sum(imf{k}.*imf{k});
th=angle(hilbert(imf{k}));
d{k}=diff(th)/Ts/(2*pi);
end
[u,v]=sort(-b);
b=1-b/max(b);
%%% set time-frequency plots
N=length(xx);
c=linspace(0,(N-2)*Ts,N-1);
figure;
for k = v(1:2)
plot(c,d{k},'k.','Color',b([k k k]),'MarkerSize',3);
hold on;
grid on;
```

```
set(gca,'FontSize',8,'XLim',[0 c(end)],'YLim',[0 50]);
xlabel('Time'),
ylabel('Frequency');
title('Subject with normal breathing in fast time domain');
end
%%% set IMF plots
M = length(imf)
N = length(xx)
c = linspace(0,(N-1)*Ts,N);
figure;
for k = 1:M
subplot(4,3,k);
plot(c,imf{k});
ylabel('EMD');
title(sprintf('IMF %d',k));
grid on;
%%% apply hamming window on each IMF
nfft = length(imf{k});
window = hamming(length(imf{k}));
[p1,f1] = periodogram(imf{k},window,nfft,fs);
%%% find rate of each IMF
[value y1] = max(p1);
value
breathing_rate_of_imf{k}= y1*fs/length(t);
set(gca,'FontSize',8,'XLim',[0 c(end)]);
%%% Minkowski distance to find the right IMF
d_mink_sum = 0;
for k1 = 1:N;
d_mink(k1) = (abs(xx(k1)-imf{k}(k1))).^2;
d_mink_sum = d_mink_sum + d_mink(k1);
end
d_m(k) = d_mink_sum^(0.5);
end
q4 = length(d_mink);
%%% plot the Minkowski distance figure
figure;
%%% set the length of M1 equals to the number of IMFs
M1 = [1 2 3 4 5 6 7 8 9 10 11];
plot(M1,d_m,'r-');
grid on;
xlabel('IMFs'),
ylabel('Minkowski distance');
title('Minkowski distance in EMD when subject is with normal breathing');
```

A.2 Modified FFT and EMD for heartbeat rate estimation

```
clear all;
close all;
clc;

%%% read radar data in csv
x = csvread('C:\Users\Susie\Desktop\data\USE\thesis\New Radar
Data\November 3\XZ_NB_LY_F_A02_FR.csv',1);
%%% set sampling frequency of radar system
fs=905.4333;
%%% select zone (where the subject is)
zone=9;
Ts= 1/fs;
%%% choose data in selected zone
L = (x(:,zone))';
%%% divide data into 30 sec segments and select one segment
signal1 = L(31*fs:60*fs);
%%% remove DC shift from radar signal
signal1 = signal1-mean(signal1);
t1 = 0:1/fs:(length(signal1)-1)/fs;
%%% plot radar signal in time domain
figure;
plot(t1(1:length(signal1)),signal1);
xlabel('t(s)');
ylabel('Amplitude');
title('Subject with normal breathing in time domain');
grid on;
s=signal1;
t=t1;
%%% pre-processing
s_fft=abs(fft(s));
k=fs*[0:1/length(t):1-1/length(t)];
nfft = length(s);
%%%Apply IIR Butterworth bandpass filter
%%%using BPF applied for every range bin
nn=3;
%normalized pass frequency
s11=(0.2)/fs;
s22=(4)/fs;
[b111,a111] = butter(nn,[s11 s22],'bandpass');
s = filter(b111,a111,(s));
```

```
%%% apply hamming window/blackman window
% window = hamming(length(s));
window = blackman(length(s));
[p1,f1] = periodogram(s,window,nfft,fs);
%%% get estimated breathing rate
[value_b y_b] = max(p1);
Fs=fs;
%%%Apply IIR Butterworth bandpass filter
%%%using BPF applied for every range bin
nn=3;
%normalized pass frequency
s11=(1.6)/fs;
s22=(4)/fs;
[b111,a111] = butter(nn,[s11 s22],'bandpass');
s = filter(b111,a111,(s));
%%% apply notch filter to remove breathing rate and its harmonics
Breathing_rate_notch= value_b;
Fc = [Breathing_rate_notch, 2*Breathing_rate_notch,
3*Breathing_rate_notch, 4*Breathing_rate_notch];
Wc = Fc/(Fs/2);
BW = Wc/10;
mycomb = zeros(4,6);
[b1,a1] = iirnotch(Wc(1),BW(1));
mycomb(1,:) = [b1,a1];
[b2,a2] = iirnotch(Wc(2),BW(2));
mycomb(2,:) = [b2,a2];
[b3,a3] = iirnotch(Wc(3),BW(3));
mycomb(3,:) = [b3,a3];
[b4,a4] = iirnotch(Wc(4),BW(4));
mycomb(4,:) = [b4,a4];
%%% remove the breathing signal from radar signal
Y = sosfilt(mycomb,s);
figure;
%%% plot the radar signal comparing signal withour breathing signal
subplot(2,1,1);
plot(t1(1:length(signal1)),signal1);
xlabel('t(s)');
ylabel('Amplitude');
title('Radar signal in time domain');
grid on;
%%% plot the signal without breathing signal to find heartbeat rate
subplot(2,1,2);
plot(t1(1:length(Y)),Y);
xlabel('t(s)');
ylabel('Amplitude');
```

```
title('Radar signal after removing breahing signal');
grid on;
%%% remove DC from signal Y
Y = Y-mean(Y);
t1 = 0:1/fs:(length(Y)-1)/fs;
t = t1;
nfftY = length(Y);
%%% apply blackman window on new radar signal without breathing signal, which is
%%% signal Y
% window = hamming(length(s));
windowY = blackman(length(Y));
[p1Y,f1Y] = periodogram(Y,windowY,nfftY,fs);
%%% plot signal Y in frequency domain
figure;
plot(f1Y,abs(p1Y))
xlim([0 3]);
xlabel('f(Hz)');
ylabel('PSD');
title('Radar signal after removing breahing signal after blackman window
 in frequency domain');
grid on;
xx = Y;

%%%%%%
%%% use EMD method to find the heartbeat rate
%%% apply EMD on signal Y to get IMFs
imf=emd(xx);
for k = 1:length(imf)
b(k)=sum(imf{k}.*imf{k});
th=angle(hilbert(imf{k}));
d{k}=diff(th)/Ts/(2*pi);
end
[u,v]=sort(-b);
b=1-b/max(b);
%%% set time-frequency plots
N=length(xx);
c=linspace(0,(N-2)*Ts,N-1);
figure;
for k = v(1:2)
plot(c,d{k},'k.','Color',b([k k k]),'MarkerSize',3);
hold on;
grid on;
set(gca,'FontSize',8,'XLim',[0 c(end)],'YLim',[0 50]);
xlabel('Time'),
ylabel('Frequency');
```

```
title('signal s in fast time domain');
end
%%% set IMF plots
M = length(imf)
N = length(xx)
c = linspace(0,(N-1)*Ts,N);
figure;
for k = 1:M
subplot(2,3,k);
plot(c,imf{k});
xlabel('t(s)');
ylabel('Amplitude');
title(sprintf('IMF %d',k));
grid on;
%%% apply hamming window on each IMF
nfft = length(imf{k});
window = hamming(length(imf{k}));
[p1,f1] = periodogram(imf{k},window,nfft,fs);
%%% find max value in frequeny domain of each IMF
[value y1] = max(p1);
Heartbeat_rate_of_imf{k} = y1*fs/length(t)
set(gca,'FontSize',8,'XLim',[0 c(end)]);
%%% Minkowski distance to find the right IMF, which is the estimated
%%% heartbeat rate
d_mink_sum = 0;
for k1 = 1:N;
d_mink(k1) = (abs(xx(k1)-imf{k}(k1))).^2;
d_mink_sum = d_mink_sum + d_mink(k1);
end
d_m(k) = d_mink_sum^(0.5);
end
q4 = length(d_mink);
figure;
M1 = [1 2 3 4 5];
plot(M1,d_m,'r-');
grid on;
xlabel('IMFs'),
ylabel('Minkowski distance');
title('Minkowski distance of Heartbeat signal in EMD');
```

A.3 Walking algorithm

```
clear all;
close all;
clc;
%%% read walking data from radar system
x = csvread('C:\Users\Susie\Desktop\data\USE\walk\XZ_WALK_Z6Z10_5MIN.csv',1);
%%% set sampling frequency
fs = 1368.22; %ZB_WALK_3MIN:912.2944   XZ_WALK_Z6Z10_5MIN: 1368.22
T = 1/fs;
%%% set total number of zones where the subject is walking
zz = 5;
%%% set total number of segments (60 * 5 sec = 300 sec)
nn = 60;
%%% loop for zone: from zone one to five
for i = 1:zz;
zone = i;
%%% select data in one zone
xx = x(:,zone);
t = 0:1/fs:length(xx)/fs;
%%% plot selected data
figure(1);
subplot(zz,1,i);
plot(t(1:length(xx)),xx);
ylabel('Amplitude (v)');
if (i==1)
title('Time domain signal in different zones: ');
end
grid on;
end
xlabel('Time(s)');
p = zeros(zz,nn);
f = zeros(zz,nn);
for i = 1:zz
zone = i;
xx = x(:,zone);
%%% loop for segments: from 1 to nn
for j = 1:nn
xxx = xx((1+(length(xx)/nn)*(j-1)):((length(xx)/nn)*j),1);
%%% remove DC shift for each segment
xxx = xxx-mean(xxx);
nfft = length(xxx);
%%% apply hamming window on each segment
```

```
window = hamming(length(xxx));
[p1,f1] = periodogram(xxx,window,nfft,fs);
figure(j+1);
subplot(zz,1,(i));
plot(f1,p1);
axis([0.1 2 0 1e5]);
grid on;
if (i==zz)
xlabel('f(Hz)');
ylabel('PSD');
end
%%% calculate energy of each segment in every zone
E = sum(p1.^2);
%%% set enery into matrix p(i,j)
p(i,j) = E;
end
end
zone = zeros(1,nn);
%%% find the max energy in each segment as the subject's position
for j = 1:nn
[w q] = max(p(:,j));
zone(1,j) = q
end
```

Appendix B

GUI interface

To graphically present the results of processing of different algorithms for various situations, we developed graphical user interface (GUI) in Matlab.

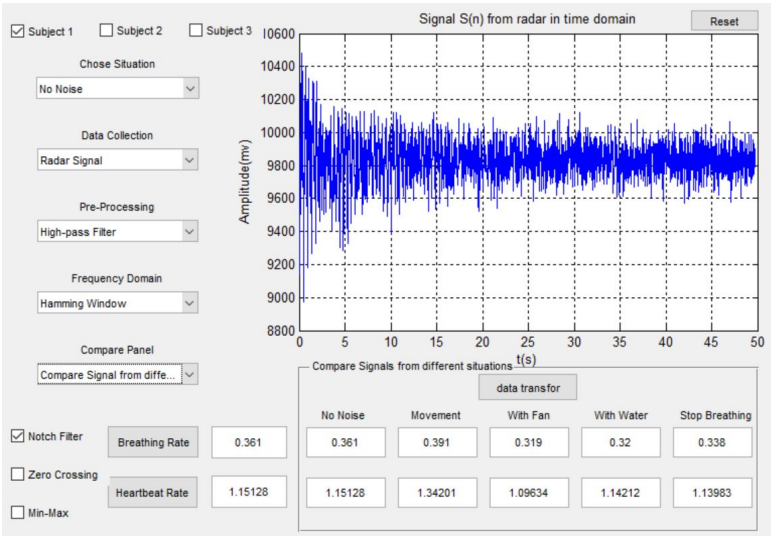

Figure B.1: GUI presenting breathing rate and hear rate in different situations

This GUI has the following functions:

- Select the experiment and the subject from the list of pre-recorded data files
- Select different situations (normal breathing, holding breath, breathing with movement, breathing with fan on, breathing with water flow)
- Select data (data from radar system, data from belt, and data from ECG sensors)

- Select window (rectangular window, Hamming window, Blackman window and so on)
- Select shown panel:
  - panel that compare with different situations (shown in Figure B.1)
  - panel that compare the estimated rate with reference rate
  - panel that compare data from different subjects
- select method to estimate breathing rate and heartbeat rate

Appendix C

Approvals

File Number: H09-14-14 **Date (mm/dd/yyyy):** 04/13/2015

Université d'Ottawa University of Ottawa
Bureau d'éthique et d'intégrité de la recherche Office of Research Ethics and Integrity

Certificate of Ethics Approval

Health Sciences and Science REB

Principal Investigator / Supervisor / Co-investigator(s) / Student(s)

First Name	Last Name	Affiliation	Role
Miodrag	Bolic	Engineering / Computer Science	Principal Investigator
Hilmi	Dajani	Engineering / Computer Science	Co-investigator
Mohamad	Forouzanfar	Harvard University	Co-investigator
Voicu	Groza	Engineering / Computer Science	Co-investigator
Mohamed	Mabrouk	Others / Others	Co-investigator
Xinyang	Zhang	Engineering / Electrical Engineering	Co-investigator
Izamil	Batkin	Engineering / Electrical Engineering	Project Coordinator
Sreeraman	Rajan	Engineering / Electrical Engineering	Project Coordinator

File Number: H09-14-14

Type of Project: Professor

Title: Processing and classification of radar signals to detect stop of breathing

Approval Date (mm/dd/yyyy)	Expiry Date (mm/dd/yyyy)	Approval Type
04/13/2015	04/12/2016	Ia

(Ia: Approval, Ib: Approval for initial stage only)

Special Conditions / Comments:
N/A

550, rue Cumberland 550 Cumberland Street
Ottawa (Ontario) K1N 6N5 Canada Ottawa, Ontario K1N 6N5 Canada
(613) 562-5387 • Téléc./Fax (613) 562-5338
http://www.recherche.uottawa.ca/deontologie/ http://www.research.uottawa.ca/ethics/index.html

Figure C.1: Approvals-1

File Number: H09-14-14 **Date (mm/dd/yyyy):** 04/13/2015

Université d'Ottawa University of Ottawa
Bureau d'éthique et d'intégrité de la recherche Office of Research Ethics and Integrity

This is to confirm that the University of Ottawa Research Ethics Board identified above, which operates in accordance with the Tri-Council Policy Statement and other applicable laws and regulations in Ontario, has examined and approved the application for ethical approval for the above named research project as of the Ethics Approval Date indicated for the period above and subject to the conditions listed the section above entitled "Special Conditions / Comments".

During the course of the study the protocol may not be modified without prior written approval from the REB except when necessary to remove subjects from immediate endangerment or when the modification(s) pertain to only administrative or logistical components of the study (e.g. change of telephone number). Investigators must also promptly alert the REB of any changes which increase the risk to participant(s), any changes which considerably affect the conduct of the project, all unanticipated and harmful events that occur, and new information that may negatively affect the conduct of the project and safety of the participant(s). Modifications to the project, information/consent documentation, and/or recruitment documentation, should be submitted to this office for approval using the "Modification to research project" form available at: http://research.uottawa.ca/ethics/submissions-and-reviews.

Please submit an annual status report to the Protocol Officer 4 weeks before the above-referenced expiry date to either close the file or request a renewal of ethics approval. This document can be found at: http://research.uottawa.ca/ethics/submissions-and-reviews.

If you have any questions, please do not hesitate to contact the Ethics Office at extension 5387 or by e-mail at: ethics@uOttawa.ca.

Germain Zongo
Protocol Officer for Ethics in Research
For Daniel Lagarec, Chair of the Sciences and Health Sciences REB

550, rue Cumberland 550 Cumberland Street
Ottawa (Ontario) K1N 6N5 Canada Ottawa, Ontario K1N 6N5 Canada
(613) 562-5387 • Téléc./Fax (613) 562-5338
http://www.recherche.uottawa.ca/deontologie/ http://www.research.uottawa.ca/ethics/index.html

Figure C.2: Approvals-2

Carleton University Research Ethics Board (CUREB)

Certificate of Ethics Clearance

Principal Investigator	Department	StudyNumber
Isar Nejadgholi	**Computer Science**	**16-107**

Co-Investigators and other researchers:

Researcher	Study Role	Position
Isar Nejadgholi	Collaborator	Post-Doctoral Fellow
Sreeraman Rajan	Faculty Supervisor	Faculty

Study Title: **Monitoring of vital signs of human using Doppler radar reflections**

Approval Date: **04/28/2016** Expiry Date: **08/31/2016** Approval Type: Final

Submitted Date	Study Component	Approval Date

Validity Term:

Comments:

Certification

The protocol describing the above-named project has been reviewed by Carleton University Research Ethics Board and the research procedures were found to be acceptable on ethical grounds for research involving human participants.

Chair, Carleton University Research Ethics Board (CUREB)

This Certificate of Clearance is valid for the above term provided there is no change in the research procedures.

Figure C.3: Approvals-3

References

[1] A. Bates, M. J. Ling, J. Mann, and D. K. Arvind. *Respiratory rate and flow waveform estimation from tri-axial accelerometer data*. International Conference on Body Sensor Networks, pp. 144-150, 2010.

[2] W. Johnston and Y. Mendelson. *Extracting breathing rate information from a wearable reflectance pulse oximeter sensor*. Conf Proc IEEE Eng Med Biol Soc., pp. 5388-5391, 2004.

[3] R. Murthy, I. Pavlidis, and P. Tsiamyrtzis. *Touchless monitoring of breathing function*. Conf Proc IEEE Eng Med Biol Soc., pp. 1196-1199, 2004.

[4] K. M. Chen, Y. Huang, J. Zhang, and A. Norman. *Microwave life-detection systems for searching human subjects under earthquake rubble and behind barrier*. IEEE Trans Biomed Eng 47, 2000, 105-114.

[5] A. D. Droitcour, V. M. Lubecke, J. Lin, and O. Boric-Lubecke. *A microwave radio for Doppler radar sensing of vital signs*. IEEE MTT-S Int Microw Symp Dig, Phoenix, 2001, 175-178.

[6] A. D. Droitcour, O. Boric-Lubecke, V. M. Lubecke, and J. Lin. *0.25 mm CMOS and BiCMOS single chip direct conversion Doppler radars for remote sensing of vital signs*.

[7] O. Boric-Lubecke, G. Awater, and V. M. Lubecke. *Wireless LAN PC card sensing of vital signs*. IEEE Conf Wireless Commun Technol, 2003, 206-207.

[8] J. Lin Y. Xiao, O. Boric-Lubecke, and V. M. Lubecke. *A Ka-band low power Doppler radar system for remote detection of cardiopul-monary motion*. Presented at the 27th IEEE Annual Engineering Medical and Biological Society Conference, Sep. 1-4, 2005.

[9] Y. Xiao, J. Lin, O. Boric-Lubecke, and V. M. Lubecke. *Frequency tuning technique for remote detection of heartbeat and respiration using low-power double-sideband transmission in Ka-band*. IEEE Trans Microw Theory Tech 54, 2006, 2023-2032.

[10] J. Mathew, Y. Semenova, and G. Farrell. *A miniature optical breathing sensor*. Optical Society of America, Photonics Research Center, Dublin Institute of Technology, Kevin St., Dublin 8, Ireland, Nov 26, 2012.

[11] K. Barrett, S. Barman, S. Boitano, and H. Brooks. *Ganong's Review of Medical Physiology*. 24th edition, 2012.

[12] S. L. DeBoer. *Newborn Emergency Home House Gecko*. Trafford Publishing p.30, ISBN 978-1-4120-3089-2, Nov 4, 2004.

[13] W. Q. Lindh, M. Pooler, C. D. Tamparo, B. M. Dahl, and J. Morris. *Delmar's Comprehensive Medical Assisting: Administrative and Clinical Competencies*. Cengage Learning. p. 573, ISBN 978-1-4354-1914-8, March 9, 2009.

[14] A. Rodriguez-Molinero, L. Narvaiza, J. Ruiz, and C. Galvez-Barron. *Normal respiratory rate and peripheral blood oxygen saturation in the elderly population*. J Am Geriatr Soc., 61(12):2238-40, Dec. 2013.

[15] *Target Heart Rates*. American Heart Association, May. 2014.

[16] *Tachycardia*. American Heart Association, 2014.

[17] I. A. Aladin, P. S. Whelton, H. M. Al-Mallah, J. M. Blaha, J. S. Keteyian, P. S. Juraschek, J. Rubin, A. C. Brawner, and D. E. Michos. *The American Journal of Cardiology*. doi:10.1016/j.amjcard.2014.08.042. ISSN 1879-1913. PMID 25439450., 114 (11), 2014.

[18] L. Chioukh, H. Boutayeb, D. Deslandes, and K. Wu. *Noise and sensitivity of harmonic radar architecture for remote sensing and detection of vital signs*. IEEE T. Microw. Theory, vol. 62, pp. 1847-1855, 2014.

[19] D. Girbau, A. Lazaro, A. Ramos, and R. Villarino. *Remote sensing of vital signs using a doppler radar and diversity to overcome null detection*. IEEE Sens. J., vol. 12, pp. 512-518, 2012.

[20] W. Massagram, V. M. Lubecke, A. Host-Madsen, and O. Boric-Lubecke. *Assessment of heart rate variability and respiratory sinus arrhythmia via doppler radar*. IEEE T. Microw. Theory, vol. 57, pp. 2542-2549, 2009.

[21] Y. Kim and L. Hao. *Human activity classication based on micro-doppler signatures using a support vector machine*. IEEE T. Geosci. Remote, vol. 47, pp. 1328-1337, 2009.

[22] G. E. Smith, K. Woodbridge, and C. J. Baker. *Naive bayesian radar micro-doppler recognition*. in IEEE Int. Conf. Radar, Adelaide, SA, Sep. 2008, p. 111-116.

[23] P. E. Cuddihy, D. J. Cleary, J. M. Ashe, and T. Yardibi. *Radar based systems and methods for monitoring a subject*. U.S. Patent 8740793 B2, Jun. 03, 2014.

[24] M. Ganesh, J. M. Ashe, L. Yu, and C. M. Graichen. *Physiology monitoring and alerting system and process*. U.S. Patent Application 20120245479 A1, Sep. 27, 2012.

[25] J. C. Lin. *Microwave sensing of physiological movement and volume change: A review*. Bioelectromagnetics, vol. 13, no. 6, pp. 557-565, 1992.

[26] K. M. Chen, Y. Huang, J. Zhang, and A. Norman. *Microwave life-detection systems for searching human subjects under earthquake rubble and behind barrier.* IEEE Trans. Biomed. Eng., vol. 47, no. 1, pp. 105-114, 2000.

[27] A. D. Droitcour, O. Boric-Lubecke, V. M. Lubecke, J. Lin, and G. T. A. Kovacs. *Range correlation and I/Q performance benefits in single-chip silicon Doppler radars for noncontact cardiopulmonary monitoring.* IEEE Trans. Microw. Theory Tech., vol. 52, no. 3, pp. 838-848, 2004.

[28] J. C. Lin. *Non-invasive microwave measurement of respiration.* Proceedings of IEEE, vol. 63, Issue: 10, Oct. 1975. pp.1530-1530, June 28 2005.

[29] H. R. Chuang, Y. F. Chen, and K. M. Chen. *Automatic Clutter-Canceler for Microwave Life-Detection Systems.* IEEE Instrum. Meas. Mag., vol. 40. No. 4, Aug, 1991.

[30] D. Addis. *Monitoring stress levels.* W.O. Patent 151607 A1, Nov. 15, 2012.

[31] J. Armitstead. *Method for detecting and discriminating breathing patterns from respiratory signals.* U.S. Patent 88992 A1, April 15, 2012.

[32] J. M. Ashe. *Unobtrusive Suicide Warning System, Final Technical Report, Phase III.* Technical report, Document No.: 243922, Oct. 2013.

[33] D. R. Morgan and M. G. Zierdt. *Doppler radar cardiopulmonary sensor and signal processing system and method for use therewith.* U.S.Patent 7 753 894 B2, Jul 13, 2010.

[34] A. Singh and V. Lubecke. *Respiratory monitoring using a Doppler radar with passive harmonic tags to reduce interference from environmental clutter.* 31st Annual International Conference of the IEEE EMBS Minneapolis, Minnesota, USA, Sep. 2009.

[35] B. K. Park, O. Boric-Lubecke, and V. M. Lubecke. *Arctangent demodulation with DC offset compensation in quadrature Doppler radar receiver systems.* IEEE Trans. Microw. Theory Tech., vol. 55, pp. 1073-1079, May 2007.

[36] C. Li and J. Lin. *Random Body Movement Cancellation in Doppler Radar Vital Sign Detection.* IEEE Trans. Microw.Theory Tech., vol. 56, pp. 3143-3152, 2008.

[37] L. Chioukh, H. Boutayeb, L. Li, L. Yahia, and K. Wu. *Integrated Radar Systems for Precision Monitoring of Heartbeat and Respiratory Status.* AaiaPasific Microwave Conference, pp. 405-408, 2009.

[38] G. Sun, M. Kubota, M. Kagawa, N. Q. Vinh, A. Kurita, and T. Matsui. *A Screening Method Based on Amplitude Probability Distribution Analysis for Detecting the Disordered Breathing Using Microwave Radar Respiration Signals.* Proceedings of APMC 2012, Kaohsiung, Taiwan, 2012.

[39] M. Kagawa, K. Ueki, H. Tojima, and T. Matsui. *Noncontact Screening System with Two Microwave Radars for the Diagnosis of Sleep Apnea-Hypopnea Syndrome.* IEEE EMBS, Osaka, Japan, 3-7, July, 2013.

[40] C. Li, J. Cummings, J. Lam, E. Graves, and W. Wu. *Radar remote monitoring of vital signs.* IEEE Microw. Mag., vol. 10, pp. 47-56, 2009.

[41] J. Kranjec, S. Begus, J. Drnovsek, and G. Gersak. *Novel methods for noncontact heart rate measurement: A feasibility study.* IEEE T. Instrum. Meas., vol. 63, pp. 838-847, 2014.

[42] A. Brewster and A. Balleri. *Extraction and analysis of micro-Doppler signatures by the Empirical Mode Decomposition.* Radar Conference (RadarCon), 2015 IEEE, Issue Date: May 2015.

[43] I. Mostafanezhad, E. Yavari, O. Boric-Lubecke, V. M. Lubecke, and D. P. Mandic. *Cancellation of Unwanted Doppler Radar Sensor Motion Using Empirical Mode Decomposition.* IEEE sensors journal, Vol. 13, NO. 5, May 2013.

[44] R. M. Narayanan, M. C. Shastry, P. H. Chen, and M. Levi. *Through-the-wall detection of stationary human targets using doppler radar.* Progress In Electromagnetics Research B, Vol. 20, 147-166, 2010.

[45] J. C. Lin. *Microwave sensing of physiological movement and volume change: A review.* Bioelectromagnetics 13, 1992, 557-565.

[46] Y. Xiao C. Li and J. Lin. *Experiment and spectral analysis of a low-power Ka-band heartbeat detector measuring from four sides of a human body.* IEEE Trans. Microw. Theory Tech., vol. 54, no. 12, pp. 4464-4471, Dec. 2006.

[47] A. DeGroote, G. Cheron M. Wantier, M. Estenne, and M. Pavia. *Chest wall motion during tidal breathing.* J Appl Physiol 83, 1997, 1531-1537.

[48] G. Ramachandran and M. Singh. *Three-dimensional reconstruction of cardiac displacement patterns on the chest wall during the P, QRS, and T-segments of the ECG by laser speckle interferometry.* Med Biol Eng Comput 27, 1989, 525-530.

[49] K. M. M. Prabhu. *Window functions and their applications in signal processing.* Boca Raton, Florida : CRC Press, 2014.

[50] G. Rilling, P. Flandrin, and P. Goncalves. *On empirical mode decomposition and its algorithms.* IEEE-EURASIP, Laboratoire de Physique (UMR CNRS 5672), Ecole Normale Superieure de Lyon 46, all'ee d'Italie 69364 Lyon Cedex 07, France, 2003.

[51] A. Herrero, J. Sedano, B. Baruque, H. Quintian, and E. Corchado. *10th International Conference on Soft Computing Models in Industrial and Environmental Applications.* Springer, May 31, 2015.